2020-06-24

Identification of a myotubularin-related phosphatase that regulates autophagic flux and lysosome homeostasis

Elizabeth A. Allen
University of Massachusetts Medical School

IDENTIFICATION OF A MYOTUBULARIN-RELATED PHOSPHATASE THAT REGULATES AUTOPHAGIC FLUX AND LYSOSOME HOMEOSTASIS

A Dissertation Presented

By

Elizabeth A. Allen

Submitted to the Faculty of the
University of Massachusetts Graduate School of Biomedical Sciences, Worcester
in partial fulfillment of the requirements for the degree of

DOCTOR OF PHILOSOPHY

JUNE 24, 2020

CANCER BIOLOGY

IDENTIFICATION OF A MYOTUBULARIN-RELATED PHOSPHATASE THAT REGULATES AUTOPHAGIC FLUX AND LYSOSOME HOMEOSTASIS

A Dissertation Presented
By
Elizabeth A. Allen

This work was undertaken in the Graduate School of Biomedical Sciences
Program in Cancer Biology

Eric H. Baehrecke, Ph.D., Thesis Advisor

Dorothy P. Schafer, Ph.D., Member of Committee

Leslie M. Shaw, Ph.D., Member of Committee

Neal Silverman, Ph.D., Member of Committee

Michael Overholtzer, Ph.D., External Member of Committee

Cole M. Haynes, Ph.D., Chair of Committee

Mary Ellen Lane, Ph.D.,
Dean of the Graduate School of Biomedical Sciences

June 24, 2020

Dedication

For
Rosemarie T. Chabot
May 23, 1957 – September 22, 2016

When I was little, you told me that I could be anything I wanted to be when I grew up. As an adult, I've been many things – a food-service worker, a mail-carrier, a firewood-processor machine operator, a mother, an endurance athlete. I spent time studying fine arts, literature, and later, biology. Underneath all of these different hats, I've remained most importantly, your daughter. Thank you for sharing so much of yourself with me. Even though you aren't physically here, I know that you remain with me because I have your outlook, your attitude, and of course, your genes. I love and miss you always.

Acknowledgements

First, I would like to thank my mentor Eric for his endless support during my graduate studies. I am grateful for his patience and understanding, for the time he spent editing my writing, and for helping me to think critically about my work. He has provided me with so many opportunities both at UMMS and in the broader scientific community, and I am fortunate to have had such an encouraging mentor.

Next, I want to thank all Baehrecke lab members, past and present. It is quite special to work in an environment where everyone is passionate about their research but also so supportive of one another. I am grateful for all of the friendly banter and serious discussions. Special thank you to Panos for always having an answer to my seemingly endless questions, especially when his answer ended with, “But, you can just do what you want.” This group of people truly made me enjoy being in lab every day. And to Yan, who may not be a Baehrecke lab member according to paperwork, but who is a member of our group in every other way. Thank you for patiently showing me how to do new things, for talking me through every step, and for giving me the encouragement and confidence to do it all on my own. I’m so glad you became part of our group.

I would like to thank my committee members for all of their advice and feedback about my project. I am extremely grateful to have committee members who treat me as a colleague. I feel fortunate to have gone into my TRAC meetings feeling a sense of mutual respect as both scientists and human beings. I would like to thank Cole for agreeing to chair my committee and for his rational advice. I would like to thank Leslie and Neal for our side discussions about my project and how to organize this dissertation. I would also like to thank Dori for her mentorship over the years, first as a rotation mentor and later on my TRAC. Most of all, I would like to thank my committee as a whole for their encouragement to pursue my goals and to keep my mind open to possibilities.

Thank you to the entire LRB 4th floor community for creating an environment that’s both friendly and professional. Special thank you to Do Kim for your mentorship in helping to plan the Cancer Biology Research Seminar. And to Art Mercurio and Michelle Kelliher for the opportunity to TA the Cancer Biology course.

Thank you to my 2015 GSBS 1st year classmates and colleagues. I feel fortunate to have had such a great group of human beings surrounding me during these last five years.

Last, but certainly not least, thank you to my family and friends, who provide unconditional support. To my dad, who finally came around to the idea that grad

school is a good thing. To Skyler, who has always been understanding and supportive and continues to impress me with her maturity about life and human nature. To Jim, for his encouragement, for always reminding me to be accountable, and for helping me laugh more. To Johnna and Allyson, who continue to answer my questions about life and science and never hold back their honest opinions. And finally, to Tracy and Melissa, who reached out with support while I was writing this dissertation and kept me motivated with thoughts of future adventures in the woods.

ABSTRACT

Macroautophagy (autophagy) is a vesicle trafficking process that targets cytoplasmic cargoes to the lysosome for degradation and underlies multiple human disorders. Pioneering work in *Saccharomyces cerevisiae* defined the core autophagy machinery, but animals possess autophagy regulators that were not identified in yeast. Autophagic flux occurs when autophagy rate increases or decreases in response to various cellular cues, such as nutrient availability. Indeed, dysregulated autophagy rates contribute to disease, making autophagy-modulation a therapeutic avenue to treat cancer, neurodegenerative disorders, and other diseases.

To identify novel regulators of autophagy in animals, I investigated autophagy in the context of animal development using *Drosophila*. In my dissertation, I screened for phosphoinositide phosphatases that influence autophagy, and identifed *CG3530/dMtmr6*, a previously uncharacterized phosphatase. CG3530/dMtmr6 is homologous to the human MTMR6 subfamily of myotubularin-related 3-phosphoinositide phosphatases. I showed that dMtmr6 functions as a regulator of autophagic flux in multiple *Drosophila* cell types, and the MTMR6 family member *MTMR8* functions similarly in autophagy of higher animal cells. Decreased *dMtmr6* function resulted in autophagic vesicle accumulation, lysosome biogenesis, and impaired both fluid phase endocytosis in the fat body and phagocytosis in embryonic macrophages. Additionally, *dMtmr6* is required for development and viability in *Drosophila*. In human cells, lysosome

homeostasis requires both the MTMR8 PH domain and catalytic cysteine residue, but only the PH domain is required to maintain autophagic flux. Collectively, this work identified a role for dMtmr6 and MTMR8 in autophagic flux and lysosome homeostasis.

TABLE OF CONTENTS

LIST OF TABLES

Tables in Chapter I

Tables in Appendices

LIST OF FIGURES

Figures in Chapter I

Figures in Chapter II

Figures in Chapter III

Figures in Appendices

List of copyrighted materials produced by the author

Figures and text in **Chapter I**, **Part I** (General Introduction) were previously published in accordance with copyright law.

Allen, E.A. and Baehrecke, E.H. (2020) Autophagy in animal development. *Cell Death and Differentiation*. 27(3):903-918. doi:10.1038/s41418-020-0497

List of abbreviations

ALR	Autolysosome Reformation
APF	After Puparium Formation
ATG/Atg	Autophagy related gene
Atg8a	Autophagy related gene 8a, LC3B ortholog
CC	Coiled-coil
Cos7	cell line derived from *Cercopithecus aethiops* kidney
FLP/FRT	flippase/flippase recognition target
FYVE	conserved in Fab1, YOTB, Vac1 and EEA1
HeLa	Human cervical carcinoma cell line, Henrietta Lacks
LAMP1	Lysosome-Associated Membrane Protein 1
LC3B	Microtubule-associated protein 1 light chain 3B, MAP1LC3B
mitf	melanocyte-inducing transcription factor, TFEB ortholog
MTMR	myotubularin-related phosphatase
mTORC1	Mechanistic Target of Rapamycin Complex I
p62	encoded by *SQSTM1* (autophagy cargo adapter)
PE	phosphatidylethanolamine
PH	plekstrin homology
GRAM	domain in glucosyltransferases, myotubularins and other membrane-associated proteins
PI	phosphoinositide
PS	phosphatidylserine

PtdIns	phosphatidylinositol
PTEN	phosphatase and tensin homolog
ref(2)p	refractory to sigma P (autophagy cargo adapter)
TFEB	Transcription factor EB
TR-avidin	Texas Red avidin, fluorescent ligand for endocytosis
VPS/Vps	vacuolar protein sorting
WIPI	WD-repeat protein interacting with phosphoinositides

Preface

Figures and text in **Chapter I**, **Part I** (General Introduction) were previously published.

Allen, E.A. and Baehrecke, E.H. (2020) Autophagy in animal development. *Cell Death and Differentiation*. 27(3):903-918. doi:10.1038/s41418-020-0497

The work presented in **Chapter II** represents unpublished work that is under review at *Journal of Cell Biology*.

Allen, E.A., Amato, C. Fortier, T., Velentzas, P., Wood, W., and Baehrecke, E.H. A conserved myotubularin-related phosphatase regulates autophagy by maintaining autophagic flux. *J Cell Biol* (under revision).

Contributions of the authors are addressed at the beginning of each chapter.

CHAPTER I

Introduction

In the first section of this introduction, I describe the different types of eukaryotic autophagy that exist and set out the key molecular players that regulate each step of the process. I explain why we study animal development to understand the mechanisms that underly autophagy. In the second section, I discuss the role of phosphoinositides in cellular membrane trafficking, with a special focus on autophagy. Finally, I describe the scope and rationale of this project.

Autophagy in animal development*

Macroautophagy (autophagy) delivers intracellular constituents to the lysosome to promote catabolism. During development in multiple organisms, autophagy mediates various cellular processes, including survival during starvation, programmed cell death, phagocytosis, organelle elimination, and miRNA regulation. Our current understanding of autophagy has been enhanced by developmental biology research during the last quarter of a century. Through experiments that focus on animal development, fundamental mechanisms that control autophagy and that contribute to disease were elucidated. Experiments in

* Part I is adapted from a previously published review article (Allen and Baehrecke, 2020). E. Allen conceived and wrote most of the article, and E. Baehrecke edited the manuscript for publication.

multiple organisms reveal conserved mechanisms of tissue remodeling that rely on the cooperation between autophagy and apoptosis to clear cell corpses, and defects in autophagy and apoptotic cell clearance can contribute to inflammation and autoimmunity. Moreover, autophagy and its components offer potential mechanisms with which to remove many of the harmful aggregates that underlie neurodegenerative diseases. In this section, I provide an overview of key developmental processes that mediate autophagy in multiple animals.

Autophagy: lysosomes, membranes, and molecules

The addition and removal of cells and tissues require transient shifts between anabolism and catabolism during animal development. These processes intersect at the lysosome, an organelle originally regarded as the cell's trash can. Since its discovery in 1955 by Christian de Duve (de Duve et al., 1955), the lysosome has emerged as a cellular signaling center (Settembre et al., 2013; Mony et al., 2016; Lawrence and Zoncu, 2019) that facilitates degradation, homeostasis, and growth. Autophagy delivers cargoes to the lysosome in response to intra- and extracellular cues to facilitate the turnover of cellular components.

Three distinct types of autophagy exist in higher eukaryotes: microautophagy, chaperone-mediated autophagy (CMA), and macroautophagy, which differ both mechanistically and morphologically **(Fig. 1.1)**. In 1966, Christian de Duve and Robert Wattiaux coined the term microautophagy (de Duve and

Wattiaux, 1966) to describe a process by which existing endo-lysosomal membranes protrude or invaginate to sequester cargoes. Microautophagy has been most studied in yeast, and is either selective, which degrades specific cellular components, or non-selective, which targets random cytosolic components. Microautophagy in higher organisms remains elusive, and is better understood in the context of endosomal microautophagy (e-MI), in which late endosomal membranes generate invaginating vesicles that internalize ubiquitinated membrane proteins (Santambrogio and Cuervo, 2011). Similarly, single proteins can be degraded by CMA, which delivers target proteins to the lysosome via a molecular chaperone. In this case, heat shock protein family A (Hsp70) member 8 (HSPA8) recognizes substrate proteins with a KFERQ-motif (Chiang et al., 1989), and delivers them to lysosomal-associated membrane protein 2A (LAMP2A) (Cuervo and Dice, 1996) for unfolding, translocation across the lysosomal membrane, and subsequent degradation (Salvador et al., 2000; Agarraberes et al., 1997).

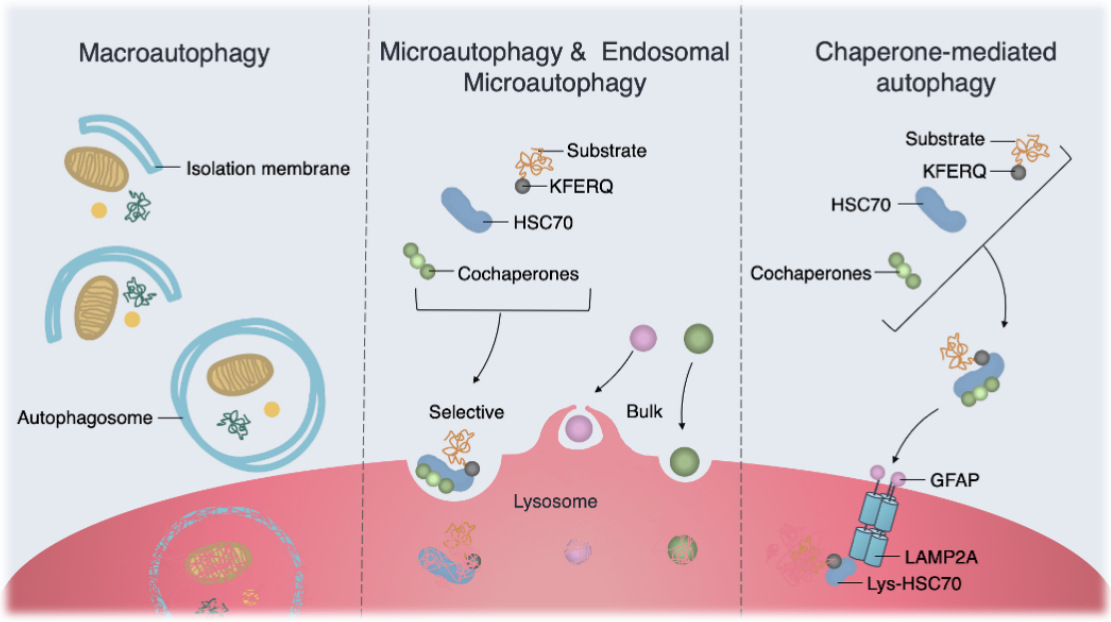

Figure 1.1 Autophagic pathways converge at the lysosome. Autophagic cargoes are degraded by lysosomal enzymes. In macroautophagy, a double-membrane isolation membrane elongates, expands, and seals to make an autophagosome around cytoplasmic components before fusing with the lysosome. Microautophagy and endosomal microautophagy deliver small cargoes directly to the lysosome either without or with chaperones, respectively. Chaperone-mediated autophagy requires the lysosome-associated membrane protein 2A (LAMP2A), in addition to molecular chaperones.

Macroautophagy (hereafter autophagy) requires the biogenesis of specialized membranes that sequester cytoplasmic cargoes, including mitochondria, for delivery to the lysosome. In their foundational report in 1962, Ashford and Porter discovered that in glucagon-stimulated rat hepatocytes, lysosome numbers increased and in many cases, contained mitochondria (Ashford and Porter, 1962), which demonstrated both hormone- and starvation-induced autophagy for the first time. Shortly thereafter, Arstila and Trump provided evidence that autophagy exists as a sequential process that begins with the formation of a double-membraned autophagosome, which is free of hydrolytic enzymes, and this structure is later observed as a single membrane autolysosome, often containing partially degraded organelles and lysosomal enzymes (Arstila and Trump, 1968). Later studies in the yeast *Saccharomyces cerevisiae* revealed the core autophagy machinery that is encoded by over 30 *ATG* (autophagy-related) genes (Takeshige et al., 1992; Thumm et al., 1994; Tsukada and Ohsumi, 1993; Ohsumi, 2001), most of which are conserved in higher animals (Yang and Klionsky, 2010; Levine and Klionsky, 2004) **(Table 1.1)**.

Table 1.1. Autophagy gene orthologs across organisms.

S. cerevisiae	*C. elegans*	*D. melanogaster*	*H. sapiens*
ATG1	*unc-51*	*Atg1*	*ULK1, ULK2*
ATG13	*epg-1*	*Atg13*	*KIAA0652*
ATG17		*Atg17*	*FIP200, RB1CC1*
	epg-7		
	epg-9	*Atg101*	*ATG101*
VPS30/ATG6	*bec-1*	*Atg6*	*BECN1*
VPS34	*vps-34*	*Vps34/Pi3K59F*	*VPS34/PIK3C3*
VPS15	*vps-15*	*Vps15/ird1*	*VPS15/PIK3R4*
ATG14	*epg-8*	*Atg14*	*ATG14/barkor*
		CG6116	*UVRAG*
		endoB	*SH3GLB1*
		buffy	*BCL2*
			AMBRA1
ATG3	*atg-3*	*Atg3*	*ATG3*

S. cerevisiae	*C. elegans*	*D. melanogaster*	*H. sapiens*
ATG4	*atg-4.1, atg-4.2*	*Atg4*	*ATG4A, ATG4B, ATG4C, ATG4D*
ATG5	*atg-5*	*Atg5*	*ATG5*
ATG7	*atg-7*	*Atg7*	*ATG7*
ATG8	*lgg-1, lgg-2*	*Atg8a, Atg8b*	*MAP1LC3A, MAP1LC3B, MAP1LC3C, GABARAP, GABARAPL2*
ATG10	*atg-10*	*Atg10*	*ATG10*
ATG12	*lgg-3*	*Atg12*	*ATG12*
ATG16	*atg-16.1, atg-16.2*	*Atg16*	*ATG16L1, ATG16L2*
ATG18	*atg-18*	*Atg18a, Atg18b*	*WIPI1, WIPI2*
	epg-2		
	epg-3	*Tango5*	*VMP1*
	epg-4	*tank*	*EI24*
	epg-5	*Epg5*	*EPG5*
	epg-6		*WIPI3, WIPI4*
ATG2	*atg-2*	*Atg2*	*ATG2*

S. cerevisiae	*C. elegans*	*D. melanogaster*	*H. sapiens*
ATG9	*atg-9*	*Atg9*	*ATG9A, ATG9B*
	pgl-3		
	rab-7	*Rab7*	*RAB7*
	sepa-1		
	sqst-1	*ref(2)p*	*SQSTM1/p62*
LST8	*mlst-8*	*Lst8*	*MLST8*
TEP1	*daf-18*	*Pten*	*PTEN*
TOR1, TOR2	*let-363*	*Tor*	*TOR*
KOG1	*daf-15*	*raptor*	*Raptor*
RHB1	*rheb-1*	*Rheb*	*Rheb*
TSC11	*rict-1*	*rictor*	*Rictor*

Autophagy membrane dynamics are characterized by sequential formation of morphologically distinct autophagic structures **(Figure 1.1)**. Following autophagy initiation, an isolation membrane forms and expands around cargoes to eventually seal and form a double-membrane autophagosome. The autophagosome fuses with the lysosome to generate an autolysosome. Following degradation, autophagy commences with autolysosome reformation via the tubulation and scission of proto-lysosomes that mature and later contribute to the lysosomal pool.

Specific *ATGs* and their regulators control different stages of autophagy **(Fig. 1.2)**, and the intricacies of their molecular regulation are extensively described elsewhere (Yang and Klionsky, 2010; Mercer et al., 2018). Briefly, autophagosome formation requires the unc-51-like kinase (ULK/Atg1) complex, the class III phosphatidylinositol 3-kinase (PtdIns3K)/Vps34 complex I (PI3KC3), two ubiquitin-like protein (Atg12 and Atg8/LC3) conjugation systems, and the transmembrane proteins ATG9/Atg9 and VMP1 (Ganley et al., 2009; Nakatogawa, 2013; Itakura and Mizushima, 2010). The protein kinase mechanistic target of rapamycin complex 1 (mTORC1/TORC1), which includes mTOR, regulatory-associated protein of mTOR (Raptor), mammalian lethal with Sec13 protein 8 (mLst8/Lst8), proline-rich AKT substrate 40 kDa (PRAS40), and DEP-domain-containing mTOR-interacting protein (Deptor), functions upstream of autophagy (Saxton and Sabatini, 2017). mTORC1 is typically activated at the lysosome by both growth factors and nutrients, and promotes the activity of translation-

regulating factors, such as the eukaryotic initiation factor 4E binding protein and the ribosomal protein S6 kinase. Meanwhile, mTORC1 represses autophagy via ULK-complex phosphorylation (Saxton and Sabatini, 2017). When nutrient levels drop, mTORC1 repression occurs, and autophagy proceeds with the activation of the ULK complex, PI3KC3-mediated generation of PI(3)P at early autophagosomal membranes, the ATG12 complex, and the conjugation of ATG8 family proteins to the membrane lipid phosphatidylethanolamine (PE) (Saxton and Sabatini, 2017; Itakura and Mizushima, 2010). Following closure, autophagosomes undergo a maturation process that includes PI(3)P turnover and removal of ATG8 proteins by members of the ATG4 protease family, as well as recruitment of fusion machinery, which includes RAB7, the homotypic vacuole fusion and protein sorting (HOPS) tethering complex, SNARES, and others (Reggiori and Ungermann, 2017). Upon lysosome fusion, the inner membrane of the autophagosome and its contents are degraded by lysosomal enzymes, and amino acids and sugars are effluxed out of the lysosome via specific transporters, including the sugar efflux Spinster (SPNS), which is required for degradation, autolysosome reformation, and reactivation of mTORC1 (Rong et al., 2011; Yu et al., 2018b).

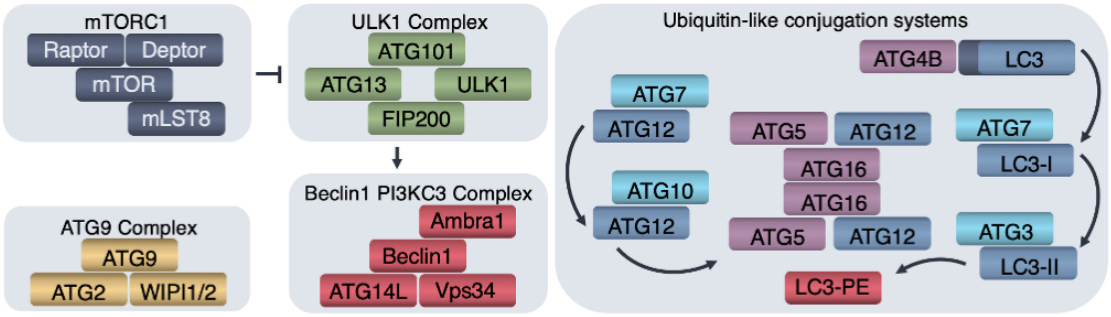

Fig. 1.2. Autophagic components. Conserved autophagy molecules regulate macroautophagy in development. Please refer to the text for further descriptions.

Autophagy and apoptotic corpse clearance in development

During development, autophagy and apoptosis work together to eliminate massive numbers of cells. Autophagy has been associated with dying cells during development of diverse taxa. During apoptosis, dying cells are quickly engulfed by phagocytosis, an internalization process by which extracellular constituents are sequestered and processed within a single-membrane phagosome that is eventually degraded by the lysosome. Efficient apoptotic corpse removal requires that apoptotic cells generate cell-surface “eat-me” signals and secrete “come-get-me” signals, and also, that phagocytic cells migrate to cell death sites, recognize, and take-up the dying cells (Grimsley and Ravichandran, 2003) **(Fig. 1.3)**. Several lines of evidence support a role for autophagic components within both apoptotic and phagocytic cells during developmental programmed cell death. One specialized process called LC3-associated phagocytosis (LAP) uses autophagy proteins in a non-canonical manner to facilitate engulfment of extracellular cargoes(Heckmann and Green, 2019). Unlike other types of autophagy, LAP requires intracellular generation of reactive oxygen species to promote maturation of macrophage phagosomes. However, a role for LAP in development remains to be discovered.

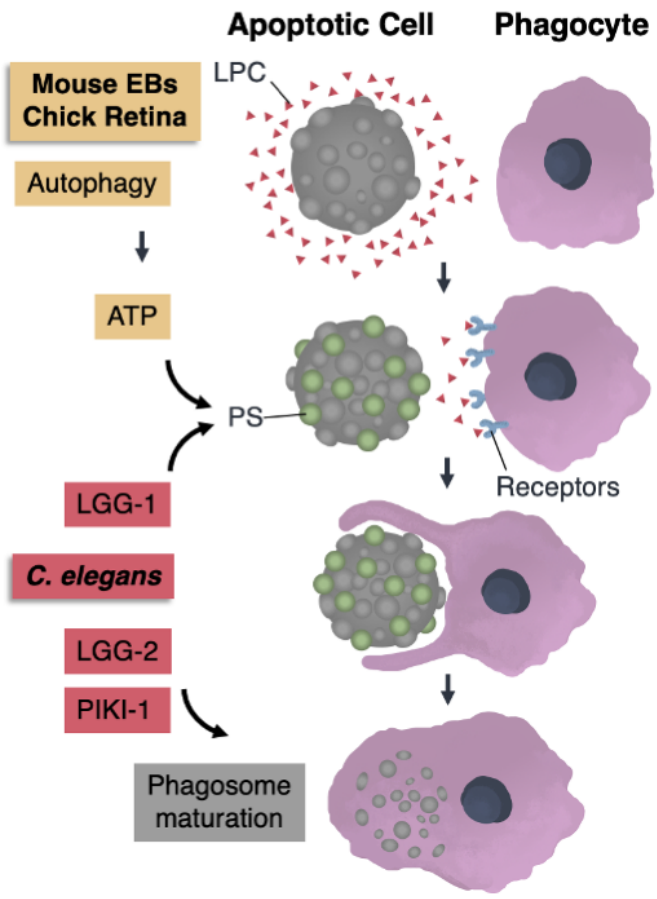

Fig. 1.3. Apoptotic corpse cell clearance. Dying cells release "find me" signals, such as lysophosphatidylcholine (LPC), which are recognized by phagocytic cells. Dying cells expose cell-surface phosphatidylserine (PS) in a context-specific manner (refer to text for details). Phagocyte receptors recognize PS, engulf and internalize corpse cells, and phagosomes mature along a lysosome-destined pathway that requires some autophagy components.

Autophagic corpse clearance in C. elegans

Much of our understanding of cell death pathways stems from experiments in *C. elegans*. Like in mammals, autophagy cooperates with apoptosis to facilitate corpse clearance in worms. However, unlike flies and mammals, *C. elegans* lack professional phagocytes, and instead, apoptotic cells rely on neighboring cells for engulfment.

During *C. elegans* embryogenesis, 113 cells undergo programmed cell death (Conradt et al., 2016) followed by corpse clearance. Worm embryos with mutations in genes that regulate multiple steps in autophagy contain more cell corpses than controls (Huang et al., 2013; Cheng et al., 2013), while corpse clearance does not require specialized autophagy cargo adapter or receptor molecules that mediate clearance of protein aggregates or P granules (Cheng et al., 2013). Autophagy genes are not required for corpse engulfment but instead cooperate with the class II PI3 kinase PIKI-1 to promote PI(3)P-dependent phagosome maturation (Cheng et al., 2013). Differential roles exist for LGG-1/GABARAP and LGG-2/LC3 in apoptotic corpse clearance in *C. elegans* embryos (Jenzer et al., 2019). Apoptotic cells and phagosomes are both enriched with LGG-1 and LGG-2. However, LGG-1 promotes apoptotic-cell phosphatidylserine (PS) exposure, while LGG-2 mediates phagosome-lysosome interactions. Unlike mouse embryoid bodies (EBs) and chick retina (discussed below), autophagy gene mutations fail to impair PS exposure in *C. elegans* embryonic cell corpses (Huang et al., 2013).

During the first larval stage, *C. elegans* Q neuroblasts divide asymmetrically, and their smaller daughter cells undergo apoptotic death. In the phagocyte, sequential function of autophagy proteins ATG-18 and EPG-5 promotes phagosome maturation and enables corpse degradation but not removal (Li et al., 2012). This process is, however, UNC-51- and ATG-7-independent because *unc-51* and *atg-7* mutant worms lack Q-cell corpse-clearance defects (Li et al., 2012). Further, adult *C. elegans* hermaphrodites undergo a germ cell death in which surrounding gonadal sheath cells phagocytose germ cell corpses. Here, corpse degradation requires BEC-1, ATG-18, and UNC-51 (Ruck et al., 2011). Both *bec-1* mRNA and BEC-1::GFP are detectable throughout development, with highest *bec-1* mRNA expression during embryogenesis (Takacs-Vellai et al., 2005) and BEC-1::GFP in differentiating organs. Interestingly, loss of both maternal and zygotic *bec-1* results in early embryonic lethality, but animals with maternally-derived wild-type BEC-1 live to early adulthood despite motility defects and vacuole accumulation in various tissues (Takacs-Vellai et al., 2005; Ruck et al., 2011). However, it remains difficult to determine the exact role for BEC-1 in development because, in addition to impaired autophagy, *bec-1* mutants display endocytosis and retrograde transport defects (Ruck et al., 2011), and evidence indicates that BEC-1/Beclin 1 exists in at least two complexes, an autophagy- and an endocytosis-specific complex.

Corpse clearance in Drosophila embryogenesis

During the final stages of *Drosophila* embryogenesis, an extra-embryonic tissue called the amnioserosa is eliminated by programmed cell death that involves both autophagy and caspases. At dorsal closure, approximately 90% of amnioserosa cells internalize and degenerate, while basal extrusion followed by anoikis accounts for cell death in the remaining 10% of amnioserosa cells (Reed et al., 2004), and phagocytic macrophages engulf the dying amnioserosa cells (Mohseni et al., 2009). In caspase-deficient embryos, amnioserosa tissue persists several hours beyond when control embryo amnioserosa degenerates (Mohseni et al., 2009). However, autophagic activity increases in late dorsal closure stage embryos prior to amnioserosa cell death in both wild-type and caspase-deficient embryos (Mohseni et al., 2009). Autophagy suppression by activated growth signaling delays amnioserosa degeneration, and autophagy activation by *Atg1* misexpression promoted early amnioserosa dissociation and cell death, which could be suppressed by caspase inhibition (Mohseni et al., 2009). Similarly, autophagy promotes, but is not required for amnioserosa basal cell extrusion during dorsal closure stage (Cormier et al., 2012). Thus, developmental autophagy precedes caspase-dependent amnioserosa cell death, which suggests that autophagy could mediate caspase activation in specific contexts.

Corpse clearance during vertebrate embryogenesis

In rodents, developmental programmed cell death occurs early in embryogenesis with cavitation that commences just prior to gastrulation. The solid mass of ectoderm cells undergoes programmed cell death to form the pro-amniotic cavity (Coucouvanis and Martin, 1995). An *in vitro* model of this process utilizes mouse embryonic stem cells, which form undifferentiated cell aggregates and develop into simple EBs. Simple EBs contain an outer layer of endodermal cells and an inner solid mass of ectodermal cells that undergo programmed cell death to form cystic EBs.

Using EBs, it was discovered that *atg5* and *beclin1* are required for the removal of dead cells by phagocytic cells during cavitation (Qu et al., 2007). A ubiquitous dying-cell eat-me signal, PS, translocates from the inner to the outer leaflet of the plasma membrane lipid bilayer early during apoptosis. In addition, dying cells secrete lysophosphatidylcholine (LPC), a potent chemoattractant signal recognized by professional phagocytes, including macrophages. Both PS exposure and LPC secretion are essential for apoptotic cell engulfment (Grimsley and Ravichandran, 2003). In autophagy gene-deficient EBs, corpse clearance and cavitation fail because dying cells lack outer-leaflet PS, secrete lower levels of LPC compared to wild-type EBs, and have reduced ATP levels (Qu et al., 2007). The defects in PS exposure, LPC secretion, and ATP levels are reversible after treating EBs with methylpyruvate, a cell-permeable tricarboxylic acid cycle substrate, which also restores corpse clearance and cavitation.

A similar role for autophagy in corpse clearance exists in chick retinal development. The embryonic chick retina is a well-characterized model in which the processes of neural development and cell death coexist. Retinal neuroepithelium proliferates, generating the retinal ganglion cells, which are the first neurons, and simultaneously, cell death occurs centrally. Autophagy is active in the E4 chick retina, in the E5 neuroepithelium and retinal ganglion cells, and in all layers of the E9 retina. At each of these stages, autophagy can be inhibited by exposure to 3-methyladenine (3-MA) (Mellén et al., 2008, 2009). Autophagy inhibition by 3-MA in E4 organotypic neuroretinal cultures results in apoptotic cell body accumulation with cells that fail to expose PE and harbor reduced ATP levels, and methylpyruvate treatment rescues these defects (Mellén et al., 2008). However, 3-MA treatment produces differential spatiotemporal effects. In E5 retinas, 3-MA impairs dorsotemporal area cell-corpse clearance. Meanwhile 3-MA has no effect on the clearance of dying cells at the optic nerve and optic fissure area, and E9 retinal ganglion cell programmed cell death remains unaffected by 3-MA. Interestingly, mouse *Atg5*$^{-/-}$ embryos feature a defect in apoptotic-corpse engulfment in retina and lungs (Qu et al., 2007). Taken together, these studies provide evidence that autophagy-dependent ATP production promotes PS-mediated apoptotic cell clearance in some developmental programmed cell death contexts, but not all.

Autophagy in post-embryonic animal development

Autophagy participates in post-embryonic animal development where it can mediate gene silencing, cell-fate determination and promote survival in stressful environments. In fact, multiple animals require autophagy either to survive periods of developmental nutrient restriction or to facilitate developmental cell death during tissue remodeling.

Autophagy in C. elegans development during stress

C. elegans normally develop through four continuous larval stages. However, when environmental conditions are insufficient to support successful reproduction, such as either limited food supply, high population density or increased temperature, *C. elegans* enter a specialized and reversible developmental stage called the dauer diapause to survive. In this case, developmental arrest occurs at the second molt, and instead of proceeding to a typical third larval stage, animals cease feeding, increase lipid storage, and become thin and dense, mainly as result of hypodermal shrinkage. Autophagy increases during dauer stage, and the remodeling that occurs during dauer formation requires *bec-1*, *atg-1*, *atg-7*, *atg-8*, and *atg-18* (Meléndez et al., 2003).

Autophagy in the mouse embryo to neonate transition

Following birth and termination of the placental nutrient supply, a critical wave of autophagy occurs during the mouse early neonatal period. Indeed, autophagy is massively induced in most tissues of the mouse immediately after birth and it continues through one to two days (Kuma et al., 2004b). This autophagic wave is essential because neonatal lethality occurs within one day of birth in either *Atg3* (Sou et al., 2008), *Atg5* (Kuma et al., 2004a), *Atg7* (Komatsu et al., 2005), *Atg9* (Saitoh et al., 2009), or *Atg16L1* (Saitoh et al., 2008) knockout mice. These knockout mice feature decreased tissue and plasma amino acid levels several hours after birth, which suggests that autophagy provides amino acids during this nutritionally limited time period. Additionally, either *Atg3*-, *Atg5*-, or *Atg7*- knockout mice have low birth weights.

It was unknown how autophagy-derived amino acids were used in neonates during this starvation period until the discovery that the Rag GTPases play a critical role (Efeyan et al., 2012). Indeed, it is now understood that Rag GTPases signal glucose and amino-acid concentrations to mTORC1, and ultimately regulate autophagy in neonates. Like autophagy gene-knockout mice, constitutively active RagA ($RagA^{GTP}$) knock-in mice fail to survive the neonatal starvation period (Efeyan et al., 2012). Shortly after birth, $RagA^{GTP/GTP}$ fasted neonates lack mTORC1 inhibition, fail to induce autophagy, and remain hypoglycemic until death. In fasted wild-type littermates, mTORC1 inhibition and hypoglycemia occur, and plasma amino-acid levels drop, but after prolonged fasting, plasma glucose levels

recover. Presumably, the amino acids produced by autophagy during the early neonatal period are required to sustain gluconeogenesis in the liver, and constitutive RagA activity ultimately results in lethal energetic exhaustion in neonates (Efeyan et al., 2012). Thus, following birth, the Rag GTPases sense the disruption of the placental nutrient supply, leading to a pro-survival autophagic program that maintains whole-animal homeostasis through the embryo to neonate transition.

Autophagy in Drosophila metamorphosis

Around the time that de Duve and Wattiaux described autophagy (de Duve and Wattiaux, 1966), studies in insects provided a first line of evidence that autophagy is associated with tissue degradation during metamorphosis, the transition from the larval to adult stages. In 1965, Schin and Clever showed that during metamorphosis in the midge, *Chironomus tentans*, salivary-gland cells undergo lysosome-mediated degradation (Schin and Clever, 1965). Locke and Collins also revealed that just prior to metamorphosis, fat body cells of the butterfly *Calpodes ethlius* sequester cytoplasmic contents within membranes (Locke and Collins, 1965). Shortly thereafter, similar tissue regressions were reported, such as in the prothoracic glands of other insects (Scharrer, 1966) and in the salivary glands of other species (Schin and Laufer, 1973). In 1977, Beaulaton and Lockshin provided evidence that during *Lepidoptera* metamorphosis intersegmental muscles are

degraded by autophagy (Beaulaton and Lockshin, 1977). Decades later, our group elucidated several mechanisms by which autophagy degrades the intestine and salivary glands during development to mediate non-apoptotic cell death in *Drosophila melanogaster* (Lee and Baehrecke, 2001; Baehrecke, 2003; Denton et al., 2009; Berry and Baehrecke, 2007a).

Animal metamorphosis requires both a continuous nutrient supply for growth and an intricate crosstalk between autophagy and apoptosis for rapid body-plan remodeling. The *Drosophila* life cycle includes the larval, pupal, and adult stages, each of which requires unique body morphologies to support stage-specific needs, including feeding, body pattern remodeling, and reproduction. Following embryogenesis and hatching, larvae feed continually, and rapid growth occurs across the three larval stages in about 4 days. Growth arrest occurs at the onset of pupariation, the cuticle hardens and larval tissues are removed while adult tissues develop over approximately 4 days.

In *Drosophila*, autophagy is associated with multiple larval tissues during metamorphosis **(Fig. 1.4)**. Autophagy is induced in the *Drosophila* fat body just prior to pupariation (Rusten et al., 2004). At the onset of pupariation, the *Drosophila* larval intestine undergoes rapid cell size reduction and caspase-independent cell death by autophagy, and at 10-12 hours after pupariation the salivary glands begin to undergo cell death that depends upon both caspases and autophagy. These developmental programs occur in response to the metamorphosis-inducing steroid hormone 20-hydroxyecdysone (ecdysone), which

increases temporally, first at the end of the larval period and again at 10-12 hours after puparium formation. Ecdysone promotes a transcriptional program that includes upregulation of autophagy genes (Lee et al., 2003), and flies with mutations in genes that promote ecdysone signaling have reduced levels of autophagy genes and fail to form autophagic structures (Lee and Baehrecke, 2001; Lee et al., 2002; Baehrecke, 2003).

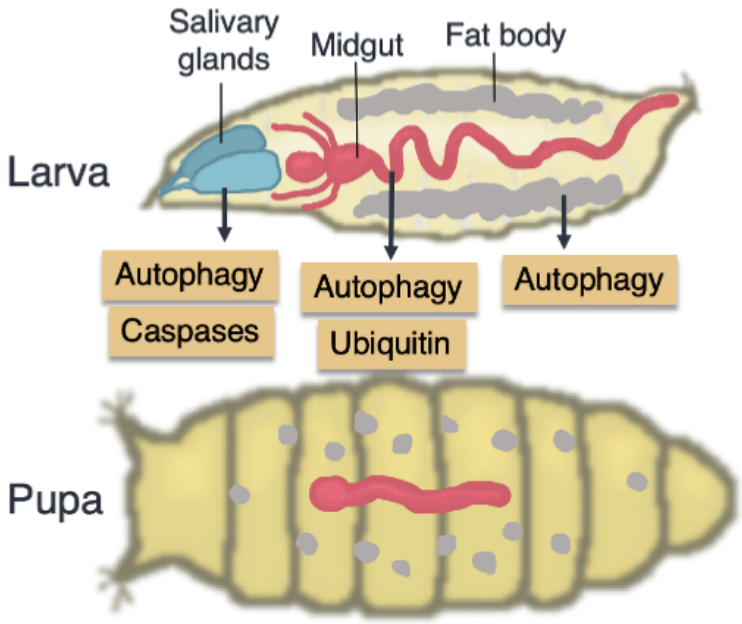

Fig. 1.4. Autophagy in *Drosophila* metamorphosis. During *Drosophila* metamorphosis, autophagy is required for the breakdown of larval tissues, where in specific contexts may function with other cell death pathways.

An important regulator of cell growth, the conserved class I phosphoinositide 3-kinase (PI3KC1) pathway signals through p110 and Akt to activate TOR in nutrient-rich conditions, which inhibits autophagy via the Atg1/ULK complex (Kamada et al., 2000) and promotes protein synthesis. In the *Drosophila* fat body, PI3KC1 signaling suppresses autophagy throughout larval development until the last larval stage when ecdysone signaling inhibits PI3KC1 signaling and activates autophagy (Rusten et al., 2004). Indeed, dominant-negative ecdysone receptor expression in fat body reduces autophagy in late larval fat body, and the ecdysone analog RH5849 stimulates autophagy in early third larval stage fat body (Rusten et al., 2004).

Autophagy during salivary gland cell death requires cell growth arrest. Expression of the PI3KC1 activity-reporter tGPH inversely correlates with the autophagy reporter GFP-LC3. Indeed, salivary glands in feeding larvae express high levels of cortical tGPH and contain very few GFP-LC3 spots while 6 h after puparium formation glands lose cortical tGPH, and by 13.5 h APH glands contain numerous GFP-LC3 spots (Berry and Baehrecke, 2007b). Misexpression of PI3KC1 positive-regulators, such as Dp110 (the PI3K active subunit), Akt, and activated Ras^{V12}, produces overgrown salivary glands and prevents gland autophagic degradation in a TOR-dependent manner (Berry and Baehrecke, 2007b). Autophagic salivary gland clearance also fails in the absence of the proton-coupled pyruvate transporter *hermes*, which is a *SLC16A11* ortholog that mediates TOR signaling (Velentzas et al., 2018). In salivary gland cells without

hermes, increased TOR activity suppresses autophagy, which impairs cell clearance, but reduced TOR function in *hermes*-deficient cells promotes gland clearance (Velentzas et al., 2018).

Drosophila salivary gland cell death requires miRNA-mediated post-transcriptional gene regulation. In salivary glands that are undergoing developmental cell death, the miRNA *mir-14* is both necessary and sufficient for autophagy, but not caspase activity or hormone signaling, and *mir-14* misexpression can induce premature autophagy in salivary glands (Nelson et al., 2014). Mechanistically, *mir-14* targets inositol 1,4,5-triphosphate kinase 2 (*ip3k2*), and *ip3k2* mediates inositol 1,4,5-triphosphate (IP3) signaling via endoplasmic reticulum calcium release. Furthermore, salivary gland cell death by autophagy requires both the calcium-binding protein Calmodulin and IP3 signaling. Interestingly, no role exists for either *mir-14* or IP3-mediated Calmodulin signaling in starvation-induced autophagy in the *Drosophila* fat body (Nelson et al., 2014).

Larval salivary gland clearance requires both autophagy and caspases (Martin and Baehrecke, 2004; Berry and Baehrecke, 2007b). Unlike other developmental contexts in which dying cells are engulfed by phagocytic cells, salivary gland degradation does not require *Drosophila* phagocytes (Martin and Baehrecke, 2004; Lin et al., 2017a). However, autophagy in *Drosophila* salivary gland cells is regulated non-autonomously. *Drosophila* macroglobulin complement-related (Mcr), a complement ortholog signals through the immune receptor Draper in neighboring cells to regulate autophagy but not caspase activity

during developmental salivary gland cell death (Lin et al., 2017a). A similar Mcr-Draper signaling axis-induced autophagy exists in the macrophage in response to wound healing. Src42A phosphorylates Draper and is required for salivary gland clearance (McPhee et al., 2010), and in the absence of Mcr, constitutively active Src42A expression is sufficient to promote gland clearance (Lin et al., 2017a). However, neither Draper nor Mcr facilitates starvation-induced autophagy in the fat body.

Drosophila larval midgut degradation occurs early in metamorphosis. Within 4 hours after the onset of pupariation, midgut cells undergo cell size reduction, and despite activation of both caspases and autophagy, only autophagy is essential for midgut cell size reduction that is associated with cell death. Indeed, caspase-inhibition permits and autophagy-inhibition delays midgut removal (Denton et al., 2009). Both developmentally programmed cell size reduction and autophagic vesicle formation in midgut cells require the canonical autophagy components Atg1, Atg2, Atg5, Atg6, Atg8a, Atg12, Atg13, Atg16, Atg18, and Vps34. However, midgut developmental cell death by autophagy, which includes mitochondrial clearance, occurs independent of Atg7 and Atg3 and instead requires the E1 enzyme Uba1 (Chang et al., 2013). Cells that possess defective *Uba1* fail to shrink and show reduced autophagic puncta compared to controls (Chang et al., 2013). However, despite Atg8a puncta formation, Uba1 activates ubiquitin but fails to activate Atg8a (Chang et al., 2013). Remarkably, both Atg8a puncta formation and cell size reduction require ubiquitin, but apparently not Atg8a-lipidation (Chang et

al., 2013). In addition, the ubiquitin binding domain-encoding Vps13D protein is required for midgut cell autophagy, size reduction, and clearance of mitochondria (Anding et al., 2018). Thus, midgut autophagy during *Drosophila* metamorphosis represents a unique context in which both canonical and non-canonical autophagy molecules participate with ubiquitin for rapid cargo clearance and cell size reduction.

We owe our current understanding of the mechanisms that regulate autophagy to research that spans the last quarter of a century. As a result of experiments that focus on developmental biology, we gained knowledge about mechanisms that underlie autophagy in different cell contexts that are relevant to disease. Indeed, through our ongoing analyses in *Drosophila* tissues, we continue to uncover new mechanisms in autophagy and related degradative pathways. Thus, future work on developmentally programmed autophagy has great potential to advance our understanding of autophagy in both normal and disease settings.

Phosphoinositides in autophagy

Phosphoinositides (PIs) are minor membrane lipids with major roles in cell biology from plants to animals. While relatively short-lived, PIs affect essential cellular processes including cell migration, signaling, ion channel gating, and intracellular membrane dynamics (Balla, 2013; Schink et al., 2016; Di Paolo and De Camilli, 2006). Importantly, autophagy requires specific phosphoinositide conversion to transition from one step of the process to the next. Here, I introduce the different species of phosphoinositides and explain how they function in the endolysosomal system, autophagy, and disease.

Phosphoinositides: small, significant, and dynamic

PIs are phosphorylated biproducts of phosphatidylinositol (PtdIns) and are generated by numerous kinases and phosphates. Phosphorylation occurs at one or more of the six -OH groups on D-*myo*-inositol **(Fig. 1.5 A)**, a 6-carbon ring that assumes a “chair” conformation. D-*myo*-inositol is linked by a phosphodiester linkage at its D1 position to a membrane-embedded diacylglycerol backbone (**Fig. 1.5 B)**, leaving the inositol headgroup exposed to the cytoplasm. Only the D3, D4, and D5 headgroups are reversibly phosphorylated *in vivo*, either in combination or individually to generate seven PI derivatives **(Fig. 1.5 C)**.

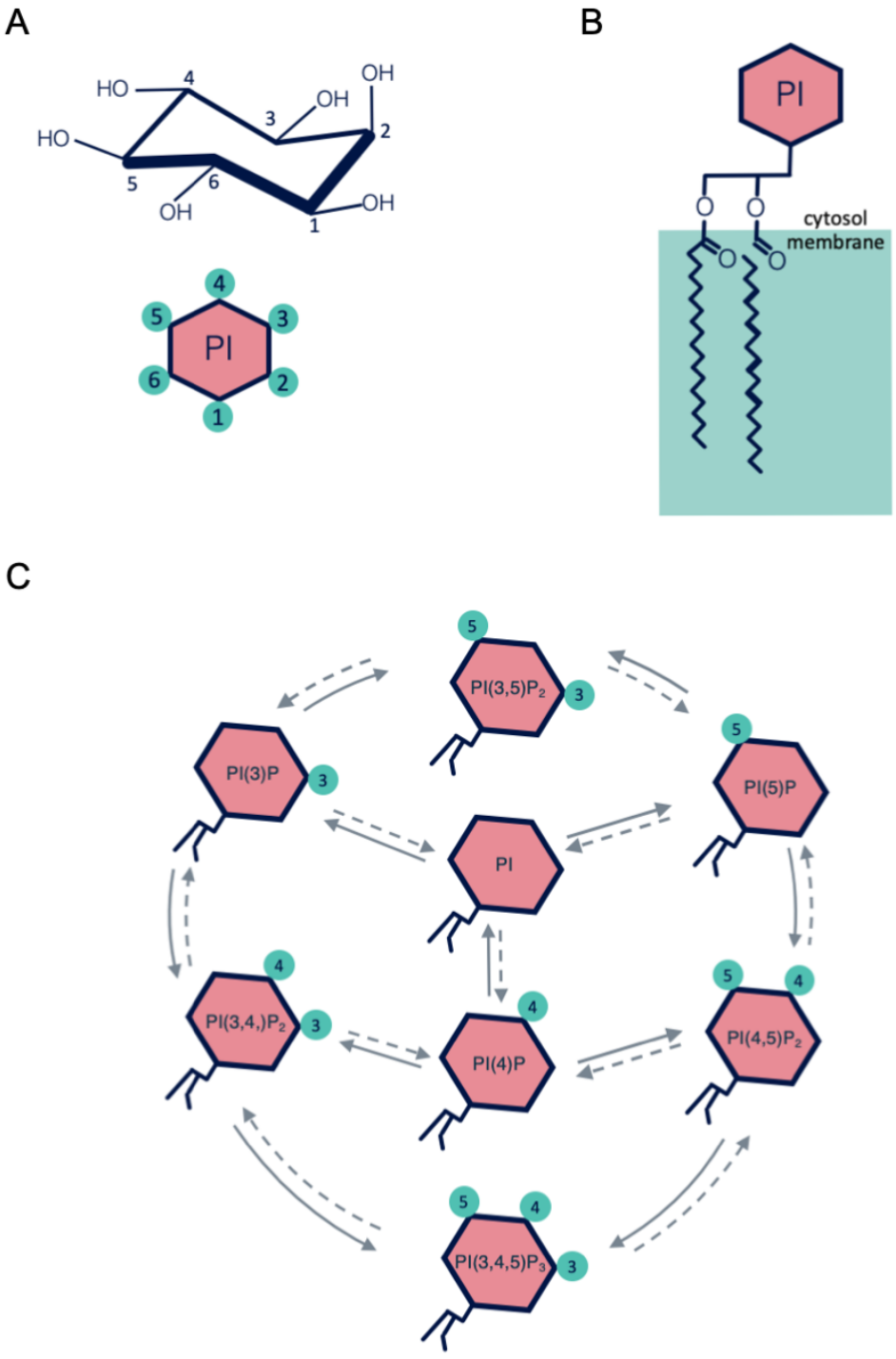
A
HO
4
OH
3
OH
2
HO
5
6
OH
OH
1
PI
B
PI
cytosol
membrane
C
PI(3,5)P2
PI(3)P
PI(5)P
PI
PI(3,4,)P2
PI(4)P
PI(4,5)P2
PI(3,4,5)P3

Figure 1.5. Phosphoinositide structure and cycle. (A) Structure of D-*myo*-inositol in the staggered chair conformation and simplified (below) with D carbons numbered. (B) Phosphatidylinositol consists of a membrane-embedded diacyl-glyceride moiety linked to a cytosolic inositol headgroup. (C) Reversible phosphorylation of the D3, D4, and D5 hydroxy groups yields seven phosphoinositides. Solid lines indicate kinase-mediated phosphorylation, and dashed lines indicate phosphatase-mediated hydrolysis.

Although they make up only about 10% of eukaryotic membrane lipid content, PIs mediate discrete cellular functions based on where they localize within cellular compartments. Dynamic changes and temporal enrichment of PIs at specific membrane domains results in a general distribution pattern throughout the cell. For example, PI(4,5)P_2, PI(3,4)P_2, and PI(3,4,5)P_3 enrichment occurs mainly at the plasma membrane, but PI(4,5)P_2 is also found with PI(4)P on recycling endosomes and in the trans-Golgi network. Early endosomes and autophagosomes contain PI(3)P while late endosomes and lysosomes contain PI(3,5,)P_2.

Depending upon the species, membrane location, and coincidence with other PI moieties, PIs generally participate in three roles: they (1) regulate integral membrane proteins like ion channels, (2) exist as substrates for PI-specific phospholipases that produce water-soluble inositol phosphates, and (3) localize to membranes as activation- or recruitment-sites for cytosolic proteins (Cullen, 2011). Proteins that interact with PIs harbor evolutionarily conserved low-affinity PI-binding motifs, such as PH (plekstrin homology), FYVE [Fab1, YOTB, Vac1, EEA1 (early endosomal antigen one)], and PX (phox homology), that function at enrichments-sites for their corresponding PI. In some cases, low-affinity binding properties are exponentially enhanced when PI binding proteins form oligomers, which provides an additional mode of spatiotemporal control to phosphoinositide conversion.

Dr. Mary Munson gave a helpful analogy during my first year of graduate school in her membrane trafficking lecture. Membrane identity is like a bar code system for a parcel-delivery service. The parcel's barcode determines its fate around the globe. Likewise, a membrane's phosphoinositide code determines its fate within the cell. Proteins with PI binding-domains scan membranes for their PI barcodes and direct a vesicle's course of action, often by further modifying the barcode. This system of checks and changes is critical for effective endolysosomal membrane dynamics.

Phosphoinositides in the endolysosomal system and autophagy

The endolysosomal system represents numerous intracellular membrane-compartments, including endosomes, recycling endosomes, late endosomes, and the lysosome. The autophagy pathway converges with the endolysosomal system at both late endosomes and lysosomes. Within the endosomal system, opposing forces carry out cargo degradation and retrieval. The endosomal sorting complex required for transport (ESCRT) machinery is well-characterized for its role in membrane scission and multivesicular body (MVB) biogenesis (Wollert et al., 2009). ESCRT proteins contain ubiquitin-binding domains that recognize those cargoes targeted for degradation. Conversely, cargo retrieval occurs when endosomal proteins are recycled this requires the retromer complex. Retromer is

best known for its roles in endosome-to-Golgi trafficking and endosomal protein sorting, but retromer also regulates cell polarity and cargo recognition.

Phosphoinositide conversion is critical in the endolysosomal system, and PI(3)P is the system's trademark PI. A majority of endosomal PI(3)P is generated by PI3KC3/VPS34, the same PI3K that functions in autophagy induction. Instead of ATG14L, UVRAG interacts with the Beclin 1-VPS34 complex where it regulates endosomal PI(3)P **(Fig. 1.6)**. Interestingly, the Beclin 1-VPS34 complex can further interact with Rubicon, which suppresses both autophagic and endocytic maturation and degradation (Matsunaga et al., 2009). Autophagosome formation and maturation also require PI(3)P. Generated by the Beclin 1-VPS34 complex during early autophagosome formation, PI(3)P recruits WIPI proteins which recruit the LC3 conjugation machinery **(Fig. 1.2)** to further promote autophagosome biogenesis. Later, PI(3)P is required to recruit factors that mediate autophagosome-lysosome fusion (Nakamura and Yoshimori, 2017).

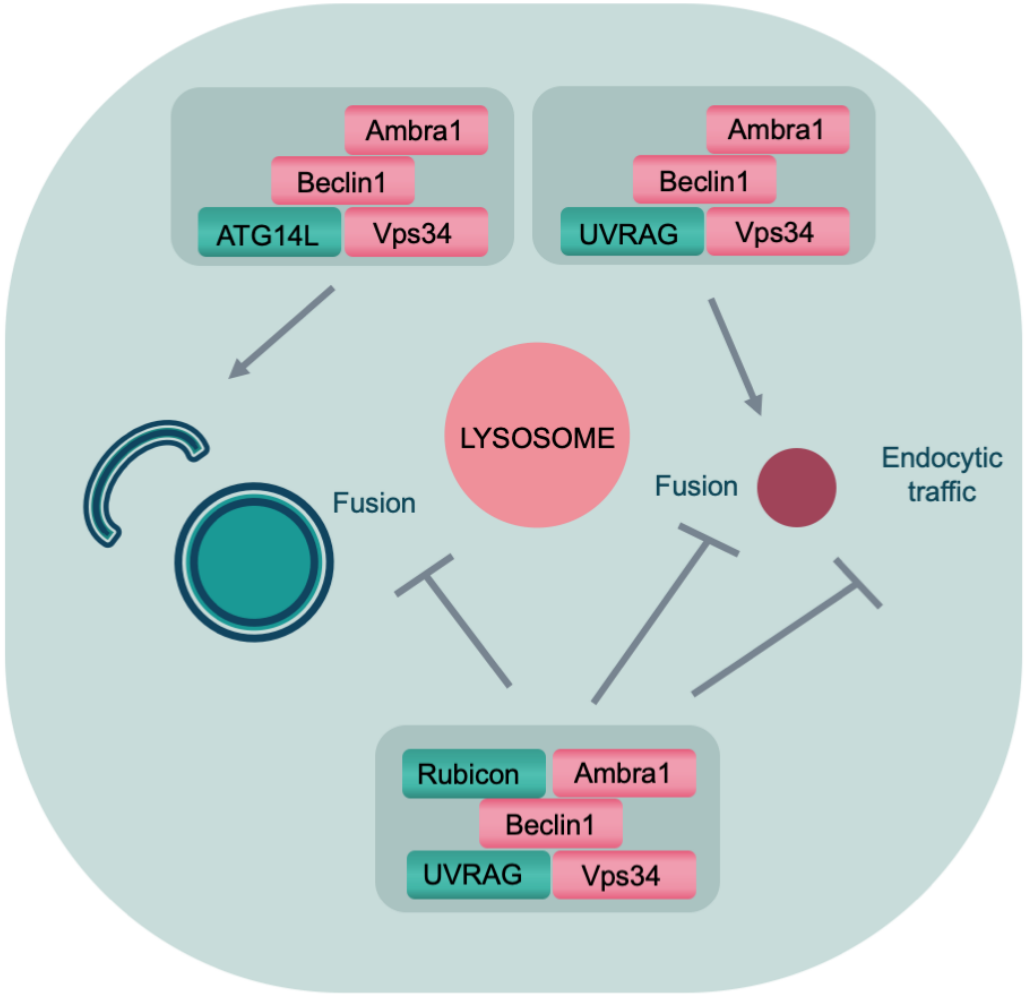

Figure 1.6. Beclin1-VPS34 complexes regulate the endolysosomal system. In mammals, the Atg14L complex functions in early autophagosome formation. The UVRAG complex functions in the endocytic pathway to promote endocytic traffic as well as late stage autophagy for autolysosome reformation. The Rubicon-UVRAG complex suppresses autophagy and prevents degradation in both the autophagic and endocytic pathways.

PI(3)P also promotes endolysosomal maturation. Here, PI(3)P is required for Rab7 activation, ESCRT recruitment, and microtubule-dependent translocation of late endosomes and lysosomes toward the cell periphery (Wallroth and Haucke, 2018). Conversion of PI(3)P to $PI(3,5)P_2$ by the PtdIns and PI(3)P 5-kinase PIKfyve, which binds PI(3)P by its FYVE domain, promotes further maturation. $PI(3,5)P_2$ is a low-level phosphoinositide that remains challenging to detect. Despite low levels, $PI(3,5)P_2$ is critical to cellular homeostasis because the loss of PIKfyve or either of its functional binding partners (scaffold protein, VAC14, and PI 5-phosphatase, FIG4) depletes $PI(3,5)P_2$, and significantly impairs endolysosomal function and autophagy (Wallroth and Haucke, 2018). Thus, endolysosomal function is exquisitely sensitive to the balance of phosphoinositide levels.

During autophagic degradation, lysosomal components are recycled into new lysosomes **(Fig. 1.7)**. Specifically, starvation leads to autolysosome reformation (ALR), in which tubules form, bud off, and give rise to lysosomes (Yu et al., 2010). Phosphoinositide conversion remains paramount for ALR. First, PI 4-kinase, PI4KIIIß phosphorylates PI to generate PI(4)P, and this promotes proper sorting of lysosomal components into tubules (Sridhar et al., 2013). The PI(4)P 5-kinase, PI4P5K1B, converts PI(4)P to $PI(4,5)P_2$ which is essential for tubulation from the autolysosome (Rong et al., 2012). Later, scission of proto-lysosomes from the tubules requires PI4P5K1A. Here, $PI(4,5)P_2$ generation leads to clathrin recruitment at tubules and tubule budding and recruitment of the motor protein KIF5B, which generates tubulation through a pulling force (Rong et al., 2012; Du

et al., 2016). Given their roles in virtually all aspects of the endolysosomal system, PIs remain a relevant and exciting research area in autophagy.

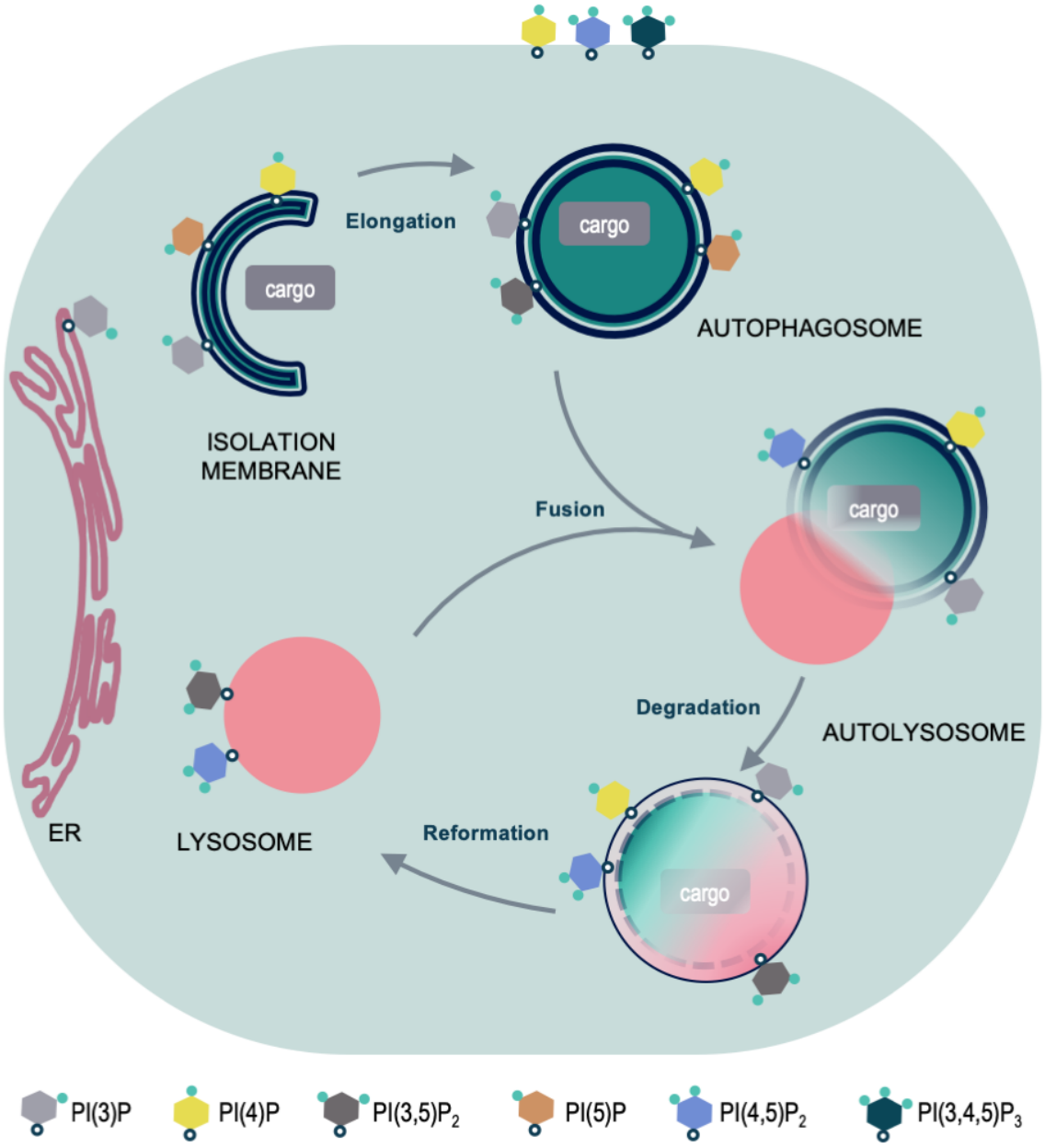

Figure 1.7. Phosphoinositides in autophagy. Phosphoinositides contribute to each step of autophagy, and discrete phospholipid pools demarcate the various autophagic organelles. ER, endoplasmic reticulum.

Myotubularin-related phosphoinositide phosphatases

Myotubularin-related phosphatases (MTMRs) are a conserved family **(Table 1.2)** of 3-phosphatases with specificity for PI(3)P and PI(3,5)P_2. The 14 *MTMR* gene family members are further divided into six subfamilies, each having a single putative *Drosophila* counterpart. Meanwhile, the *C. elegans* family of *MTMRs* lacks both *MTMR10* and *MTMR14* family members, and mice lack *MTMR8.* Interestingly, Zebrafish have additional *MTMR1* and *MTMR7* orthologs.

Table 1.2. Model organism orthologs of myotubularin-related phosphatases

Human	Fly	Worm	Mouse	Zebrafish	
MTM1	*Mtm*	*mtm-1*	*Mtm1*	*mtm1*	
MTMR1			*Mtmr1*	*mtmr1a*	*mtmr1b*
MTMR2			*Mtmr2*	*mtmr2*	
MTMR3	*CG3632/Mtmr3*	*mtm-3*	*Mtmr3*	*mtmr3*	
MTMR4			*Mtmr4*	*mtmr4*	
MTMR6	*CG3530/Mtmr6*	*mtm-6*	*Mtmr6*	*mtmr6*	
MTMR7			*Mtmr7*	*mtmr7a*	*mtmr7b*
MTMR8			-	*mtmr8*	
MTMR9	*CG5062/Mtmr9*	*mtm-9*	*Mtmr9*	*mtmr9*	
MTMR10	*CG14411/Mtmr10*	-	*Mtmr10*	*mtmr10*	
MTMR11		-	*Mtmr11*	*mtmr11*	
MTMR12		-	*Mtmr12*	*mtmr12*	
MTMR5/SBF1	*Sbf*	*mtm-5*	*Sbf1*	*sbf1*	
MTMR13/SBF2			*Sbf2*	*sbf2*	
MTMR14/Jumpy	*Mtmr14/EDTP*	-	*Mtmr14*	*mtmr14*	

The human MTMR protein family members share a common structural core that consists of a PH-GRAM domain, a catalytic phosphatase domain, and a coiled-coil domain **(Fig. 1.8)**. Further division into subfamilies, yields additional conserved regions such as DENN, FYVE, PDZ-binding, and PH domains. Included in both **Table 1.2** and **Figure 1.8** is MTMR14/Jumpy, which contains the conserved catalytic phosphatase domain, but lacks both the PH-GRAM and coiled-coiled (CC) domains. Thus, Jumpy is not considered a *bona fide* MTMR by the field. Among the other 14 MTMR proteins, eight possess catalytic activity towards PI(3)P and PI(3,5)P_2 (MTM1, MTMR1-4, and MTMR6-8), and the remaining seven are catalytically inactive. The conserved active site *Cys-X_5-Arg* motif, which is a characteristic of protein tyrosine phosphatases, is inherently altered in the inactive family members. However, inactive MTMRs heterodimerize specifically with catalytically active family members via the CC-domain and regulate their stability, substrate specificity, and localization (Laporte et al., 2003). Similarly, some active MTMRs homodimerize via the CC-domain, but that MTMR3- and MTMR4-CC-domain mutants can homo- and heterodimerize suggests that these family members interact through another interface (Lorenzo et al., 2006).

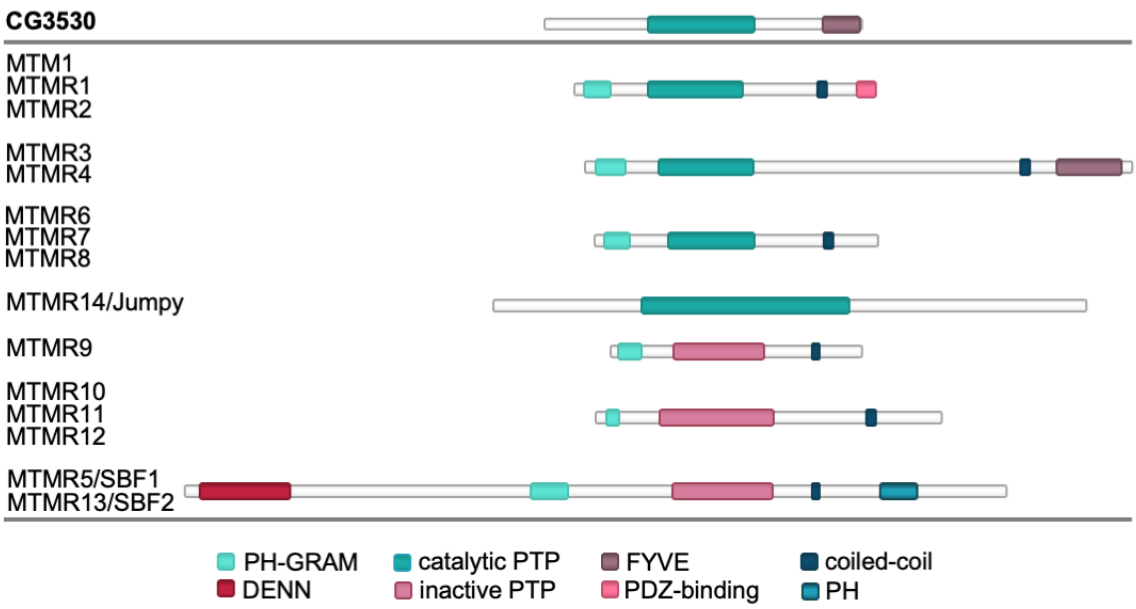

Figure 1.8 Structural organization of myotubularin-related phosphatases. A scaled representation of the human myotubularin protein family, *Drosophila* CG3530 (top), and MTMR14/Jumpy, with their conserved domains. The MTMR family is further grouped into six subfamilies, but MTMR14/Jumpy, though show here, is not universally accepted as a MTMR family member because it lacks a PH-GRAM domain.

MTMRs in the endolysosomal pathway and autophagy

Historically, MTMRs have been studied in terms of their relationship to human disease (detailed below). While these analyses identified important mechanisms underlying the function of MTMRs in the endolysosomal system, most research remained focused on MTM1, MTMR1, and MTMR2.

Recently MTMR4 was shown to play a role in macrophage phagocytosis and phagosome maturation. MTMR4, which contains a FYVE domain, facilitates phagosomal PI(3)P turnover (Sheffield et al., 2019). In this setting, *MTMR4* overexpression reduced actin protrusion formation and impaired phagocytosis, while *MTMR4* depletion expedited phagosome maturation. By live imaging, the authors showed YFP-MTMR4 transiently localized to PI(3)P-enriched phagophore sites, and shortly thereafter, the PI(3)P reporter signal declined, coinciding with decline of YFP-MTMR4. In a human lung cancer cell line, MTMR4 localized to and regulated PI(3)P on late endosomes and autophagosomes (Pham et al., 2018). *MTMR4*-knockdown resulted in enlarged early endosomes and impaired endosome maturation and the formation of late endosomes, lysosomes, autophagosomes, and autolysosomes. Moreover, despite an appropriate decrease in mTORC1 activity following starvation, *MTMR4*-knockdown impaired starvation-induced nuclear localization of TFEB, which is a transcription factor that promotes autophagy and lysosome biogenesis.

In C*. elegans*, MTM-3 promotes autophagosome maturation into lysosomes by degrading late autophagosomal PI(3)P pools (Wu et al., 2014). Similarly, human MTMR3 negatively regulates autophagy, suppresses autophagosome enlargement, but lacks a role in degradation (Taguchi-Atarashi et al., 2010). Interestingly, MTMR3 interacts with mTORC1, and MTMR3-overexpression inhibits mTORC1 activity, dependent upon both the PH-GRAM and phosphatase domains (Hao et al., 2016). Furthermore, the PH-GRAM, but not the FYVE domain was required for PI(3)P binding by MTMR3.

MTMR8 was also implicated in autophagy (Zou et al., 2012a; b). Largely focusing on the biochemical aspects of interactions between MTMR8 and its inactive binding partner, MTMR9, the authors demonstrated MTMR8 substrate specificity toward PI(3)P. Of note, MTMR8 could degrade both PI(3)P and PI(3,5)P_2. They further showed that starvation promotes MTMR8-MTMR9 dissociation. Further, they showed that on its own, *MTMR8*-knockdown or -misexpression had little effect of autophagy, but when *MTMR8* and *MTMR9* were co-depleted, or misexpressed together, autophagy was influenced. They showed that co-depletion of *MTMR8* and *MTMR9* resulted in WIPI-1 puncta formation and a reduction in p62 protein levels. Meanwhile, misexpression of both *MTMR8* and *MTMR9* impaired WIPI-1 puncta formation and increased p62 protein levels. While these data indicate that MTMR8 and MTMR9 functionally regulate aspects of autophagy, they lack analyses of important autophagy markers like LC3B.

Myotubularin-related proteins and human disease

The MTMR family features several human disease-related genes (Raess et al., 2017b). Specifically, three cause monogenic disorders. *MTM1* mutations cause X-linked centronuclear myopathy (myotubular myopathy, OMIM: 310400), which features hypotonia at birth, muscle weakness, respiratory distress, and the inability to move the eyes and eyebrows (Laporte et al., 1996). *MTMR2* mutations cause Charcot-Marie-Tooth (CMT) neuropathy type 4B1 (CMT4B1, OMIM: 601382), and mutant *MTMR13/SBF2*, an inactive family member, causes CMT4B2 (Azzedine et al., 2003; Bolino et al., 2004; Senderek et al., 2003). Both types of CMT are autosomal recessive demyelinating neuropathies that affect peripheral nerves and promote muscular atrophy with distal limb weakness. Interestingly, a rare form of X-linked spastic paraplegia (SPG16, OMIM: 300266) has been mapped to Xq11.2, which is at the *MTMR8* locus (Steinmuller et al., 1997; Tamagaki et al., 2000). While we lack a direct link between *MTMR8* and SPG16, it should be noted that similarities exist between SPG16 disease symptoms and the diseases described above that are caused by MTMR family-member mutations. Indeed, SPG16 only affects males and in addition to intellectual disability, is characterized by deficiencies in the peripheral nervous system and musculature. SPG16 patients often present with delayed motor development, spasticity, and progressive ataxia that affects speech, eyesight, and bladder and bowel function. With better access to genome exome sequencing, we may see a direct connection between MTMR8 and SPG16 in the future.

Several MTMRs are connected to multifactorial diseases, including cancers. When compared to adjacent, healthy tissue, patient breast tumor samples contained elevated MTMR3 protein levels, and high *MTMR3* gene expression levels correlated with poor survival and relapse (Wang et al., 2019b). Triple-negative breast cancer cells expressed higher levels of MTMR3 protein than other breast cancer cells. Further, *MTMR3*-knockdown in triple negative breast cancer cells reduced cell proliferation and induced autophagy and cell death. Indeed, PI(5)P production by either MTMR3-mediated PI(3,5)P_2 hydrolysis or PIKfyve-mediated PI phosphorylation promotes cell motility in both fibroblasts and cancer cell lines (lung, rhabdomyosarcoma, and osteosarcoma) as well as a *Drosophila* model of cell migration (Oppelt et al., 2014, 2013). Conversely, *MTMR3*-depletion in gastric cancer cells increased proliferation, migration, and invasion, and induced autophagy (Lin et al., 2017b). Despite opposite effects in different cancer cell types, these data are consistent with the idea that autophagy has dual roles in cancer. Like MTMR3 expression in breast cancer, high MTMR6 expression was associated with ovarian cancer, and *MTMR6*-depletion in ovarian cancer cells reduced cell proliferation and enhanced cell death (Wang et al., 2019a). Future studies should address how MTMR6 might promote ovarian cancer cell growth and proliferation. Also linked to cancer, low MTMR7 expression levels in stromal tissues, but not the tumor correlated with colorectal cancer disease severity (Weidner et al., 2016). In patients, decreased MTMR7 protein expression in the stroma correlated with tumor grade, size, and stage, as well as poor prognosis.

Indeed, stromal cells in patients with benign tumors had high MTMR7 expression. Further, loss of MTMR7 protein expression occurred most often in patients with either type 2 diabetes mellitus or insulin-like growth factor 2 (*IGF2)* loss of imprinting, an effect that typically results in increased IGF2 signaling and growth. In colorectal cancer cell lines, MTMR7 expression reduced cellular PI(3)P levels and inhibited growth and proliferation signaling downstream of IGF2. This suggests, that the loss of MTMR7 in colorectal cancer patients could promote growth through the tumor microenvironment. Future studies should address the potential role of MTMRs in tumor-stromal crosstalk.

Metabolic syndrome is associated with an increased risk for type 2 diabetes mellitus and cardiovascular disease (Wilson et al., 2005). Clinically, symptoms include obesity, glucose intolerance, hypertension, and dyslipidemia, and both genetic and environmental factors contribute to disease development and progression. Interestingly, single nucleotide polymorphisms (SNPs) in *MTMR9* conferred susceptibility to elevated visceral fat levels and obesity in a Japanese population with metabolic syndrome. Interestingly, MTMR9 plays a role in macropinocytosis, a cellular process in which actin drives the plasma to internalize large amounts of extracellular fluid and solutes (Maekawa et al., 2014). While speculative, *MTMR9* deficiencies in metabolic disorder could be a result of impaired cellular uptake in adipose tissue and subsequent lipid storage. Further investigations should address how MTMR9 could promote metabolic syndrome

and test if macropinocytosis is impaired in adipose tissue from *MTMR9*-deficient metabolic syndrome patients.

Transmissible disease susceptibility and infection are also linked to MTMRs. Variant Creutzfeldt-Jakob disease (vCJD) is a lethal disease that is primarily caused by dietary exposure to bovine spongiform encephalopathy agent and manifests as prion accumulation in body tissues, including brain. Patients suffer from rapidly progressive neurodegeneration. Because the disease manifested in a small number of people relative to mass exposures, it was thought that genetic variation might underlie susceptibility (Sanchez-Juan et al., 2012). Indeed, a specific, SNP in *MTMR7*, was identified as a risk factor for vCJD following genome-wide association studies. Given that *MTMR7* expression is enriched in brain tissues (Raess et al., 2017b), future studies should address how the vCJD-specific SNP in *MTMR7* promotes disease susceptibility.

Immunodeficiency viruses are known to replicate and disseminate rapidly in the gastrointestinal tract. Simian immunodeficiency virus (SIV) is commonly accepted as the retrovirus that gave rise to human immunodeficiency virus (HIV). In an effort to identify regulatory factors that promote SIV infection in the intestine, *MTMR6* mRNA transcripts were identified as significantly reduced during the peak viral replication period (Mohan et al., 2014). In addition to viral replication and dissemination, intestinal $CD4^+$ T cell depletion occurs during SIV infection. T cell activation relies upon increases in intracellular Ca^{2+} levels, and this process is mediated by K^+ channels. Interestingly, the Ca^{2+}-activated K^+ channel, KCa3.1 is

activated by PI(3)P and negatively regulated by MTMR6 (Srivastava et al., 2006). Furthermore, *MTMR6*-overexpression impairs CD4+ T cell proliferation, which further supports the idea that *MTMR6* expression promotes SIV infection mechanisms.

While MTMRs are associated with human disorders, they are largely understudied. Compared to PTEN, a phosphoinositide phosphatase and tumor suppressor gene that is mutated frequently in a large number of cancers, little research has been done on MTMRs **(Fig. 1.9 A)**. Very few MTMRs appear to be disease-drivers, but as introduced above, MTMRs underlie processes that contribute to disease progression. Furthermore, a clear link between MTMRs, autophagy, and cancer exists. As mentioned in Part I of this introduction, tissue in *Drosophila* undergo autophagy, thus providing an *in vivo* system in which to study autophagy. Similar to humans, *Drosophila* Mtmrs remain understudied **(Fig. 1.9 B)**. By using *Drosophila* tissues that undergo autophagy, research could uncover additional regulatory roles for myotubularins and new mechanisms that underlie disease.

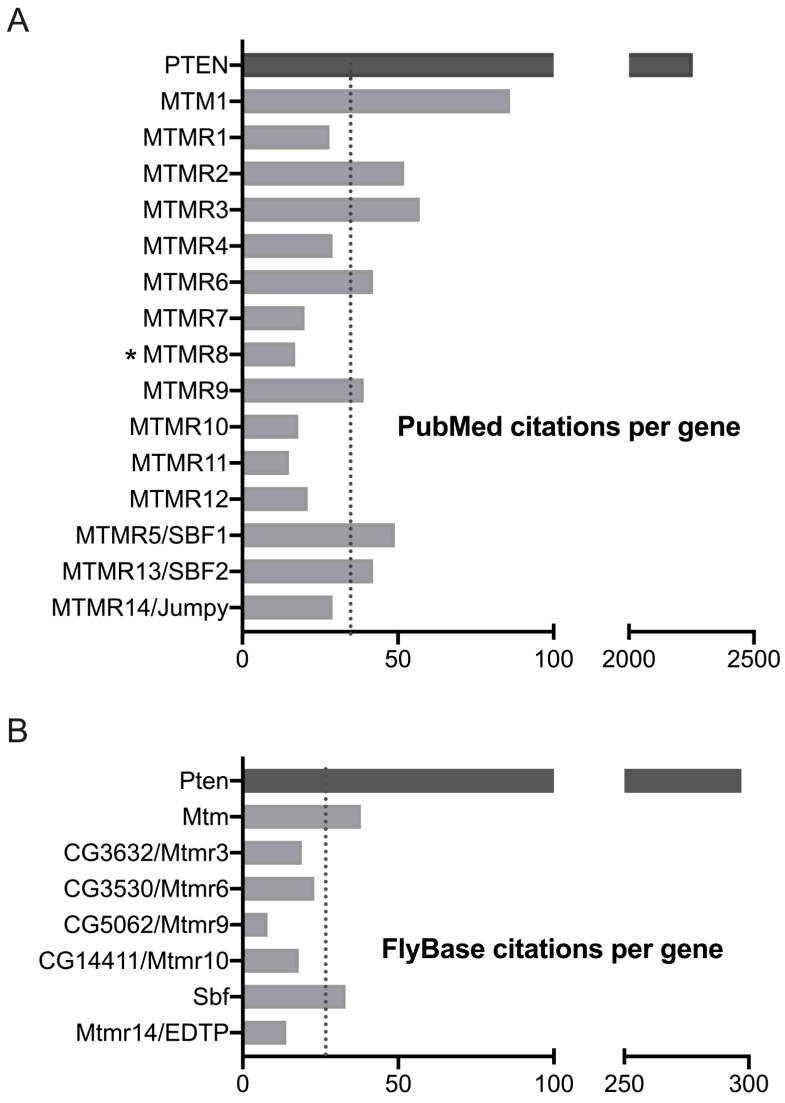

Fig. 1.9. Publication number per gene. Number of publications, including research and review articles, for the indicated human or fly gene listed on PubMed (A) and FlyBase (B), respectively. A notable phosphoinositide phosphatase, the tumor suppressor PTEN is included for comparison.

Thesis rationale

Myotubularin-related phosphatases occupy various roles across endolysosomal and autophagic membranes. However, we lack a complete understanding of the role for MTMRs in autophagy, and *in vivo* analyses remain limited. In response to nutritional and developmental cues, several *Drosophila* tissues undergo autophagy, offering multiple experimental systems in a single animal and a platform in which we can interrogate the role of MTMRs in autophagy. I identified *CG3530* as novel regulator of autophagy in the *Drosophila* larval midgut during an *in vivo* RNAi phosphatome screen. This uncharacterized gene is an ortholog of the human MTMR6, MTMR7 and MTMR8 subfamily, the latter of which has a reported, but largely unexplored role in autophagy. For my thesis project, I sought to define the role of *CG3530* and its human counterpart, MTMR8 in autophagy using a combination of *in vivo* and cell culture analyses. Given that *CG3530*-depletion enhanced our autophagy-reporter signal, it was important to assess whether its function was to inhibit autophagosome biogenesis or promote autolysosome degeneration. It was also important to determine if *CG3530* functions in other membrane-mediated degradation processes, such as endo- and phagocytosis. By comparing and understanding CG3530 and MTMR8 functions, this dissertation aims to

advance our understanding of how myotubularin-related proteins contribute to autophagy.

CHAPTER II

A conserved myotubularin-related phosphatase regulates autophagy by maintaining autophagic flux

Elizabeth A. Allen[1], Clelia Amato[2], Tina Fortier[1], Panagiotis Velentzas[1], Will Wood[2] and Eric H. Baehrecke[1,*]

[1]Department of Molecular, Cell, and Cancer Biology, 423 Lazare Research Building, 364 Plantation St., University of Massachusetts Medical School, Worcester, MA 01655, USA

[2]Centre for Inflammation Research, The Queen's Medical Research Institute, University of Edinburgh, 47 Little France Crescent, Edinburgh, EH16 4TJ, UK

Contribution Summary

E. Allen and E.H. Baehrecke conceptualized the experiments. E. Allen performed and analyzed most of the experiments. C. Amato performed and analyzed macrophage phagocytosis in embryos, T. Fortier performed TEM, and P.V. performed *Vps34* and *Atg9* epistasis in fat body. E. Allen wrote the original manuscript with contributions from the other authors.

ABSTRACT

Macroautophagy (autophagy) targets cytoplasmic cargoes to the lysosome for degradation. Like all vesicle trafficking, autophagy relies on phosphoinositide identity, concentration and localization to execute multiple steps in this catabolic process. Here we screen for phosphoinositide phosphatases that influence autophagy in *Drosophila*, and identify *CG3530*. CG3530 is homologous to the human MTMR6 subfamily of myotubularin-related 3-phosphatases, and therefore we named it dMtmr6. dMtmr6, which is required for development and viability in *Drosophila*, functions as a regulator of autophagic flux in multiple *Drosophila* cell types. The MTMR6 family member *MTMR8* has a similar function in autophagy of higher animal cells. Decreased *dMtmr6* and *MTMR8* function results in autophagic vesicle accumulation and influences endolysosomal homeostasis.

INTRODUCTION

Cells rely on macroautophagy (hereafter autophagy) to deliver sequestered cytoplasmic cargoes to lysosomes for degradation. Basal autophagy levels maintain cellular homeostasis, and activated autophagy mitigates several cellular stresses, including nutrient deprivation. Autophagy begins with the formation of an isolation membrane that elongates and encloses cargoes to eventually form a closed double-membrane autophagosome that fuses with lysosomes to become an autolysosome (Yu et al., 2018a). Lysosomal enzymes, including cathepsins, breakdown autophagic cargoes into macromolecules, which are later effluxed into the cytoplasm for use in anabolic cellular processes. Pioneering yeast experiments defined the core autophagic molecular mechanisms (Tsukada and Ohsumi, 1993). However, metazoans such as *Drosophila melanogaster* possess an enhanced repertoire of autophagic machinery beyond those required in yeast, thus providing a multicellular *in vivo* experimental system to study autophagy (Mulakkal et al., 2014; Zhang and Baehrecke, 2015).

From initiation to completion, autophagy is regulated by over 30 conserved core autophagy-related (Atg/ATG) proteins (Galluzzi et al., 2017). Autophagy initiation and autophagosome biogenesis require the Atg1/ULK1 serine/threonine kinase complex, the vacuolar protein sorting (Vps34) class III phosphoinositide 3-kinase complex, and the Atg8 conjugation system. Autophagosome-lysosome

fusion utilizes dozens of proteins, including many shared with the endocytic pathway and the autophagosomal SNARE protein Syntaxin 17 (Takáts et al., 2013; Itakura et al., 2012). When lysosomal enzymes complete autophagic cargo degradation, then autolysosome reformation (ALR) contributes to regeneration of the lysosomal pool, which further promotes homeostasis (Yu et al., 2010). Both excessive and insufficient autophagy can promote disease by dysregulating autophagic flux, a term which describes the quantity of autophagic degradation (Dowling et al., 2015; Levine and Kroemer, 2019; Yoshii and Mizushima, 2017), making rate-control a key component to each step of autophagy.

Vesicular membrane-identity and -trafficking rely largely upon phosphoinositide (PI) identity, concentration, and coincidence (Schink et al., 2016). PI kinases and phosphatases can switch the 3-, 4-, and 5- hydroxyl group phosphates of the inositol ring to generate seven distinct cellular PIs. Membrane-embedded PIs recruit effectors to control membrane dynamics via multiple mechanisms, including membrane-fusion, -scission, and -shaping. In the endolysosomal system, PI(3)P is the major PI species on endosomes following PI conversion from PI(4,5)P_2, which is required for endocytosis (Wallroth and Haucke, 2018). Recycling endosomes rely on a PI(3)P loss (Campa et al., 2018) and PI(4)P gain (Ketel et al., 2016), while degradative PI(3)P-positive endosomes require PI(3,5)P_2 production by the PI(3)P 5-kinase PIKFYVE for ESCRT-III recruitment and delivery to multi-vesicular bodies (MVBs) (Kim et al., 2014; Hasegawa et al., 2017). Similar PI conversion events occur during uptake and degradation of either

extracellular fluids or particles by macropinocytosis or phagocytosis respectively (Zoncu et al., 2009), and phagosome maturation coincides with PI(3)P reduction (Levin et al., 2015). Likewise, autophagy progression from start to finish relies upon phosphoinositide identity changes. Autophagy initiation requires recruitment of the class III PI3K complex I to pre-autophagosomal structures (Funderburk et al., 2010), which results in PI(3)P production and recruitment of autophagosome-forming effectors (Lystad and Simonsen, 2016). Meanwhile, autophagosome-lysosome fusion requires multiple PI conversion events. For example, fusion requires production of PI(4)P at autophagosomes by PIK4IIα (Wang et al., 2015), as well as lysosomal PI(3,5)P_2 synthesis by PIKFYVE (De Lartigue et al., 2009) and hydrolysis by INPP5E (Hasegawa et al., 2016). After fusion, a transient PIP5K-mediated PI(4,5)P_2 increase on the lysosomal surface recruits clathrin machinery (Rong et al., 2012), which is followed by OCRL-mediated PI(4,5)P_2 turnover to PI(4)P for autophagic lysosome reformation (De Leo et al., 2016).

Both PI(3)P and PI(3,5)P_2 facilitate degradative membrane-driven cellular processes. Thus, as described above, enzymes that catalyze their synthesis or turnover play critical roles in trafficking membrane-bound cargoes to the lysosome. Myotubularin-related phosphatases (MTMRs) are a conserved family of 3-phosphoinositide phosphatases that are associated with diseases (Raess et al., 2017b) and regulate membrane trafficking during endocytosis and autophagy (Nicot and Laporte, 2008; Robinson and Dixon, 2006). Of the 16 human MTMRs, 9 contain the catalytically active CX_5R motif, and 7 are catalytically dead pseudo-

phosphatases due to a cysteine residue substitution. The MTMR family of enzymes are grouped into subfamilies, and the *Drosophila* genome harbors a single ortholog in each subfamily. One human MTMR subfamily consists of human MTMR6, MTMR7, and MTMR8. These all partner with MTMR9, an inactive pseudophosphatase which fails to bind PIs on its own (Zou et al., 2012b) but enhances substrate binding, catalytic activity, and protein stability of its active partners *in vitro* and in cells (Zou et al., 2009a, 2012b).

Here we identify *CG3530/dMtmr6* as a regulator of autophagy in *Drosophila*. We reveal that dMtmr6, which is homologous to the human MTMR6 subfamily of myotubularin-related 3-phosphatases, functions as an essential regulator of autophagic flux in multiple cell types and is required for *Drosophila* development. Downregulation of *dMtmr6* leads to autophagic vesicle accumulation, promotes lysosome biogenesis, and impairs both endocytosis and phagocytosis. Importantly, we show that MTMR8 has similar function in autophagy in higher animal cells. This work establishes dMtmr6 as an essential regulator of autophagic flux.

RESULTS

Drosophila CG3530/dMtmr6 negatively regulates Atg8a puncta formation and is essential for survival and development

Enzymes that regulate autophagy represent potential drug targets for human disorders (Rubinsztein et al., 2012), and and cycles of phosphorylation and dephosphorylation provide regulatory cues for autophagy and other cellular processes. However, the phosphatases that regulate autophagy remain largely unexplored. We sought to identify novel phosphatases that regulate autophagy by screening the *Drosophila* phosphoinositide phosphatases because of their links to membrane trafficking and autophagy. We used the FLP/FRT system (Golic and Lindquist, 1989; Theodosiou and Xu, 1998) to simultaneously express GFP and RNAi that target phosphatases in clones of cells within tissues that uniformly express the autophagy reporter mCherry-Atg8a.

Drosophila larval intestine enterocytes contain pmCherry-Atg8a puncta two hours after puparium formation (2 h APF) due to high levels of developmental autophagy (Denton et al., 2009). Therefore, we evaluated the effects of phosphoinositide phosphatase-RNAi on pmCherry-Atg8a expression in 2 h APF midguts (Appendix A). We identified multiple previously described regulators of autophagy, such as PTEN (not shown), as well as *CG3530/Mtmr6* (*dMtmr6* hereafter), a previously undescribed negative regulator of autophagy. Expression

of double-stranded RNA (dsRNA) targeting *dMtmr6* generates cells that contain Atg8a puncta in feeding third instar larvae (L3) when autophagy remains inactive in neighboring wild-type cells **(Fig. 1 A and B)**. At 2 h APF, *dMtmr6*-knockdown enterocytes contain both increased and enlarged pmCherry-Atg8a puncta compared to neighboring wild-type cells **(Fig. 1 B-D)**.

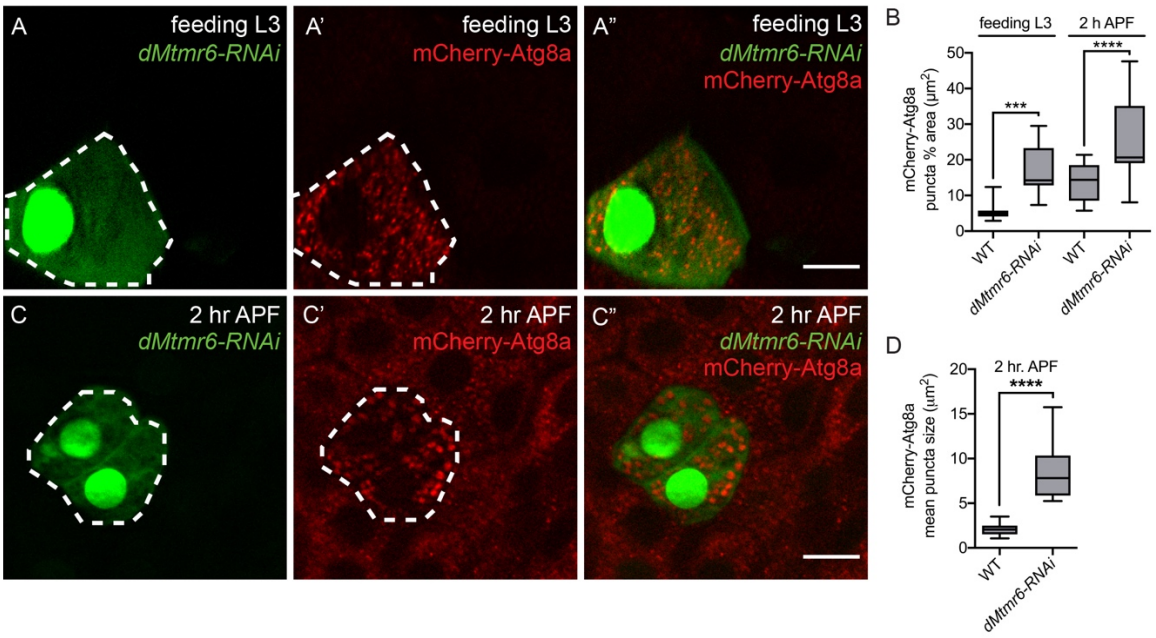

Figure 2.1. *Drosophila* CG3530/dMtmr6 negatively regulates midgut Atg8a puncta formation. (A) Control (GFP-negative) and d*Mtmr6* knockdown cells (white dotted line, green) from midguts expressing pmCherry-Atg8a during feeding L3 larval stage. (B) Quantification of pmCherry-Atg8a puncta levels in wild-type (WT) control cells and d*Mtmr6* knockdown cells of midguts from feeding L3 larvae and 2 h APF pupae. (C) Control (GFP-negative) and d*Mtmr6* knockdown cells (white dotted line, green) from midguts expressing pmCherry-Atg8a during developmental autophagy (bottom) occurring 2 hours after puparium formation (APF). (D) Quantification of pmCherry-Atg8a puncta size in WT and d*Mtmr6* knockdown cells from 2 h APF midguts. Data information: in (B and D), data are presented as mean ± min to max (n ≥ 10). Asterisks denote statistical significance (***P < 0.001 and ****P < 0.0001, using paired t test). Scale bars, 20 μm.

We sought to determine if *dMtmr6* regulates autophagy either specifically in larval intestine developmental autophagy or more broadly in multiple cell contexts, including stress-induced autophagy following nutrient deprivation. Therefore, we investigated if *dMtmr6* functions in amino acid starvation-induced autophagy in the *Drosophila* larval fat body (Scott et al., 2004). We examined fat body tissue from either fed third instar larvae that lack autophagy, or animals grown on 20% sucrose under nutrient restriction conditions for 4 hours to induce autophagy. As in midguts of the intestine, *dMtmr6* knockdown cells contain Atg8a puncta in fed larvae, and Atg8a puncta are significantly larger in *dMtmr6* knockdown cells compared to adjacent wild-type cells from starved larvae **(Fig. 2.2 A-D)**. These data indicate that *dMtmr6* functions in both developmental and starvation-induced autophagy in *Drosophila*.

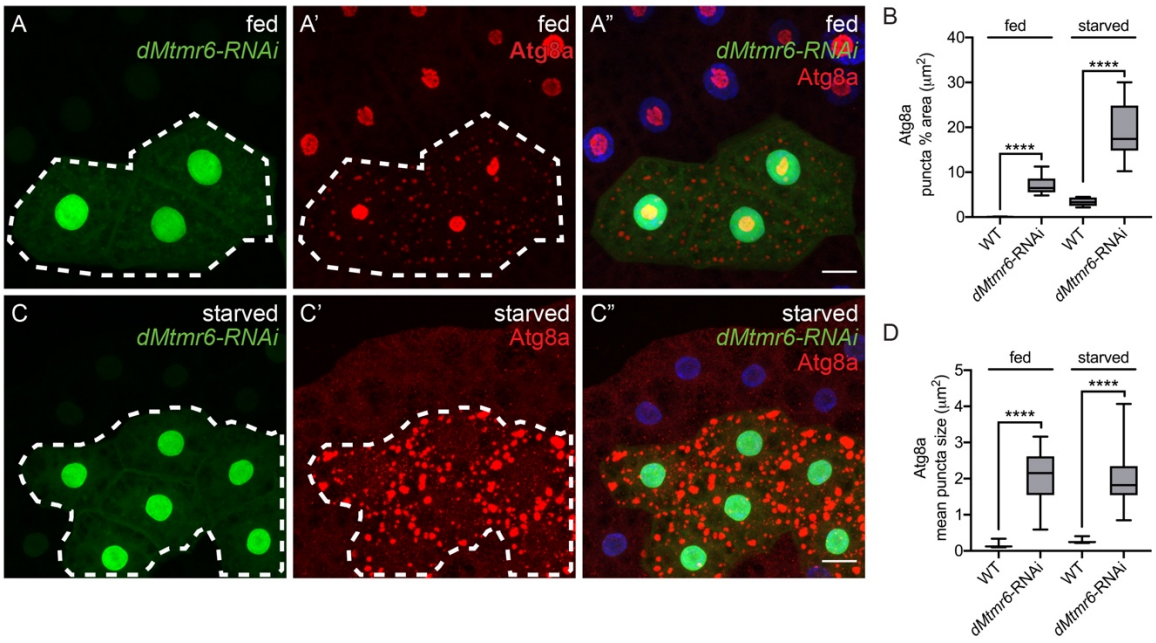

Figure 2.2. *Drosophila* CG3530/dMtmr6 negatively regulates fat body Atg8a puncta formation. (A) Larval *Drosophila* fat body with control (GFP-negative) and d*Mtmr6* knockdown cells (white dotted line, green) stained with an antibody to detect Atg8a and Hoechst to detect nuclei (blue) from fed animals. (B) Quantification of percent area of cell occupied by Atg8a puncta in WT and d*Mtmr6* knockdown cells of L3 fat body from fed or starved animals. (C) Larval *Drosophila* fat body with control (GFP-negative) and d*Mtmr6* knockdown cells (white dotted line, green) stained with an antibody to detect Atg8a and Hoechst to detect nuclei (blue) from starved animals. (D) Quantification of Atg8a puncta size in WT and d*Mtmr6* knockdown cells of L3 fat body from fed or starved animals. Data information: in (B and D), data are presented as mean ± min to max (n ≥ 10). Asterisks denote statistical significance (****P < 0.0001, using paired t test). Scale bars, 20 µm.

To better understand the function of *dMtmr6*, we deleted the *dMtmr6* open reading frame using CRISPR/Cas9 **(Fig. 2.3 A)**. Knockdown of *dMtmr6* in all tissues using both strong and weak RNAi strains results in lethality at either the early larval stage or early pupal stage, respectively **(Fig. 2.3 B)**. Importantly, homozygous loss of *dMtmr6* (*dMtmr6Δ/Δ*) is larval lethal, as is *dMtmr6Δ/Df* **(Fig. 2.3 B)**. However, some trans heterozygous mutant animals (*dMtmr6Δ/dMtmr6*^{KG01267}) survive until adult stage; *dMtmr6*^{KG01267} is a mutant allele made by P-element insertion in the 5' UTR of the *dMtmr6* B and C isoforms but not A **(Fig. 2.3 A)**, which suggests that the P-element insertion is a weak allele. To evaluate the effects of *dMtmr6* loss on autophagy, we measured protein levels from whole larvae (feeding L3). Trans-heterozygous *dMtmr6Δ/KG* and *dMtmr6Δ/Df* animals have increased levels of the cargo receptor ref(2)p (p62 in mammals) and lipidated Atg8a compared to control heterozygous animals lacking one allele of either the null *dMtmr6Δ* or weak allele *dMtmr6*^{KG01267} **(Fig. 2.3 C-C")**. We then used the FLP/FRT system to generate homozygous *dMtmr6* null mutant cell clones within wild-type tissue. As with *dMtmr6*-RNAi, *dMtmr6*-knockout results in increased amounts of Atg8a in feeding larval midguts **(Fig. 2.3 D-D')**. However, we obtain significantly fewer *dMtmr6Δ*-null mutant cell clones than control cell clones in both the midgut and fat body **(Fig. 2.3 E)**, suggesting that homozygous loss of *dMtmr6Δ* compromises cell viability. These data suggest that *dMtmr6* regulates autophagy and is critical for *Drosophila* development, and that at least in some contexts *dMtmr6* is required for cell viability.

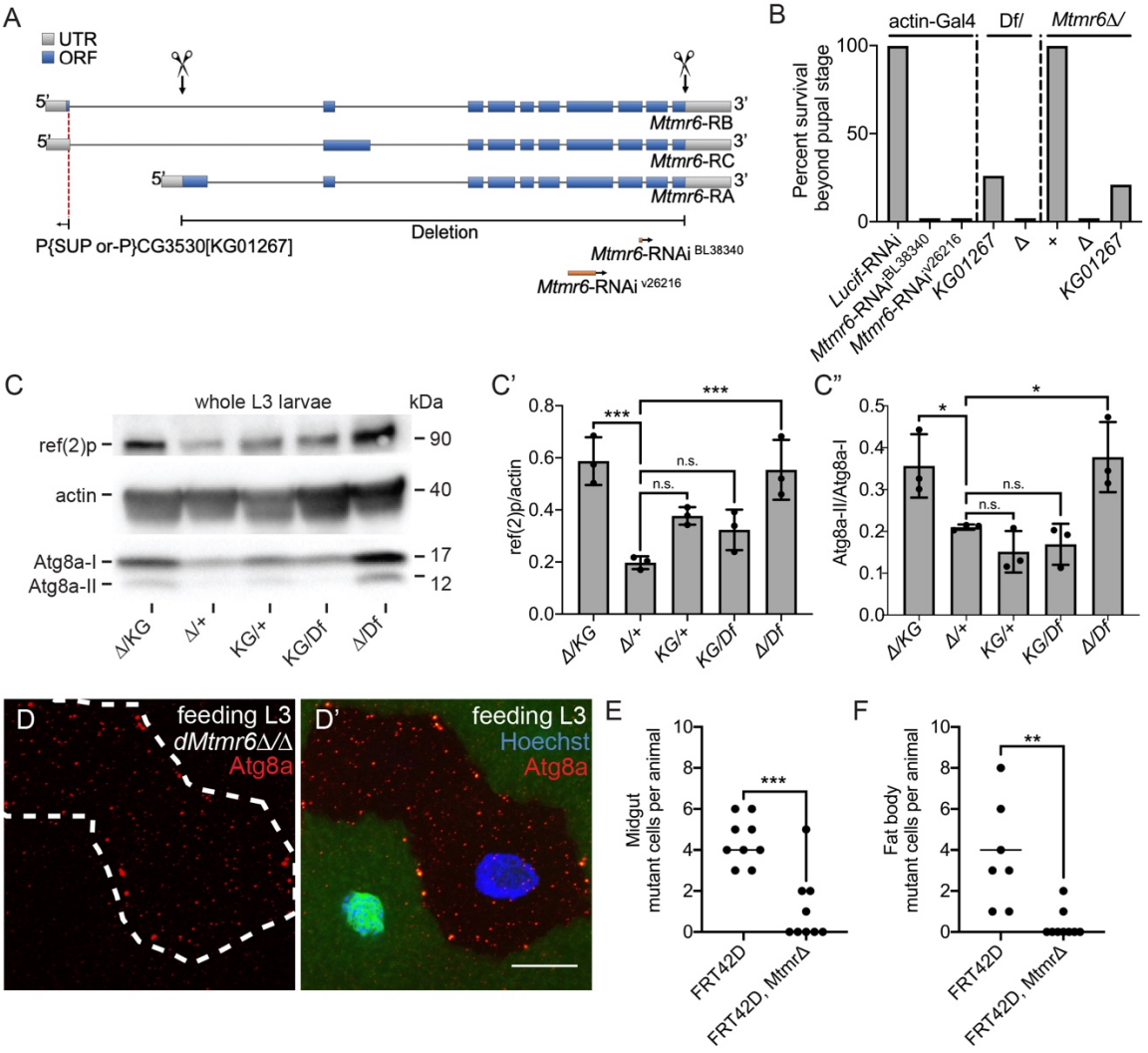

Figure 2.3. *dMtmr6* is essential for development and survival. (A) Schematic representation of *CG3530/dMtmr6*. Vertical arrows indicate the CRISPR-targeted sites and the resulting deletion. Horizontal arrows indicate P-element insertion site and RNAi target sites. (B) Quantification of the percentage of animals that survive beyond pupal stage from ubiquitous knockdown experiments (left) or mutant analyses (right). (C) Western blot from whole larvae (feeding L3) and quantifications of the ratio of lipidated Atg8a-II to cytosolic Atg8a-I and ref(2)p to actin from the indicated genotypes. (D) Feeding L3 larval midguts with *dMtmr6*-null clone cells (white dashed outline, (GFP-negative cells) within wild-type tissue (green) stained with antibody to detect Atg8a and Hoechst to detect nuclei (blue). (E) Quantification of the number of control (FRT42D, + / FRT42D, +) and mutant (FRT42D, *dMtmr6Δ* / FRT42D, *dMtmr6Δ*) clone cells generated in midgut (left) and

fat body (right) from whole larvae (feeding L3). Data information: in (B) percentage of n > 100 animals from 3 experimental replicates (C) data are presented as mean ± SD, n = 2 animals, 3 experimental replicates, and in (E) as individual values, n ≥ 3 animals, 3 experimental replicates. Asterisks denote statistical significance (*P < 0.05, **P < 0.01, ***P < 0.001), using one-way ANOVA (C) and paired t test (E and F). Scale bar, 20 μm.

dMtmr6 and mammalian MTMR8 influence autophagic flux and endolysosomal homeostasis

Our data indicate that dMtmr6 influences autophagic flux, but it is unclear at what stage flux is altered because increased Atg8a puncta could result from elevated levels of autophagic membrane biogenesis, impaired degradation, or both. We analyzed *Drosophila* fat body tissue stained with antibody to detect the autophagy cargo adapter ref(2)p to determine if lysosomal degradation of autophagic cargoes is impaired when we downregulate *dMtmr6*. Under normal conditions, ref(2)p, is internalized within the autophagosome and degraded by the autolysosome. In *dMtmr6*-knockdown fat body cells, ref(2)p levels increase compared to neighboring wild-type cells from fed and starved animals **(Fig. 2.4 A-C)**. In addition, *dMtmr6*-knockdown cells contain larger ref(2)p spots than wild-type cells from starved animals **(Fig. 2.4 D)**. These findings indicate that *dMtmr6*, influences the rate of autophagy, either by initiation, degradation, or both.

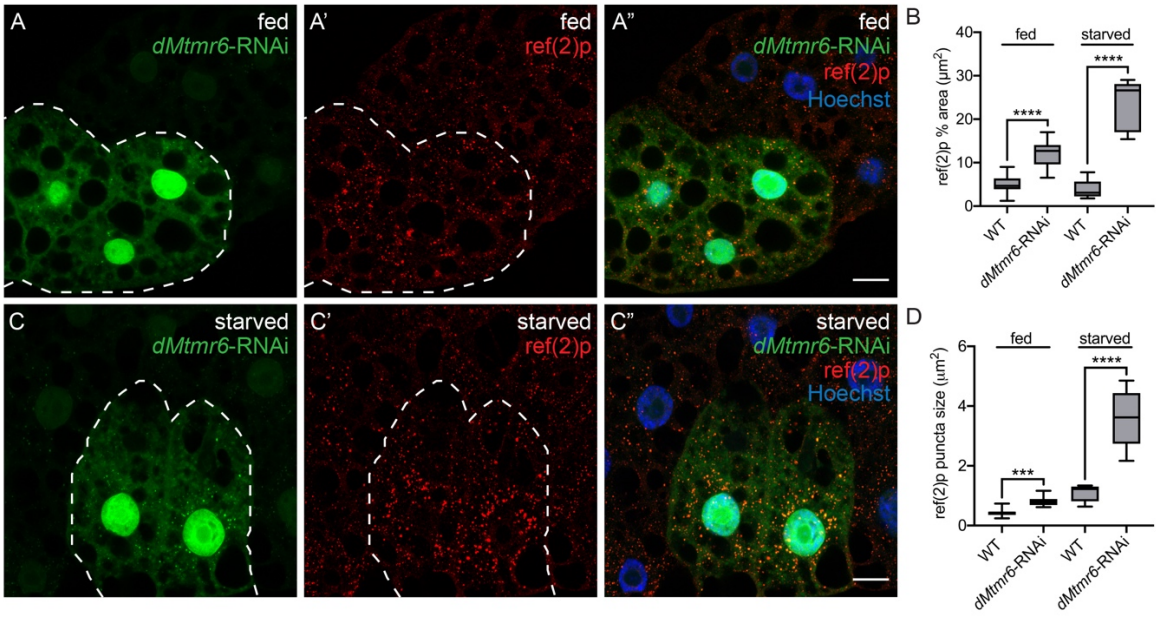

Figure 2.4. dMtmr6 influences autophagic flux. (A) Representative image of fed L3 larval fat body with control (GFP-negative) and d*Mtmr6* knockdown cells (white dashed outline, green cells) stained with an antibody to detect ref(2)p and Hoechst to detect nuclei (blue). (B) Quantification of ref(2)p percent area (□m^2) in control and d*Mtmr6* knockdown cells of L3 larval fat body from fed and starved animals (shown in A and C). (C) Representative image of starved L3 larval fat body with control (GFP-negative) and d*Mtmr6* knockdown cells (white dashed outline, green cells) stained with an antibody to detect ref(2)p and Hoechst to detect nuclei (blue). (D) Quantification of ref(2)p puncta size in control and *dMtmr6* knockdown cells of L3 larval fat body from fed and starved animals (shown in A and C). Data information: in (B and D), data are presented as mean ± min to max, n = 10 each. Asterisks denote statistical significance (***P < 0.001 and ****P < 0.0001), using paired t test. Scale bars, 20 μm.

dMtmr6 is a member of the myotubularin-related (MTMR) family of proteins and is most similar to the human MTMR6 subfamily, which includes MTMR6 (65% similar, 47% identical), MTMR7 (64% similar, 47% identical), and MTMR8 (72% similar, 55% identical) **(Fig. 2.5 A)**. The predicted catalytic domain of dMtmr6 and each of the human MTMR6-subfamily members is conserved **(Fig. 2.5 A)**. However, a key difference between fly and human is that *dMtmr6* encodes an N-terminal FYVE domain, while members of the human MTMR6-subfamily encode a coiled-coil domain **(Fig. 2.5 B)**. Previous studies suggest a negative role for human MTMR8 in autophagy and for MTMR6 in apoptosis (Zou et al., 2009a, 2012b). However, these studies focus on biochemical aspects of MTMR8, MTMR6, and their inactive binding-partner MTMR9 and provide very little information about how MTMR8 could function in autophagy. We transfected both COS-7 and HeLa cells with siRNA to downregulate either *MTMR6* or *MTMR8* and confirmed a role for *MTMR8* in autophagy in primate cells. As shown previously (Zou et al., 2009a), *MTMR6* knockdown promotes HeLa cell death but, unexpectedly, *MTMR6* knockdown in COS-7 cells did not influence viability (not shown). Like *dMtmr6* knockdown, downregulation of *MTMR8* produces increased numbers of large LC3B puncta in COS-7 cells **(Fig. 2.5 C-F)**. Recruitment of ubiquitinated cargoes to autophagic membranes requires the autophagy adapter molecule p62 (*Drosophila* ref(2)p). Importantly, reduced *MTMR8* function resulted in increased numbers of large p62 puncta in COS-7 cells **(Fig. 2.5 C, D, G and H)** and HeLa cells (not shown). We also observed increased lipidated-LC3B (LC3B-II) and p62

protein levels in *MTMR8*-siRNA-transfected COS-7 cells in both serum-fed and serum-deprived conditions **(Fig. 2.5 I)**, which suggests that MTMR8 depleted cells can respond to nutrient deprivation. Furthermore, the inhibition of lysosomal function by addition of Bafilomycin-A1 caused a further increase in LC3B-II and p62 levels **(Fig. 2.5 I)**. Similar to what we observed in *Drosophila*, we hypothesize that *MTMR8* may also regulate the rate of either autophagosome biogenesis or lysosomal degradation of cargoes in higher organisms.

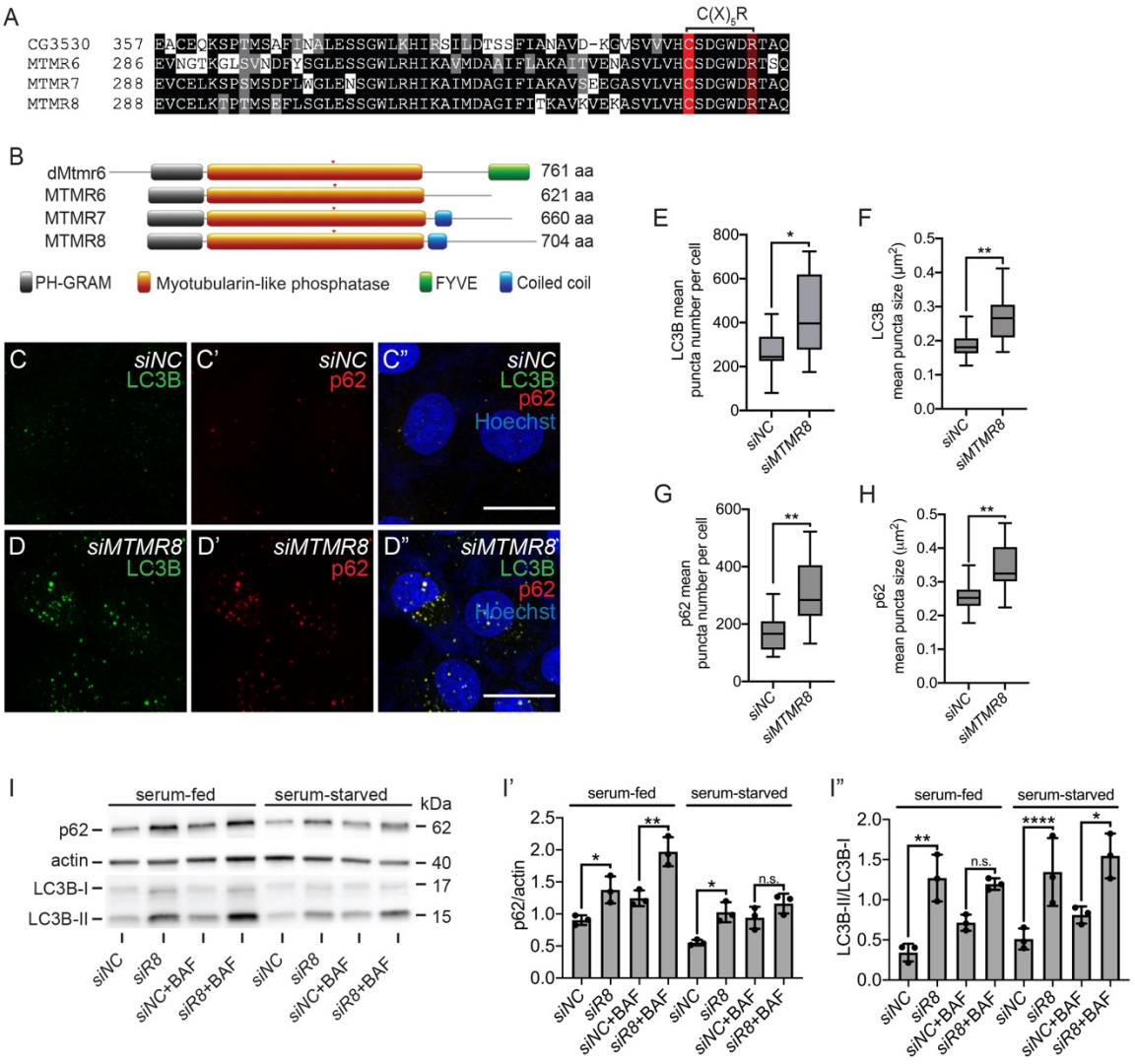

Figure 2.5. MTMR8, the human dMtmr6 ortholog, influences autophagic flux. (A) Amino acid sequence alignment of the CG3530, MTMR6, MTMR7, and MTMR8 catalytic domain (see supplemental figure 1 for full sequence alignment). (B) Schematic of the MTMR6 subfamily. *Drosophila* CG3530 contains an N-terminal FYVE domain. MTMR6, MTMR7, and MTMR8 contain a N-terminal coiled coil domain. (C and D) Representative maximum intensity projection of z-stack image from serum-fed Cos7 cells treated with scrambled siRNA (NC, top) or MTMR8-siRNA (bottom). Cells were stained with Hoechst (blue) to detect nuclei and antibodies to detect p62 (red) and LC3B (green). (E-H) Quantification of the size (area in μm^2) and number of both p62 and LC3B puncta per cell as represented in (C and D) (I) Western blot from serum-fed or serum-starved COS7 cells treated without or with Bafilomycin A1, which disrupts autophagosome-

lysosome fusion. Data information: in (E-H), data are presented as mean ± min and max, n = 12 images from 3 experimental replicates, and in (I’ and I”) data are presented as mean ± SEM from 3 experimental replicates. Asterisks denote statistical significance (*P < 0.05, **P < 0.01, and ****P < 0.0001), using unpaired t test (E-H) and one-way ANOVA (I’ and I”). Scale bars, 20 μm.

Genes whose molecular products facilitate autophagic flux are expressed through transcription factor EB (TFEB, *Drosophila Mitf*) mediated transcription. When inactive TFEB remains in the cytoplasm, but in response to starvation or during lysosome dysfunction, TFEB translocates to the nucleus to promote expression of both lysosome- and autophagy-genes (Napolitano and Ballabio, 2016). We hypothesized that if *MTMR8* inactivation impairs lysosome function, then we should see evidence of TFEB activation in *MTMR8*-depleted cells. Indeed, we detected more TFEB in the nucleus of serum-starved than of serum-fed control HeLa cells while *MTMR8*-depleted cells displayed nuclear TFEB in both serum-starved and serum-fed conditions **(Fig. 2.6 A-E)**. If MTMR8 and dMtmr6 function as orthologues, then *dMtmr6* knockdown should produce activation of the *Drosophila* TFEB ortholog, Mitf. As expected, Mitf-target gene expression increased in *Drosophila dMtmr6*-knockdown fat body compared to control (*Lucif-RNAi*) **(Fig. 2.6 F)**. Despite nutrient availability, TFEB activation occurs in cells and tissues depleted of *MTMR8* or *dMtmr6*. These results suggest that inactivation of MTMR8 or dMtmr6 may elicit lysosome dysfunction.

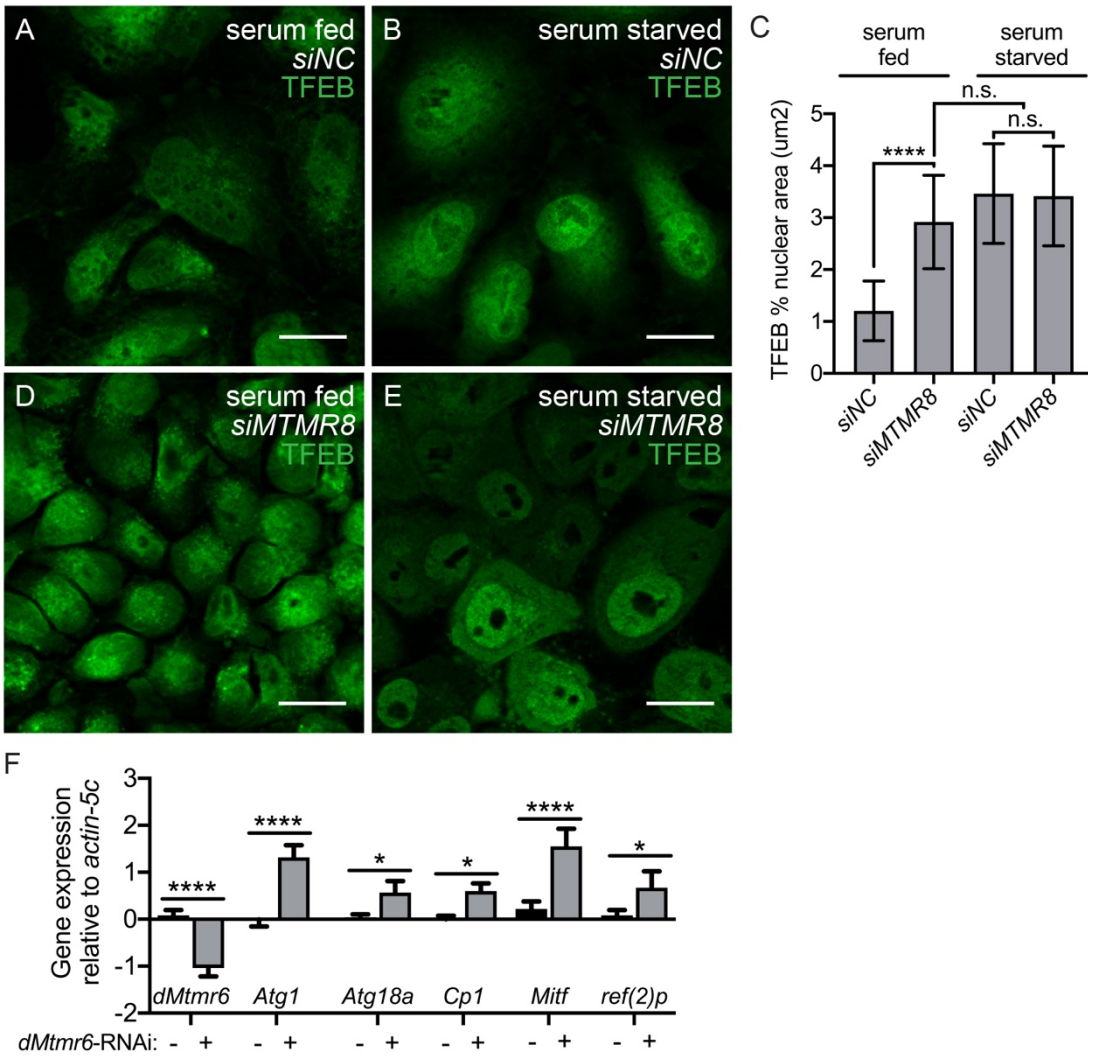

Figure 2.6. MTMR8 and dMtmr6 influence TFEB/mitf signaling. Representative maximum intensity projection of z-stack image from serum-fed (A and D) or serum-starved (B and E) siRNA-transfected HeLa cells stained with antibodies to detect TFEB (green). **(C)** Quantification of nuclear TFEB in serum-fed and -starved HeLa cells transfected with the indicated siRNA as represented in (A, B, D, and E). **(F)** Changes in *Mitf/TFEB-target gene transcription relative to *actin-5c* in fat body from *Luciferase*-RNAi (-) or *dMtmr6*-RNAi (+) fat body-specific knockdown tissue. Please note that *Mitf* is the *Drosophila TFEB* ortholog, and *Cp1* is the gene for cathepsin L protein. Data information: in (C), data are presented as mean ± SD, n = 10 random images per genotype and condition across 3 biological replicates, and in (F), data are presented as mean ± SEM (n = 3 biological replicates).

Asterisks denote statistical significance (*P < 0.05 and ****P < 0.0001) using one-way ANOVA (C) and unpaired t test in (F). Scale bars, 20 μm.

We further explored the possibility that lysosome dysfunction exists in the absence of either dMtmr6 or MTMR8. We reasoned that fusion between autophagosomes and lysosomes could be impaired, which would indicate an autolysosome formation defect and could explain increased ref(2)p/p62 and lipidated Atg8a/LC3B levels. To determine if autolysosomes form, we used the tandem GFP-mCherry-Atg8a fluorescent reporter, which is a transgene expressed under control of the Atg8a promoter (Lee et al., 2016). Dual punctate fluorescence of both GFP and mCherry reflects autophagosomes, but because GFP is pH sensitive, mCherry signal alone reflects autolysosomes. In *Drosophila* fat body from fed animals, Atg8a reporter expression is diffuse throughout the cytoplasm in control tissue and Atg8a puncta form in *dMtmr6*-depleted tissue **(Fig. 2.7 A and C)**, with the ratio of GFP to RFP being elevated in control tissue **(Fig. 2.7 B)**. By contrast, we observe lone mCherry signal in *dMtmr6*-knockdown tissue where the ratio of GFP to RFP is decreased **(Fig. 2.7 B-D)**. These data indicate that the number autolysosomes increase when *dMtmr6* function is reduced.

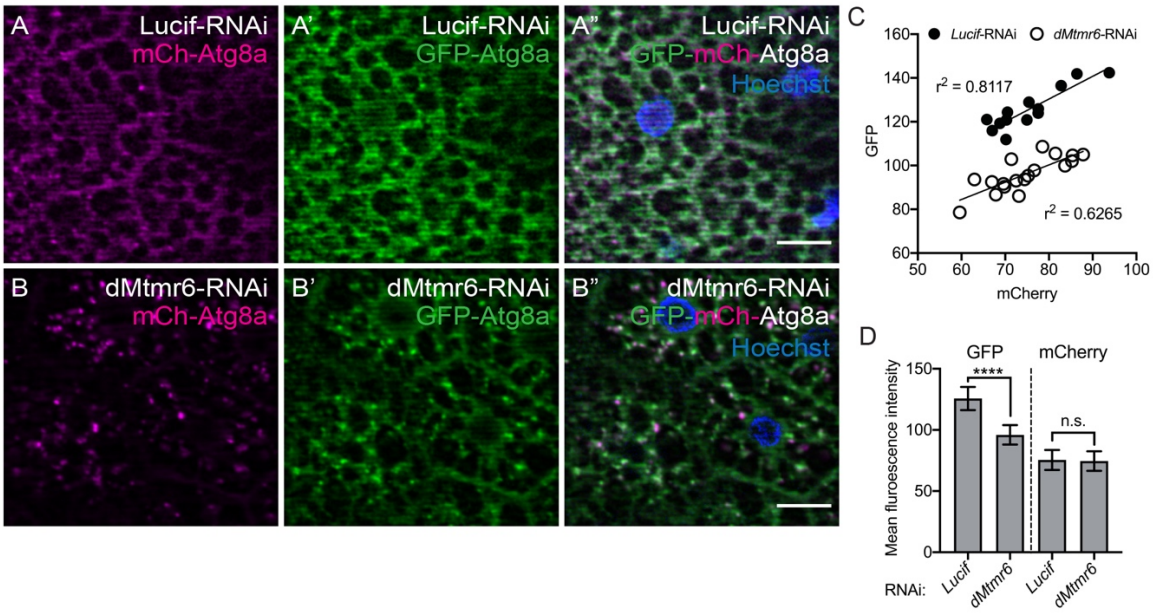

Figure 2.7. dMtmr6 depleted autolysosomes possess low pH. (A and C) Representative images of fed L3 larval fat body expressing EGFP-mCherry-Atg8a and either control *Lucif*-RNAi (A) or *dMtmr6*-RNAi (C). Tissues were stained with Hoechst (blue) to detect nuclei. (B) Quantification of correlation between average GFP intensity and mCherry intensity per fat body cell expressing either control *Lucif*-RNAi (filled circle) or *dMtmr6*-RNAi (empty circle) as represented in A and C. (D) Quantification of average fluorescence intensity of GFP and mCherry. Data information: in (B), data are presented as mean ± SD, and in (D), data are presented as the average pixel intensity of both GFP and mCherry per cell, n ≥ 5 random images taken across 3 samples from each genotype. Asterisks denote statistical significance (****P < 0.0001), using unpaired t test in (D). Scale bars, 20μm.

Reduced function of both *dMtmr6* in *Drosophila* and *MTMR8* in COS-7 cells results in large Atg8a/LC3B and ref(2)p/p62 structures. To further determine the nature of the large Atg8a-positive puncta generated by *dMtmr6* depletion, we performed transmission electron microscopy (TEM) analyses of *Drosophila* midguts 2 h after puparium formation. In control animals undergoing developmental autophagy in midgut enterocytes, the cytoplasm contains autophagosomes and autolysosomes **(Fig. 2.8 A)**. By contrast, *dMtmr6*-knockdown enterocytes possess large electron-poor vesicles throughout the cytoplasm **(Fig. 2.8 B)**. We classified these single-membrane structures as autolysosomes **(Fig 2.8 C and D)**. Importantly, we observe similar large autolysosome structures in COS-7 cells transfected with *MTMR8*-siRNA but not in control cells **(Fig. 2.8 E-H)**.

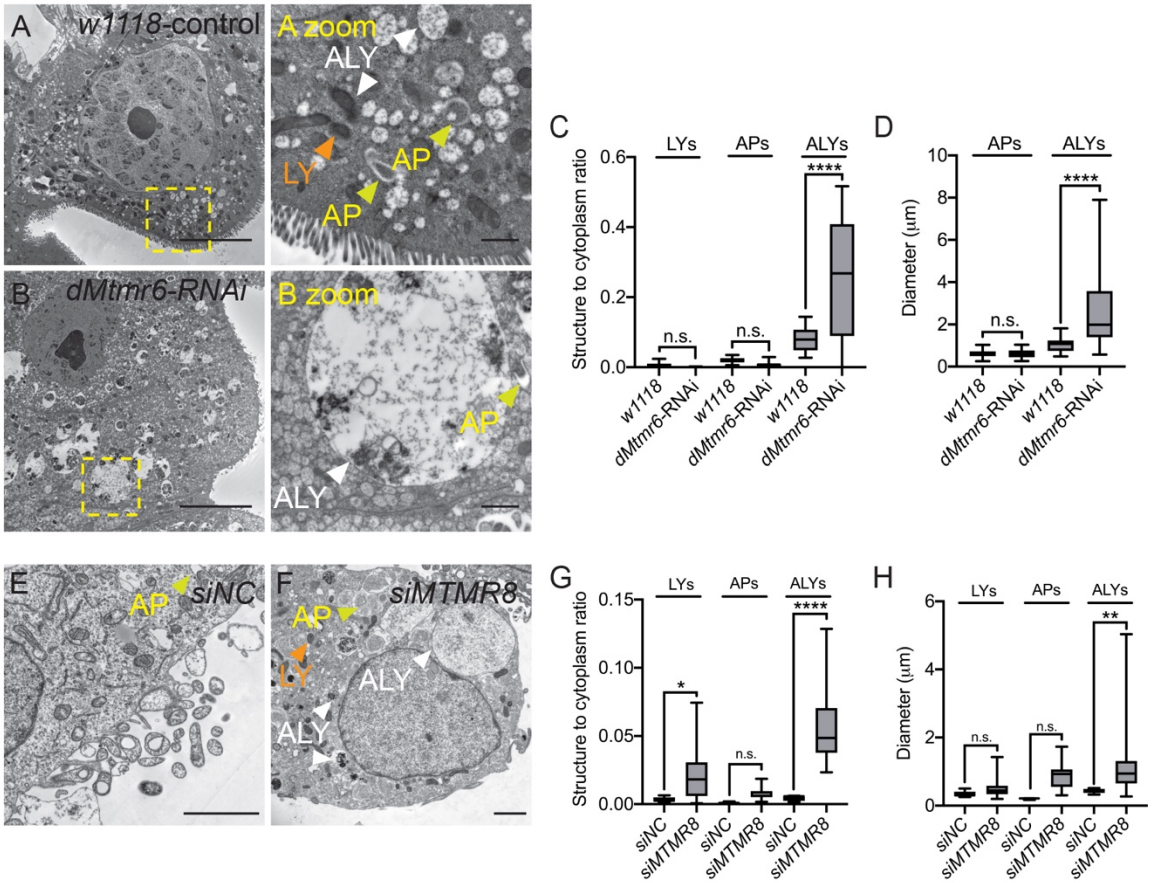

Figure 2.8. dMtmr6 and MTMR8 affect autolysosome size. (A and B) Electron micrographs of *Drosophila* larval midgut cells during developmental autophagy (2 h APF) from control *w1118* (A) or *dMtmr6* knockdown (B) tissues. Whole cell sections on left, yellow box indicates area shown at high magnification in panels on right. Arrows indicate lysosomes (LY, orange), autophagosomes (AP, yellow), and autolysosomes (ALY, white). (C) Quantification of the ratio of the indicated organelles area (□m^2) relative to the total area of cytoplasm. (D) Quantification of the diameter of indicated organelles. (E and F) Electron micrographs of serum-fed COS7 cells transfected with siRNA targeting scrambled *NC* control (E) or *MTMR8* (F). (G) Quantification of the ratio of the indicated organelles area (□m^2) relative to the total area of cytoplasm. (H) Quantification of the diameter of indicated organelles. Data information: in (C, D, G, and H) data are presented as minimum and maximum, in (G and H) n ≥ 10 random images taken across samples from 3 biological replicates, in (K and L) n = 15 images, 1 experimental replicate. Asterisks denote statistical significance (*P < 0.05, **P < 0.01, and ****P < 0.0001), using one-way ANOVA in (C, D, G, and H). Scale bars, (A and B, left panels) 10 μm; (A zoom and B zoom, right panels) 1 μm; (E and F) 2 μm.

To confirm that the large structures we observe by TEM are autolysosomes and that they occur in another mammalian cell line, we co-stained HeLa cells with LC3B and LAMP1 antibodies to detect coincidence of autophagic and lysosomal markers respectively. In serum-fed HeLa cells transfected with control siRNA, we observe very few LC3B-positive spots, and LAMP1 puncta appear throughout the cytoplasm **(Fig. 2.9 A)**. By contrast, *MTMR8*-siRNA-transfected HeLa cells contain large puncta that feature both LC3B and LAMP1 that colocalize and cluster near the perinuclear region **(Fig. 2.9 A-G)**. These data indicate that depletion of both *dMtmr6* in fly tissues and *MTMR8* in primate cells promotes the formation of large autolysosomes.

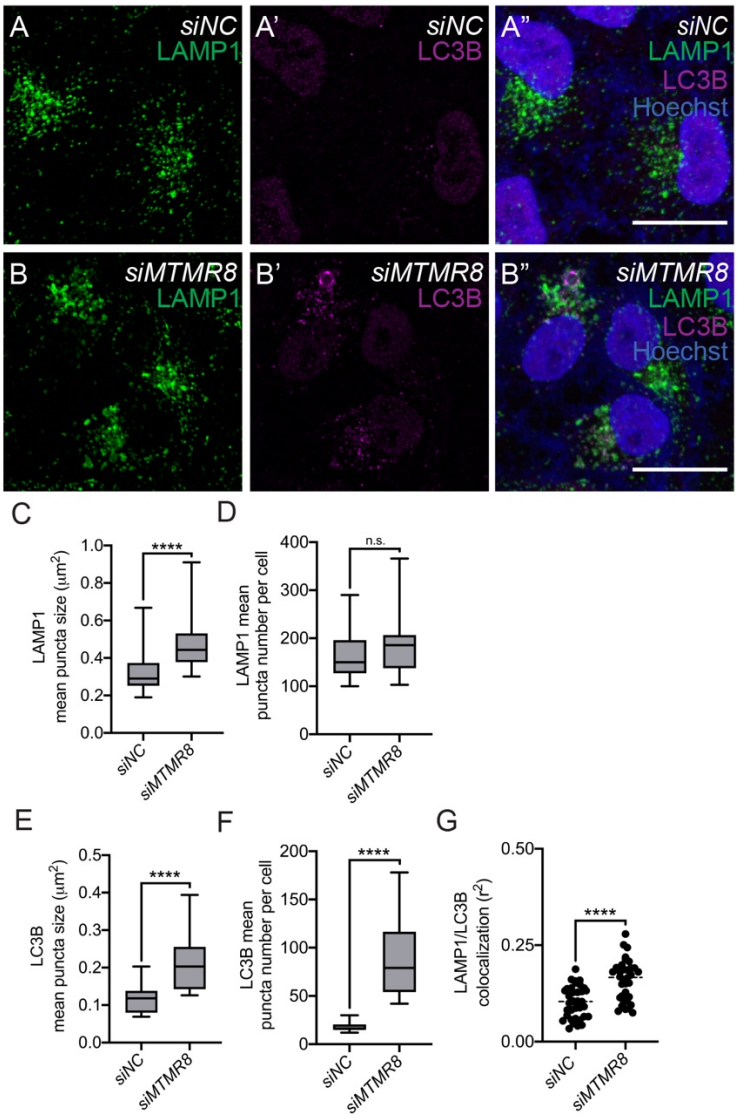

Figure 2.9. *MTMR8*-depleted HeLa cells possess autolysosomes. (M and N) Representative maximum intensity projection of z-stack image from serum-fed HeLa cells siRNA-transfected to target *NC* control (M) or *MTMR8* (N) stained with Hoechst to detect nuclei (blue) and antibodies to detect LAMP1 (green) and LC3B (magenta), indicative of lysosomes and autophagosomes, respectively. Autolysosomes contain both LAMP1 and LC3B. (O-R) Quantification of the size (area in µm^2) and number of both LAMP1 and LC3B puncta per cell as represented in M and N. (S) Quantification of LAMP1 and LC3B puncta colocalization as represented in M and N. Data information: in (C-G) data are presented as minimum and maximum; n = 10 images, 3 experimental replicates. Asterisks denote

statistical significance (****P < 0.0001), using unpaired t test in (C-G). Scale bars, 20 μm.

Autophagosomes deliver their cargoes to lysosomes for degradation, and impaired lysosome function can lead to autophagosome accumulation and prevent autolysosome resolution. Therefore, we evaluated lysosomes in larval fat body using LysoTracker, an acidophilic dye that labels acidic organelles, to determine if *dMtmr6* influences lysosome homeostasis. In fat body from fed larvae, *dMtmr6* knockdown cells contain more acidic organelles than neighboring wild-type control cells **(Fig. 2.10 A and B)**. Although *dMtmr6* knockdown cells possess increased numbers of acidic vesicles, this may not reflect an increase in functional lysosome numbers. Therefore, we evaluated cathepsin protease activity in *dMtmr6* knockdown cells to directly evaluate lysosomal enzyme function. We tested cathepsin B protease activity using Magic Red substrate, which fluoresces upon cleavage by cathepsin B. Compared to neighboring wild-type cells in fat body from fed larvae, Magic Red fluorescence levels increase in *dMtmr6* knockdown cells **(Fig. 2.10 C and D)**. We also measured cathepsin L protein levels from fed or starved larval fat body tissues. During starvation-induced autophagy, lysosome biogenesis increases and pre- and pro-cathepsin L levels rise in Luciferase-RNAi and *Atg1*-RNAi control tissues **(Fig. 2.10 E)**. However, in *dMtmr6*-depleted tissues from fed animals, pre- and pro-cathepsin L protein levels are greater than controls **(Fig. 2.10 E)**, indicating that cathepsin L biogenesis increases as a result of *dMtmr6*-knockdown. Together these data suggest that, although lysosomes display functional qualities in *dMtmr6*, lysosome homeostasis is altered.

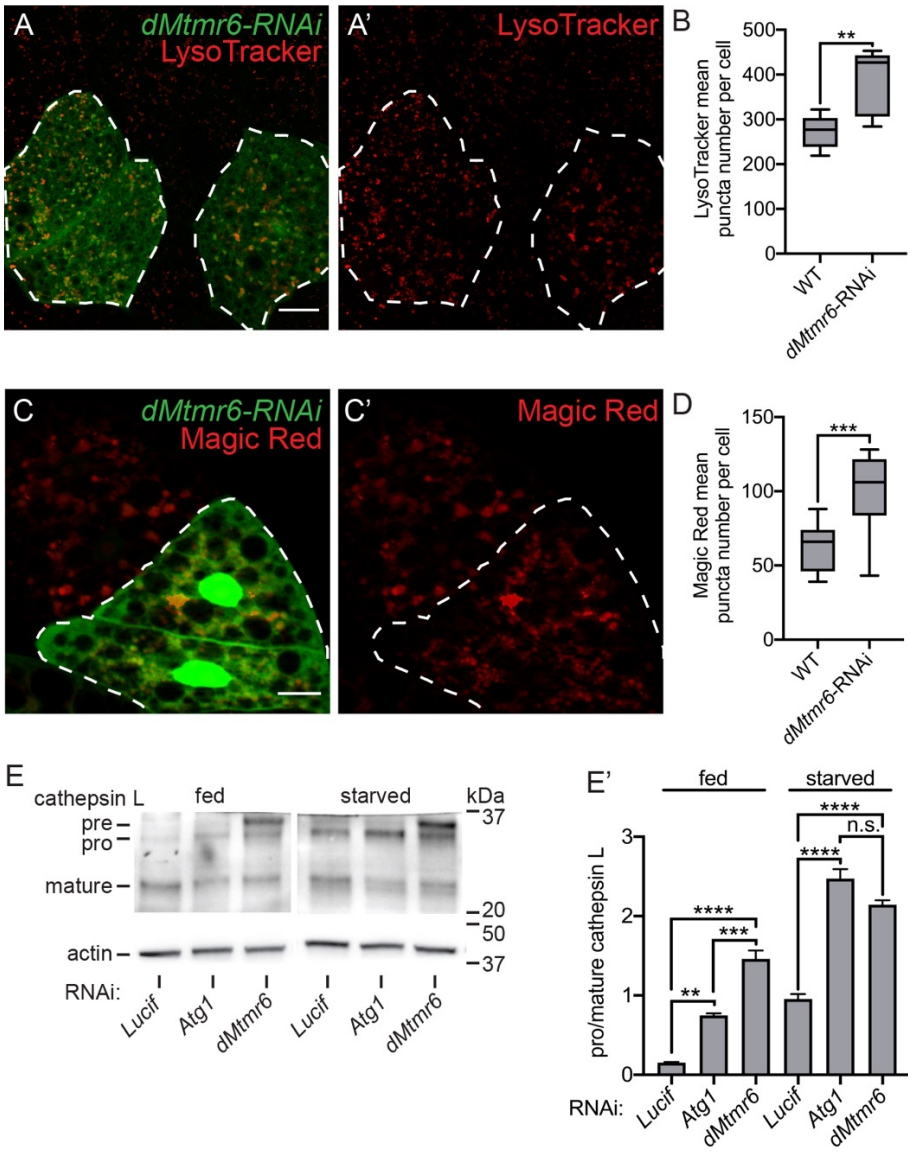

Figure 2.10. dMtmr6 and MTMR8 maintain endo-lysosomal homeostasis. (A) Representative image of fat body from fed L3 *Drosophila* larvae with control (GFP-negative) and clonal d*Mtmr6*-knockdown cells (white dotted outline, green) stained with LysoTracker Red to detect acidic vesicles. (B) Quantification of LysoTracker Red puncta number per cell in WT versus d*Mtmr6*-knockdown cells as represented in (A). (C) Representative image of fat body from fed L3 *Drosophila* larvae with control (GFP-negative) and clonal d*Mtmr6*-knockdown cells (white dotted outline, green) stained with MagicRed to detect cathepsin B protease activity. (D) Quantification of Magic Red puncta number in WT versus d*Mtmr6*-knockdown cells as represented in (C). (E) Representative western blot of fat body cathepsin L

protein levels from fed and starved fat body-specific knockdown larvae (L3) of the indicated genotype. Quantification is the ratio of pro- to mature- cathepsin L. Data information: in (C and D), data are presented as min to max, n =10; in (E) data are presented as mean ± SEM, n = 6 animals for each genotype of 3 experimental replicates. Asterisks denote statistical significance (**P < 0.01, ***P < 0.001, ****P < 0.0001 paired t test in (B and D) and one-way ANOVA in (E). Scale bars, (A and C) 20 μm.

Because lysosomal homeostasis is altered in *dMtmr6* knockdown cells, we reasoned that aspects of the endolysosomal pathway may be altered. To test whether *dMtmr6* functions in endocytosis, we monitored fluid-phase endocytosis in larval fat body via uptake of Texas Red (TR)-avidin. Control cells contained TR-avidin-positive puncta throughout the cytosol, whereas *dMtmr6* knockdown cells (GFP-positive) possessed little to no endocytic tracer **(Fig. 2.11 A and B)**. However, we observed no change in localization of the endosomal marker, Rab7 **(Fig. 2.11 C-E)**. Thus, *dMtmr6* knockdown alters endocytosis in a manner that does not appear to impact Rab7 localization.

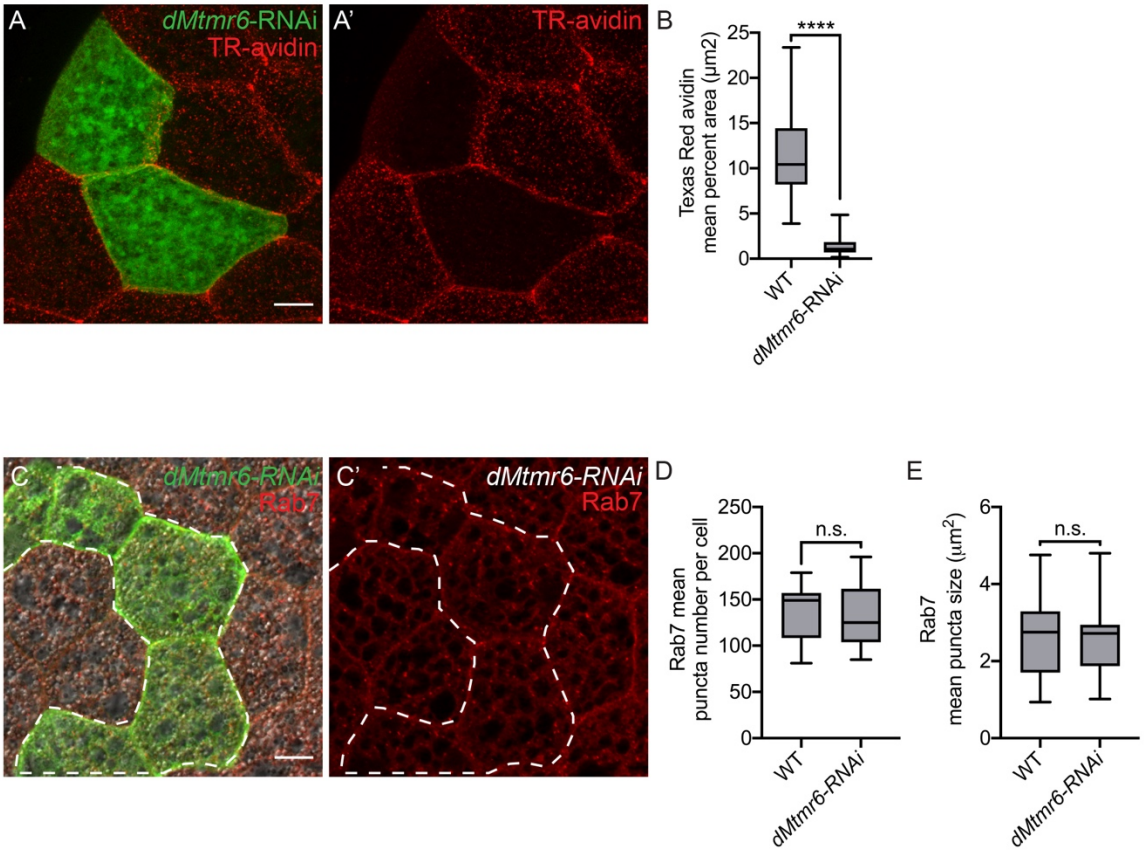

Figure 2.11. *dMtmr6* depletion impairs endocytosis but does not impact Rab7. (A) Representative image of fat body from fed L3 Drosophila larvae with wild-type (WT) control (GFP-negative) and clonal *dMtmr6*-knockdown (green cells). Tissues were fixed following ex vivo incubation with Texas Red-Avidin as described in methods. (B) Quantification of percent area (□m^2) of Texas Red Avidin in WT versus *dMtmr6* knockdown cells as represented in A. (C) Representative image of fat body from fed L3 *Drosophila* larvae with wild-type (GFP-negative) and clonal d*Mtmr6*-knockdown cells (white dotted outline, green) stained with antibody to detect Rab7 (red). (D and E) Quantification of Rab7 puncta number (D) and size (E) per cell in wild-type (WT) control and *dMtmr6*-knockdown cells as represented in (C). Data information: in (B, D, and E), data are presented as mean ± min to max (n = 10 paired WT and *dMtmr6*-knockdown cell taken across random images from 3 experimental replicates). Asterisks denote statistical significance (****P < 0.0001), using paired t test (B, D, and E). Scale bars (A and C), 20 μm.

Intracellular localization of FYVE domain-containing proteins represents PI(3)P enriched sites (Gillooly, 2000). However, *Drosophila* PI(3)P reporters remain limited to endosomal compartments, and we lack tools that are specific to autophagic PI(3)P. Nonetheless, we investigated how *dMtmr6*-depletion effects the widely-used GFP-2xFYVE endosomal PI(3)P-reporter, which utilizes two copies of the FYVE domain from the early endosomal protein Hrs fused to EGFP (Wucherpfennig et al., 2003). When we mis-expressed GFP-2xFYVE and depleted *dMtmr6* in fat body of fed larvae, we detected increased GFP-2xFYVE levels in cellular regions that are both perinuclear and away from the nucleus (aponuclear) when compared to *Lucif-RNAi* controls **(Fig. 2.12 A-F)**. Interestingly, fat body from fed *dMtmr6*-knockdown animals contained perinuclear GFP-2xFYVE distribution similar to fat body from starved control animals, even though aponuclear levels remained high in *dMtmr6-RNAi* conditions **(Fig. 2.12 B-G)**. Starvation further increased perinuclear and decreased aponuclear GFP-2xFYVE localization in *dMtmr6*-depleted cells **(Fig. 2.12 C-H)**. Despite alterations in GFP-2xFYVE localization, we saw reduced colocalization between GFP-2xFYVE and Atg8a in *dMtmr6*-knockdown cells compared to controls in both fed and starved conditions **(Fig 2.12 I-M)**. Together, these data indicate that *dMtmr6*-depletion impacts localization of PI(3)P-containing vesicles, but these vesicles remain distinct from large Atg8a-bearing structures.

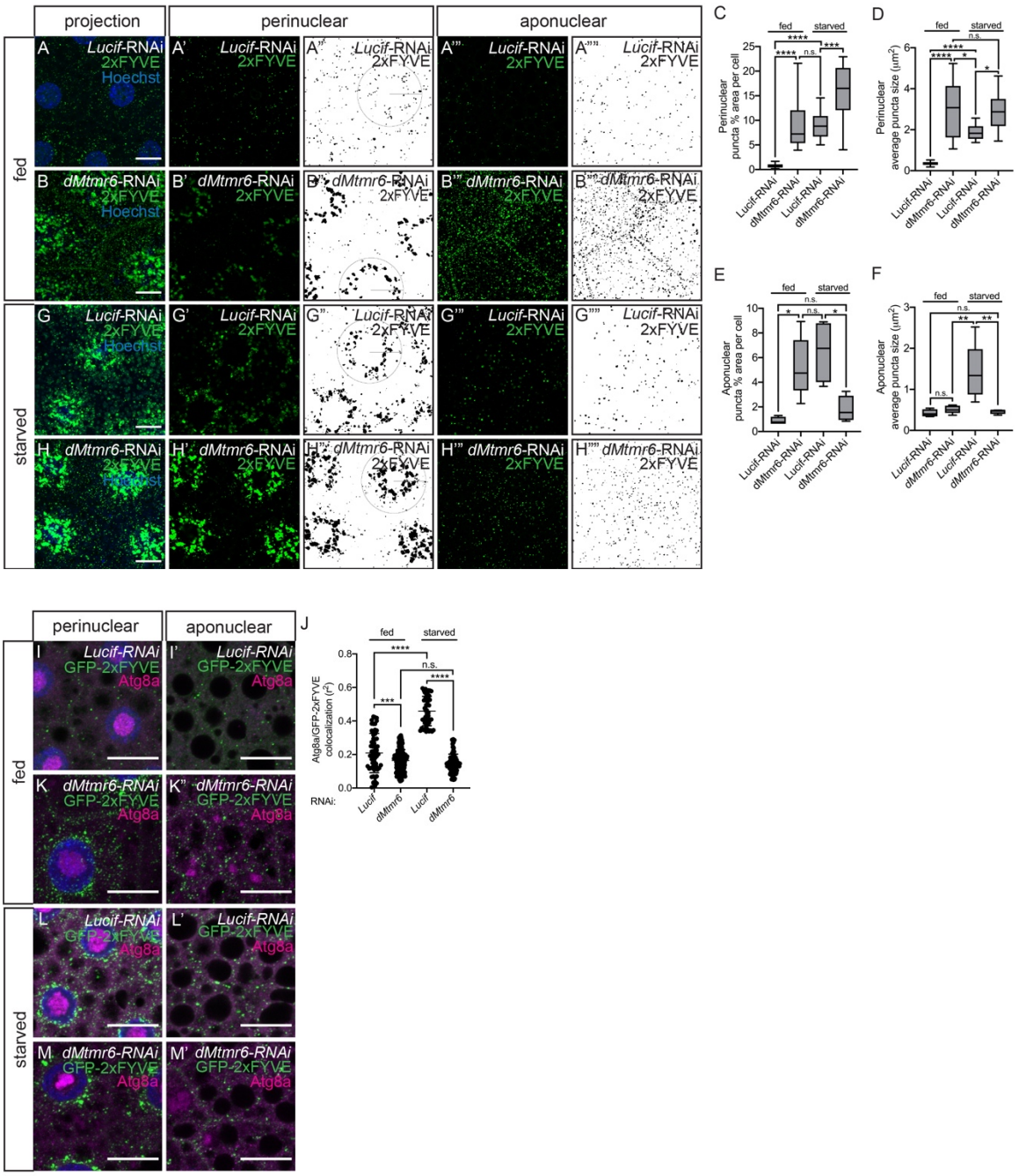

Figure 2.12. dMtmr6 influences PI(3)P reporter distribution. (A, B, G and H) Representative images of indicated regions of Drosophila fat body overexpressing the PI(3)P reporter GFP-2xFYVE from fed (A and B) and starved animals (G and H**).** (C-F) Quantification of GFP-2xFYVE puncta from regions of interest as depicted in (A", B", G" and H", perinuclear, and A"", B"", G"", and H"", aponuclear).

(I, K, L and M) Representative images of fed and starved Drosophila fat body overexpressing GFP-2xFYVE, stained with Hoechst to detect nuclei, and antibody stained to detect Atg8a. **(J)** Quantification of colocalization between GFP-2xFYVE and Atg8a as represented in (I, K, L and M). Data information: in (C-F and J), data are presented as mean ± min to max ($n \geq 10$). Asterisks denote statistical significance (*P < 0.05, **P < 0.01, ***P < 0.001, and ****P < 0.0001), using ANOVA. Scale bars, 20 μm.

Phagocytosis requires both Vps34-mediated PI(3)P generation and lysosomal degradation of extracellular cargoes (Jeschke and Haas, 2016). Given the role of dMtmr6 in autophagy and endocytosis, we hypothesized that dMtmr6 might also influence phagocytosis. To investigate this, we tested the ability of *Drosophila dMtmr6* knockdown embryonic macrophages to engulf apoptotic corpses, which are generated throughout the embryo as part of normal development. Corpse phagocytosis primes macrophages for subsequent immune responses such as recruitment to wounds and bacterial uptake (Weavers et al., 2016). Importantly, *dMtmr6*-knockdown in embryonic macrophages compromises phagocytosis, as indicated by the decreased vacuole number compared to control macrophages **(Fig. 2.13 A and B)**. These data suggest a role for dMtmr6 in phagocytosis.

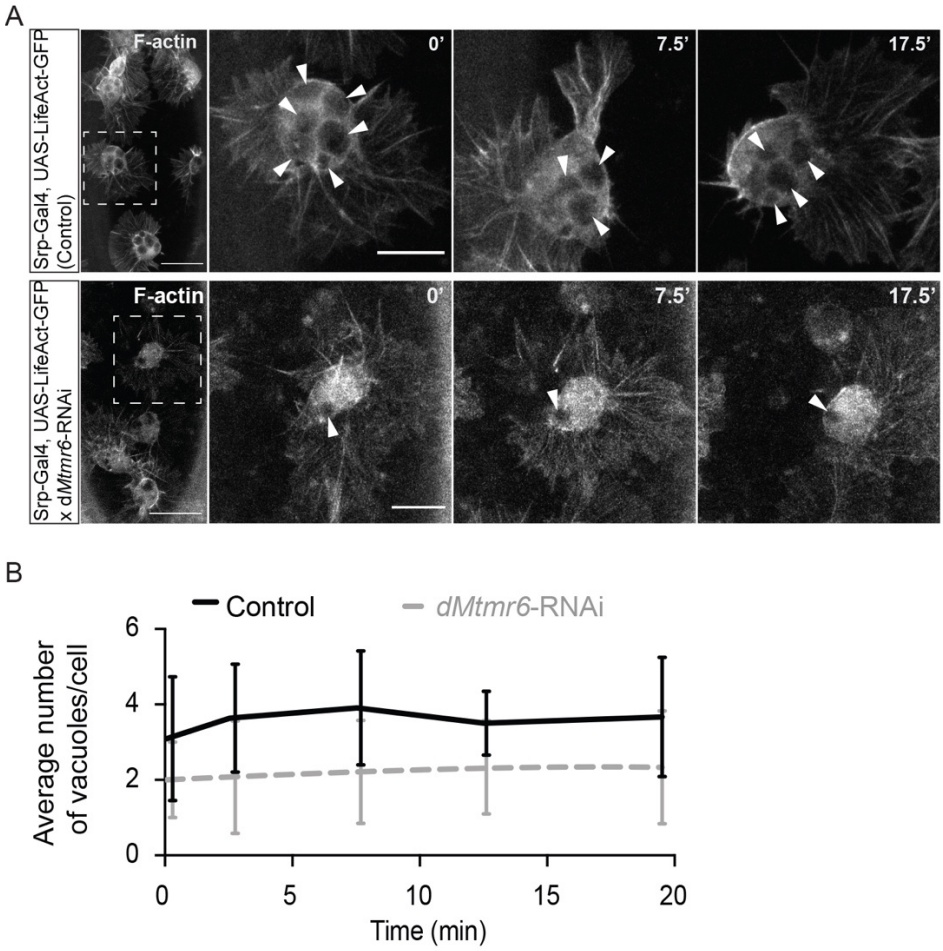

Figure 2.13. *dMtmr6* depletion impairs developmental phagocytosis. (A) Control *Drosophila* macrophage expressing GFP-labeled F-actin (top panels), which contain phagocytic vacuoles (white arrowheads) during developmental apoptotic corpse clearance in embryos, compared to *dMtmr6*-knockdown *Drosophila* macrophages expressing GFP-labeled actin (bottom panels). (B) Quantification of the number of phagocytic vacuoles in macrophages over time from control versus *dMtmr6*-knockdown cells. Scale bars in (A) first panel from left, 20 μm; second panel from left, 10□□m.

dMtmr6 mutant cells are autophagy prone

We next investigated the relationship between *dMtmr6* and upstream regulators of autophagy. Cell growth and the factors that regulate this process, such as the ribosomal protein kinase p70 S6 and the serine/threonine kinase Akt (protein kinase B), often have a reciprocal relationship with autophagy. Since our data indicate that cells with decreased *dMtmr6* function are prone to autophagy, we tested if growth signaling is altered in these cells. Indeed, fat body from feeding larvae possess reduced levels of both phosphorylated p70 S6 Kinase and phosphorylated AKT in *dMtmr6*-depleted tissue compared to controls **(Fig. 2.14 A)**. These data suggest that fat body exists in an autophagy-prone state in the absence of *dMtmr6*.

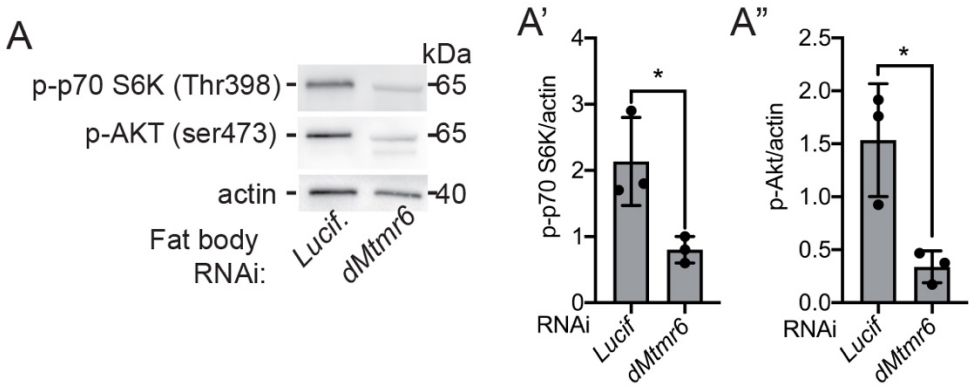

Figure 2.14. dMtmr6 influences growth signaling. (A) Representative western blot from fat body of indicated genotypes to measure levels of phosphorylated p70-S6K and phosphorylated AKT proteins relative to actin. Quantification of the ratio of phospho p70-S6K to actin (A') and phospho AKT to actin (A"). Data information: in (A' and A"), data are presented as mean ± SEM, 3 experimental replicates. Asterisks denote statistical significance (*P < 0.05) using unpaired t test (A' and A").

We queried the relationship between *dMtmr6* and the Atg1 and Vps34 kinases that are conserved regulators of autophagy (Galluzzi et al., 2017). As expected, *Atg1*-knockdown alone resulted in ref(2)p accumulation **(Fig. 2.15 A)** and inhibited Atg8a puncta formation **(Fig. 2.15 E and C)**. Surprisingly, fat body with double knockdown of *Atg1* and d*Mtmr6* possessed Atg8a lipidation, ref(2)p accumulation **(Fig. 2.15 A)**, and increased numbers of Atg8a-positive structures **(Fig. 2.15 C-D)**, but these Atg8a puncta were significantly smaller **(Fig. 2.15 D-F)**. These data suggest that dMtmr6 functions in at least a partially Atg1-independent manner.

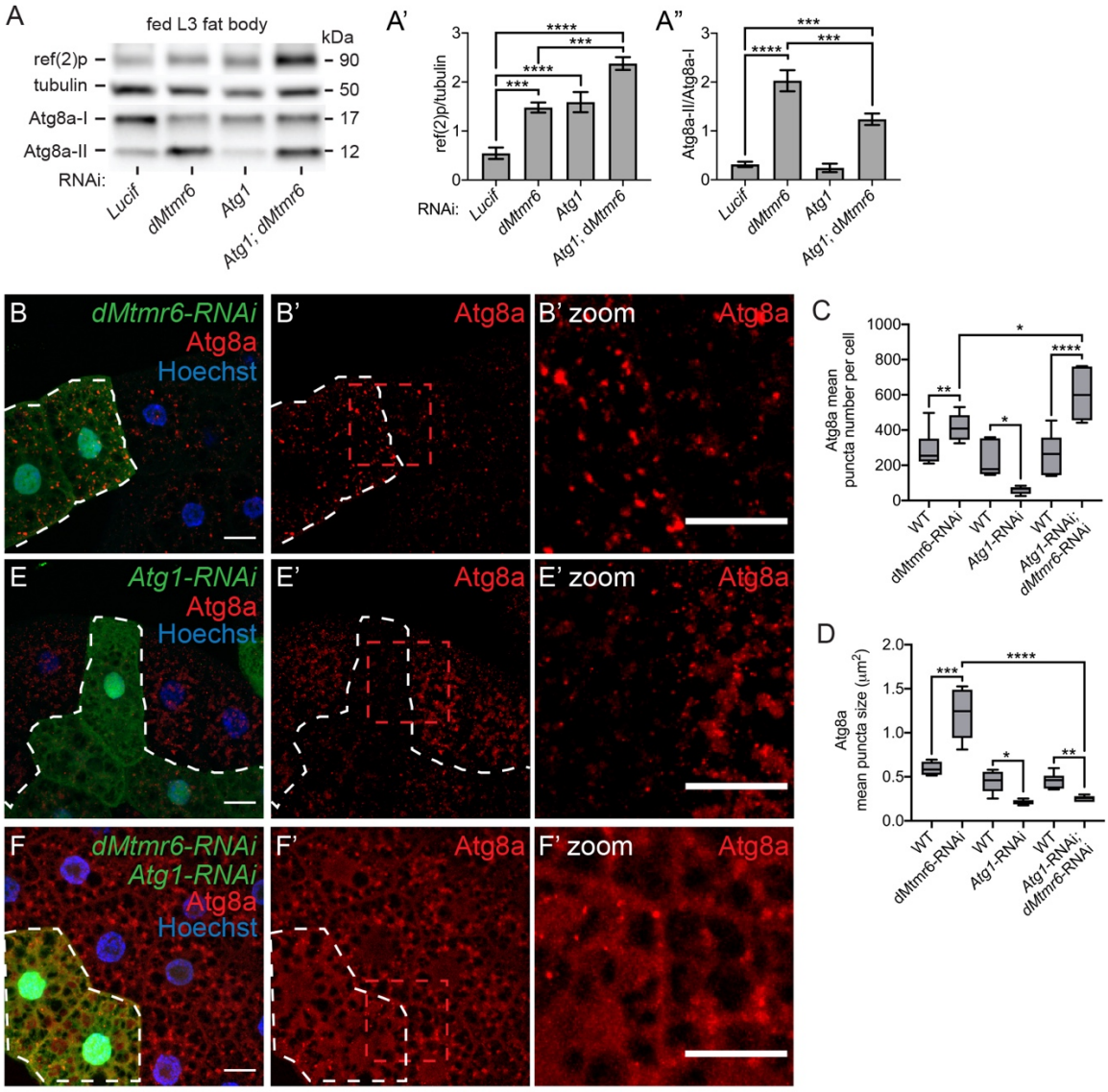

Figure 2.15. dMtmr6 regulates autophagic flux, independent of Atg1. (A) Representative western blot using fed L3 larval fat body from fat body-specific knockdown of the indicated genotypes to measure lipidated Atg8a and ref(2)p protein levels. Quantification of the ratio of ref(2)p relative to tubulin (A') and lipidated Atg8a-II relative to cytosolic Atg8a-I (A"). (D, E and F) Representative images of starved L3 larval fat body with control (GFP-negative) and knockdown cells of indicated genotypes (white dashed outline, green cells) stained with an antibody to detect Atg8a and Hoechst to detect nuclei (blue). Red box indicates area shown in zoom panels at right. (C and D) Quantification of Atg8a puncta number (C) and average size (D) as represented in (B, E, and F). Data information:

in (A and B), data are presented as mean ± SEM, 3 experimental replicates; in (C and D), data are presented as mean ± min and max ($n \geq 9$). Asterisks denote statistical significance (*$P < 0.05$, **$P < 0.01$, ***$P < 0.001$, ****$P < 0.0001$), using one-way ANOVA (A, C and D). Scale bars, 20 μm.

During autophagy, Vps34 kinase activity contributes to PI(3)P production on autophagic membranes, and *Vps34* mutant cells fail to form GFP-Atg8a puncta (Juhász et al., 2008). Because dMtmr6 is a putative PI(3)P phosphatase, we reasoned that dMtmr6 could influence the pool of PI(3)P that is supplied by Vps34. We used the FLP/FRT system to generate *Vps34* null mutant cell clones in fat body expressing *dMtmr6*-RNAi (*Lsp2-GAL4* > *UAS-dMtmr6-RNAi*) and evaluated Atg8a puncta formation in starved animals. *Vps34* null mutant cells that express *dMtmr6-RNAi* possess fewer Atg8a puncta than cells expressing *dMtmr6*-RNAi alone **(Fig. 2.16 A-B)**. In addition, we observed similar results when we tested if the loss of Atg9 could suppress Atg8a puncta formation in *dMtmr6*-knockdown tissue **(Fig. 2.16 C-D)**. Taken together, these data suggest that dMtmr6 negatively regulates Atg8a membrane-association, and that dMtmr6 function is at least partially independent of either Vps34, Atg9, or Atg1 function.

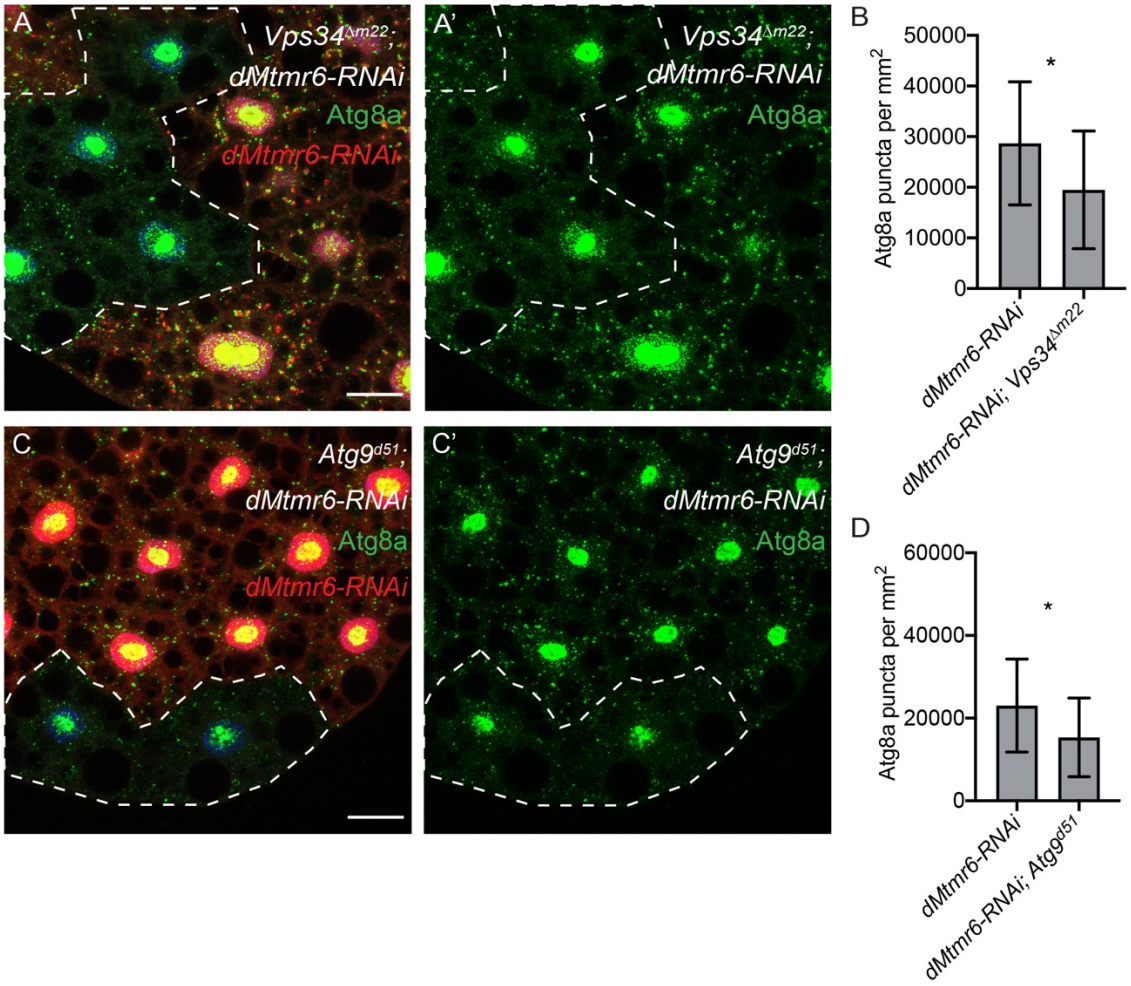

Figure 2.16. dMtmr6 regulates autophagic flux, partly independent of Vps34 and Atg9. (A and C) Representative images of starved fat body expressing *dMtmr6-RNAi* in which Vps34 (A) or Atg9 (C) homozygous null clones are induced (non-dsRed, white dashed outline) and stained with antibody to detect Atg8a. (B and D) Quantification of Atg8a puncta number (as represented in (A and C). Data information: in (B and D) data are presented as the mean ± SEM ($n \geq 9$). Asterisks denote statistical significance (*$P < 0.05$), using paired t test. Scale bars, 20 μm.

Autolysosomal homeostasis requires the MTMR8 PH-GRAM domain and catalytic cysteine residue

Despite documentation that MTMR8 hydrolyzes PI(3)P and PI(3,5)P_2 *in vitro* (Zou et al., 2012b; a), we lack evidence that the MTMR8 catalytic domain mediates autophagy. In fact, MTMR8 could influence autophagy by various membrane interactions, including PI(3)P or PI(3,5)P_2 hydrolysis (CX_5R motif) and membrane localization (PH-GRAM domain), which are required for other MTMR family members (Amoasii et al., 2012). To test these possibilities, we modified MTMR8 in HeLa cells using CRISPR/Cas9 to generate a cysteine to serine mutation (MTMR8-C338S), which is the amino acid change seen in the catalytically dead MTMR family members, and a PH-GRAM domain truncation (MTMR8ΔPH) **(Fig. 2.17 A)** (Lorenzo et al., 2006). Similar to the LAMP1 and LC3B puncta alterations in *MTMR8* knockdown cells **(Fig 2.17)**, LAMP1 and LC3B vesicles were larger in serum-fed MTMR8-C338S cells than in MTMR8 wild-type cells **(Fig. 2.17 B-E)**. Furthermore, fewer LAMP1 puncta, more LC3B puncta, and increased LAMP1/LC3B co-localization exist in MTMR8-C338S cells compared to MTMR8-WT cells **(Fig. 2.17 F-H)**. Although not significant, MTMR8-C338S influences autophagic flux in serum-fed conditions compared to control cells (not shown). These data suggest that MTMR8 catalytic activity influences autophagic flux.

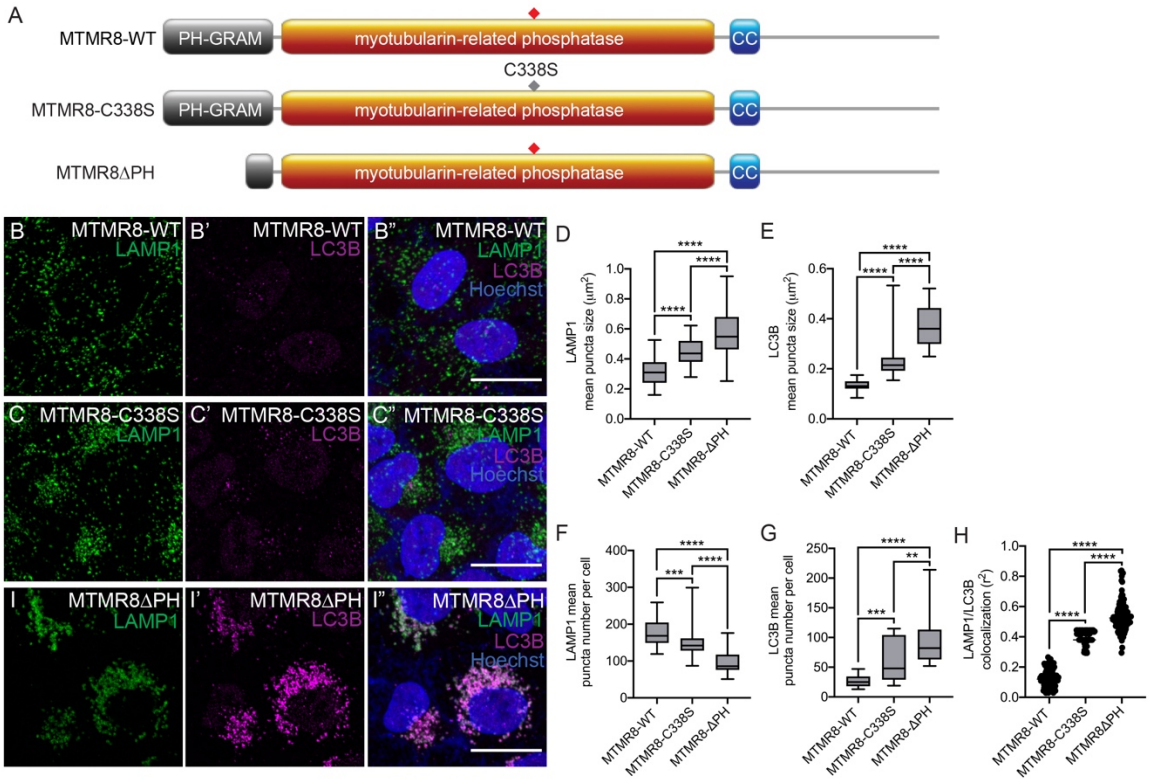

Figure 2.17. Autolysosome homeostasis requires the MTMR8 PH-GRAM domain and catalytic cysteine residue. (A) Schematic of MTMR8 constructs used in (B, C, and I). An intact PH-GRAM domain and catalytic cysteine residue exist in WT MTMR8, MTMR8-C338S features a serine in place of the catalytic cysteine, and the PH-GRAM domain is truncated in MTMR8ΔPH. (B, C, and I) Representative maximum intensity projection of z-stack image from HeLa cells with the indicated genotypes stained with Hoechst to detect nuclei (blue) and antibodies to detect LAMP1 (green) and LC3B (magenta), indicative of lysosomes and autophagosomes, respectively. Autolysosomes contain both LAMP1 and LC3B. (D-G) Quantification of the size (area in μm^2) and number of both LAMP1 and LC3B puncta per cell as represented in (B, C and I). (H) Quantification of LAMP1 and LC3B puncta colocalization as represented in (B, C and I). Data information: in (D-G), data are presented as mean ± min and max (n ≥ 5 cells per 10 random images from 3 experimental replicates in D-G, and in H, individual Z-planes from ≥ 5 cells per 10 random images). Asterisks denote statistical significance (**P < 0.01, ***P < 0.001, ****P < 0.0001), using one-way ANOVA. Scale bars, 20 μm.

We next investigated the requirement of the MTMR8PH-GRAM domain for autophagy. In striking comparison to both MTMR8-WT and MTMR8C338S cells, MTMR8ΔPH cells contain enlarged LAMP1 and LC3 puncta, reduced LAMP1 and increased LC3B puncta numbers, and significant co-localization between these two autophagic markers **(Fig. 2.17 B-I)**. Moreover, MTMR8ΔPH cells have more LysoTracker puncta than both MTMR8-WT and MTMR8-C338S cells, and LysoTracker staining significantly overlaps with LAMP1 **(Fig. 2.18 A-F)**. Thus, MTMR8 catalytic function influences autophagy, but MTMR8 membrane-localization via the PH-GRAM domain likely plays a more critical role in autolysosome homeostasis.

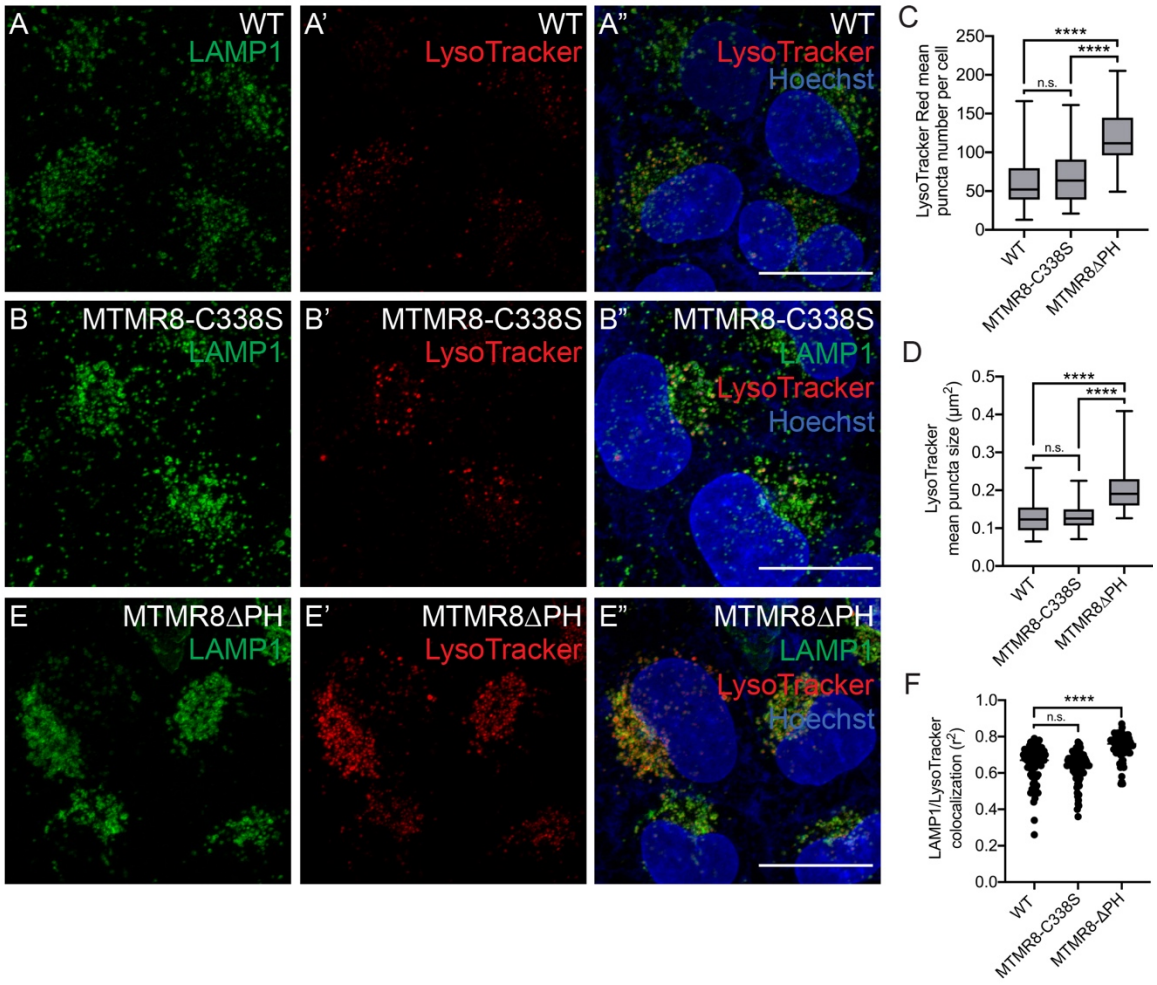

Figure 2.18. Autolysosome homeostasis requires the MTMR8 PH-GRAM domain and catalytic cysteine residue. (A, B, and E) Representative maximum intensity projection of z-stack image from HeLa cells of the indicated genotypes stained with Hoechst to detect nuclei (blue), Lysotracker to detect acidic vesicles (red), and LAMP1 antibody to detect lysosomes (green). Acidified lysosomal compartments contain both LAMP1 and LysoTracker. (C and D) Quantification of the number and size (area in μm^2) of LysoTracker puncta per cell as represented in (A, B and E). LAMP1 quantifications are in (Fig. 2.12 D and F). (F) Quantification of LAMP1 and LysoTracker puncta colocalization as represented in (A, B and E). Data information: (C-F), data are presented as mean ± min and max ($n \geq 5$ cells per 10 random images from 3 experimental replicates in C and D, and in F, individual Z-planes from ≥ 5 cells per 10 random images). Asterisks denote statistical significance (*P < 0.05, **P < 0.01, ****P < 0.0001), using one-way ANOVA (C, D, F) and unpaired t test (H). Scale bars, 20 μm.

Previous data indicate that MTMR8 favors PI(3)P, but can hydrolyze both PI(3)P and PI(3,5)P2 (Zou et al., 2012b). To investigate a role for MTMR8 in PI(3)P-regulation at autophagic membranes, we evaluated localization of WIPI2, a protein that binds early autophagic structures at PI(3)P-enriched sites (Dooley et al., 2014). We found a significant increase in WIPI2 puncta numbers in both MTMR8C338S and MTMR8ΔPH cells compared to MTMR8-WT control HeLa cells **(Fig. 2.19 J-O)**, which suggests that MTMR8 regulates PI(3)P levels at autophagic membranes. Furthermore, MTMR8C338S cells contain significantly more WIPI2 puncta than MTMR8ΔPH cells **(Fig. 2.19 K-M and O)**, indicating that the catalytic cysteine residue is important for decreasing PI(3)P levels, while the PH domain is likely important for MTMR8 recruitment to PI(3)P-bearing membranes. Moreover, WIPI2 and LC3B co-localize more in MTMR8C338S cells and less in MTMR8ΔPH cells **(Fig. 2.19 K, N, and O)**. We expected that impaired PI(3)P hydrolysis by MTMR8C338S could lead to increased WIPI2 recruitment, more LC3B conjugation, and increased WIPI2/LC3B co-localization. However, it is surprising that WIPI2/LC3B colocalization decreases in MTMR8ΔPH cells compared to MTMR8-WT control cells when WIPI2 puncta numbers increase, suggesting a possible role for the MTMR8 PH domain in WIPI2/LC3B localization.

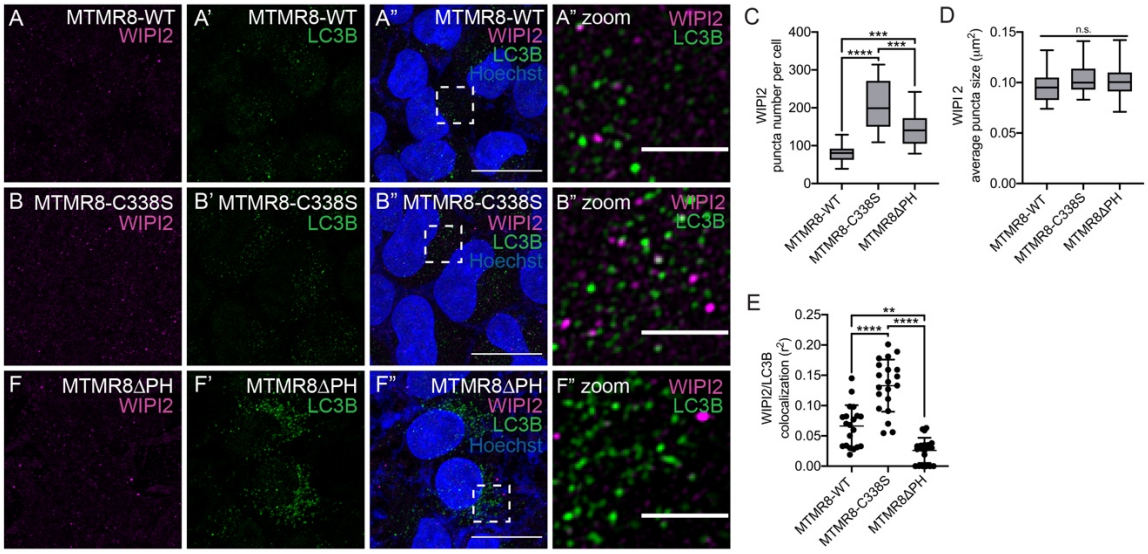

Figure 2.19. Mutations in the MTMR8 PH-GRAM domain and catalytic cysteine residue alter WIPI2 puncta levels and localization. (A, B, and F) Representative maximum intensity projection of z-stack image from HeLa cells with the indicated genotypes stained with Hoechst to detect nuclei (blue) and antibodies to detect WIPI2 (magenta) and LC3B (green). (C-E) Quantification of the number and size of WIPI2 puncta and colocalization between WIPI2 and LC3B as represented in (J, K and O). Data information: in (C-E), data are presented as mean ± min to max (n ≥ 5 cells per 10 random images from 3 experimental replicates). Asterisks denote statistical significance (**P < 0.01, ***P < 0.001, and ****P < 0.0001), using one-way ANOVA. Scale bars, 20 μm.

Previous work indicates that MTMR8 localizes to the perinuclear region (Lorenzo et al., 2006). We surmised that MTMR8 might localize to a perinuclear lysosomal pool to facilitate autolysosome resolution. We initially used CRISPR/Cas9 to tag the MTMR8 C-terminus with 3xFLAG, but we were unable to detect FLAG by either immuno-fluorescence or -blotting. Therefore, we over-expressed MTMR8. Unlike Lorenzo et al., we saw peripheral localization, and MTMR8 failed to overlap with perinuclear-localized LC3B puncta **(Fig. 2.20 A)**. Consistent with previous work (Zou et al., 2012b) and our evidence that MTMR8 influences autophagic flux **(Fig. 2.5)**, p62 protein levels decreased and lipidated LC3B levels increased in cells over-expressing MTMR8 **(Fig. 2.20 B).** Taken together, these data suggest that MTMR8 influences autophagic flux by promoting lysosome-mediated degradation.

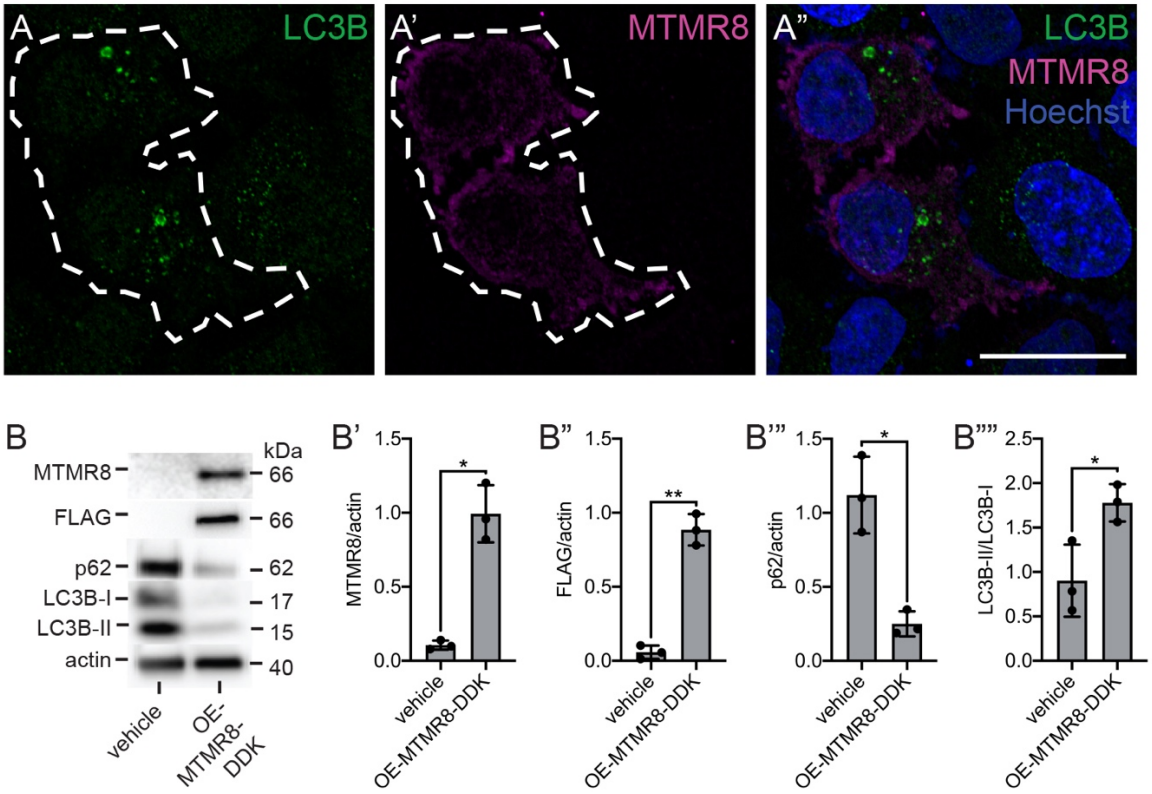

Figure 2.20. MTMR8 misexpression promotes autophagic degradation. (A) Representative maximum intensity projection of z-stack image from HeLa cells transfected with *myc-DDK-MTMR8* and antibody stained with antibodies to detect LC3B (green) and MTMR8 (magenta, white dashed line). (B) Representative western blot from HeLa cells transfected with vehicle (control, Lipofectamine 2000) or *myc-DDK-MTMR8* to detect MTMR8, DDK (FLAG), p62, and LC3B. Relative protein levels are quantified as the ratio of: MTMR8 to actin (B'), FLAG to actin (B'), p62 to actin (B'"), and LC3B-II to LC3B-I (B""). Data information: in (B), data are presented as mean ± SD (n = 3 experimental replicates). Asterisks denote statistical significance (*P < 0.05 and **P < 0.01) using unpaired t test. Scale bars, 20 μm.

DISCUSSION

We identified *Drosophila CG3530/Mtmr6* as a negative regulator of autophagy, and show that *MTMR8* has a similar function in both human and monkey cells. d*Mtmr6* maintains autophagic flux in multiple fly tissues under different conditions, including stress- and developmentally-induced autophagy. We demonstrated that dMtmr6 and MTMR8 play a critical role in regulating the amount and size of cellular Atg8a/LC3B-positive vesicles. Furthermore, these structures correlated with lysosome markers and demarcated the existence of autolysosomes. Depletion of *dMtmr6* in fly tissues or *MTMR8* in mammalian cells influences endolysosomal homeostasis and promotes autolysosome accumulation.

Myotubularin-related phosphatases dictate intracellular membrane identity and modulate membrane trafficking events, including autophagy, through PI(3)P and PI(3,5)P_2 degradation. However, differential expression of MTMRs implies that they may have cell- and tissue-specific functions (Raess et al., 2017a). According to bioinformatics studies from public data at the Genotype-Tissue Expression (GTEx) database, the roles and requirements for the different MTMRs are thought to differ according to tissue and cell type. For example, *MTMR8* is expressed at higher levels in reproductive tissues than in brain tissues, which instead, express *MTMR7*. Meanwhile, *MTMR6* is most highly expressed in the adrenal gland and testis. We tested HEK293T cells (kidney) in our analyses (not shown) and found that *MTMR8* knockdown had a less significant effect on autophagic structures than in HeLa cells (cervical). These data are consistent with the data of Raess et al.

(2017) which show lower *MTMR8* expression in kidney and higher *MTMR8* expression in cervical tissues. Like *MTMR8,* publicly available RNA-sequencing of *Drosophila* tissues indicates that *dMtmr6* is highly expressed in reproductive tissues, and both *MTMR8* and *dMtmr6* are moderately expressed in tissues of the digestive tract (Thurmond et al., 2019). Unlike *MTMR8* however, *dMtmr6* is highly expressed in head of adult flies, hinting at a role for dMtmr6 in the brain and potentially the central nervous system. Interestingly, *dMtmr6* muscle-specific knockdown impairs *Drosophila* flight (Schnorrer et al., 2010).

Tissue- and cell-specificity at least partially account for the diverse regulatory functions of the MTMR6 subfamily members and their binding partner, MTMR9. Human MTMR6 facilitates PI(3)P turnover during micropinocytosis (Maekawa et al., 2014), negatively regulates the Ca^{2+}-activated K^{+} channel KCa3.1 in CD4 T cells (Srivastava et al., 2005, 2009), and apoptosis in HeLa cells (Zou et al., 2009a, 2012a). Similar to *dMtmr6*, which regulates AKT signaling in *Drosophila* fat body (Fig. 7 A), both MTMR7 and MTMR9 regulate CD4 T-cell AKT signaling and differentiation (Guo et al., 2013), and MTMR7 regulates AKT signaling in C2C12 myoblasts. MTMR7 protein levels inversely correlate with tumor grade in colorectal cancer (CRC), and in CRC cell lines, MTMR7 inhibits proliferation and insulin-mediated AKT-ERK1/2 signaling (Weidner et al., 2016). In zebrafish embryos, MTMR8 regulates actin filament modeling (Mei et al., 2009) and both muscle (Mei et al., 2009) and vascular development (Mei et al., 2010). It is important to note that the mouse genome lacks MTMR8 and contains only MTMR6

and MTMR7. In human cells, the MTMR8/R9 complex reduces PI(3)P levels and inhibits autophagy (Zou et al., 2012b). MTMR9 mutations are associated with obesity (Yanagiya et al., 2007), metabolic syndrome (Hotta et al., 2011), and multiple prediabetes-associated symptoms (Tang et al., 2014). While a specific link to MTMR8 in disease remains to be determined, alterations in the MTMR8 locus have been implicated in glioblastoma multiforme (Waugh, 2016) and intellectual disability (Holman et al., 2013). Furthermore, a rare type of x-linked spastic paraplegia (SPG16, OMIM, 300266) is mapped to an uncharacterized locus at Xq11.2, which is where MTMR8 resides. Future studies could benefit from mining genome- and exome-sequencing databases for the influence of this MTMR family on disease.

An additional difference exists between *MTMR8* and *dMtmr6*. *MTMR8* encodes one human isoform while *dMtmr6* encodes three **(Fig. 2.3 A)**. We have not experimentally tested the significance of *dMtmr6* splice isoforms. However, publicly available data of fly gene expression during development indicates that there is ubiquitous expression of *dMtmr6* B and C isoforms throughout development (Thurmond et al., 2019). The *dMtmr6* A isoform is expressed at low levels during early embryonic development, ceases during late embryonic development, and increases progressively throughout L3 stage. In adult flies, isoform A is expressed lower in females than in males. Potentially relevant to our findings, third instar wandering fat body expresses both B and C, but not A. However, upon pupa formation when numerous tissue types undergo

developmental autophagy, all three isoforms are expressed. Thus, *dMtmr6* isoform A could play a specific role in developmental autophagy while isoforms B and C function more generally. Our data indicate that *dMtmr6* is required for survival **(Fig. 2.3 B)**, yet some trans-heterozygous animals that are *dMtmr6*^{KG01267}*/Df(2R)* survive to adults. The *dMtmr6*^{KG01267} allele retains isoform A, which indicates that, in the absence of isoforms B and C, isoform A could function in a compensatory way to support survival. Future experiments should explore the possibility of isoform-specific *dMtmr6* functions in development and cellular trafficking.

Despite evidence of autophagy initiation, *dMtmr6* and MTMR8 depletion elicits ref(2)p/p62 accumulation, indicative of impaired degradation **(Fig. 2.3 C, 2.4 A-D, and 2.5 C, D and I)**. However, autophagosome-lysosome fusion remains intact based on GFP signal reduction in *dMtmr6* fat body expressing the tandem-fluorescent Atg8a reporter **(Fig. 2.7 A-D)**. This reporter recapitulated the aberrant large autophagic puncta we saw with mCherry-Atg8a alone in *dMtmr6*-depleted fat body from fed animals and supplied evidence that upon fusion, lysosomal pH remains low enough to quench the GFP signal from autophagic structures. Furthermore, *dMtmr6* depleted cells possess elevated levels of LysoTracker and cathepsin B protease activity compared to adjacent wild-type cells **(Fig. 2.10 A-D)**. These data imply that in *dMtmr6*-deficient cells, lysosomes harbor some functional aspects required for degradation. Similarly, *MTMR8*-deficient and -mutant cells bear numerous and large vesicles that are positive for LC3B, LAMP1, and LysoTracker, indicative of acidified autolysosomes **(Fig. 2.9, 2.17 B-I, and 2.18 A-**

F). Thus, in *dMtmr6*- and *MTMR8*-depleted cells, autophagosomes form and fuse with lysosomes, which suggests that they promote post fusion endolysosomal homeostasis.

We also evaluated *Drosophila* cathepsin-L protein levels **(Fig. 2.10 E)**. Lysosomal cathepsins are synthesized as inactive preproenzymes that undergo subsequent maturation steps (Stoka et al., 2016). Following preprocathepsin synthesis in the ER, the N-terminal signal peptide is cleaved and glycosylated to generate procathepsin. Glycosylation ensures that cathepsins remain inactive until low pH triggers propeptide unfolding and either successive autocleavage or cleavage by other active cathepsins. We showed that cathepsin L undergoes maturation in *dMtmr6*-depleted *Drosophila* fat body from fed and starved animals, but the balance between prepro-, pro-, and mature cathepsin L differs compared to wild type fat body under the same conditions **(Fig. 2.10 E)**. Indeed, high levels of prepro- and procathepsin L exist in *dMtmr6*-knockdown tissue. For this, one possible explanation is that *dMtmr6*-deficiency influences cathepsin L processing. However, we can detect mature cathepsin L, and an alternative possibility is that *dMtmr6*-depletion prompts lysosome biogenesis. This idea is further supported by our evidence of augmented mitf(TFEB) target-gene transcription in *dMtmr6*-depleted tissues **(Fig. 2.6 F)**, denoting activation of autophagy and lysosome biogenesis (Sardiello et al., 2009). It appears that *MTMR8*-depleted cells undergo a similar response because TFEB localized to the nucleus of HeLa cells under both serum-fed and serum-starved conditions.

Phosphorylated p70 S6K and Akt levels are reduced in *Drosophila dMtmr6*-knockdown fat body from fed animals compared to control animals **(Fig. 2.14)**, which likely explains the influence of dMtmr6/MTMR8 on Mitf/TFEB. Indeed, both phospho-p70 S6K and -Akt are indicators of mTORC1 activity, and phosphorylation is indicative of ample nutrients and growth factors (Liu and Sabatini, 2020). When active, mTORC1 localizes to lysosomes and inhibits TFEB nuclear localization (Settembre et al., 2012), and Akt represses TFEB nuclear localization independent of mTORC1 (Palmieri et al., 2017). Conversely, starvation and lysosome stress prompts mTORC1 dissociation from lysosomes, TFEB nuclear translocation, and autophagy induction (Settembre et al., 2012). During prolonged starvation, cells require mTORC1 reactivation to replenish the lysosome pool (Yu et al., 2010). Furthermore, active mTORC1 is required for lysosomal tubulations, which is a critical step in autolysosome reformation (Yu et al., 2010). Once reactivated, mTORC1 functions upstream of PIK3C3 to produce a small pool of autolysosomal PI(3)P, and loss of PIK3C3 activity, despite active mTORC1, prevents tubule scission. Our genetic epistasis analyses indicated that *dMtmr6* functions at least in a partially independent manner of class III PIK Vps34 **(Fig. 2.16 A and B)**. As mentioned above, our data suggest that *dMtmr6* functions at the autolysosome to facilitate degradation. In *Drosophila* blood cells, the class II PI3K, Pi3K68D coregulates endolysosomal size and cortical dynamics with mtm, an MTMR family member, via a pool of PI(3)P (Velichkova et al., 2010). However, endolysosomal size in blood cells is also *Atg1* and *Vps34*-dependent, unlike

dMtmr6. The results of our phosphatase screen indicate that mtm does not play a role in fat body or developmental midgut autophagy **(Appendix A)**. Moreover, we do not think that *dMtmr6* plays a role in cortical remodeling of blood cells. We were able to observe actin filaments (as seen by LifeAct localized accumulation) at extending protrusions in both control and *dMtmr6*-depleted blood cells **(Fig. 2.13 F and G)**, which strongly suggests that *dMtmr6* does not play a direct role in actin filament turn-over.

We showed that *dMtmr6*-depleted macrophages contained fewer phagocytic vacuoles than control blood cells **(Fig. 2.13 F and G)**. Phagocytosis requires Vps34 to produce PI(3)P, and like autophagy, terminates as lysosomal hydrolases degrade cargoes (Jeschke and Haas, 2016). During *Drosophila* embryonic development, apoptotic corpses are removed by macrophages, a process that primes these blood cells for ensuing immune responses later in life (Weavers et al., 2016). Our findings imply that *dMtmr6* supports macrophage corpse-uptake. Similarly, we saw impaired uptake of TR-avid by fluid-phase endocytosis in *dMtmr6*-depleted fat body cells **(Fig. 2.11 A and B)**. In the nematode *Caenorhabditis elegans*, MTM-1, MTM-6, and MTM-9 facilitate fluid-phase endocytosis in coelomocytes (Dang et al., 2004; Xue et al., 2003), and MTM-1 negatively regulates apoptotic corpse engulfment (Neukomm et al., 2011; Zou et al., 2009b). Thus, MTMRs have an evolutionarily conserved role in these diverse but related trafficking processes.

Here we demonstrate that dMtmr6 and MTMR8 negatively regulate late-stage autophagy and play a critical role in regulating autophagic flux. Our analyses revealed critical requirements for dMtmr6 and MTMR8 in preventing expansion of the Atg8a/LC3B compartment, leading to autolysosome accumulation, and impairing autophagic flux in multiple cell and tissue types. Defects in autophagic flux underlie lysosomal storage disorders and neurodegenerative diseases, including Parkinson's and Huntington's. Thus, it remains important to identify novel drug targets to modulate autophagy levels. Future studies of MTMR6 family members will reveal if they are useful targets to mitigate human diseases.

MATERIALS AND METHODS

Fly stocks

Drosophila melanogaster were raised on standard cornmeal-molasses-agar medium. We performed fly crosses and experiments at 25°C unless noted otherwise. We used *UAS-Luciferase* as the wild-type control for RNAi experiments. We used CRISPR/Cas9 to delete the *dMtmr6* open reading frame (Well Genetics, Taiwan). To generate RNAi-expressing cell clones, we crossed *yw hsFlp*; pmCherry-*Atg8a*; *Act*>CD2> Gal4, *UAS-GFP* (nls) virgin females to *UAS-RNAi* males. To generate tissue-specific knockdown, we crossed *Np1*-Gal4 virgins for intestinal-knockdown or *CG*-Gal4 virgins for fat body knockdown to *UAS-RNAi* males. For *dMtmr6* mutant cell clones we crossed *yw hsFlp*; *FRT42D, ubi-RFP* virgin females to *FRT42D, dMtmr6Δ* males. For *Vps34* and *Atg9* mutant clones, we crossed *yw hsFlp*; *FRT42D, ubi-RFP*; *Lsp2*-Gal4 to either *yw hsFlp; FRT42D, Vps34*$^{\Delta m22}$*/cyo; dMtmr6-RNAi*^{BL38340} or *yw hsFLP; FRT42D, Atg9*^{d51}*/cyo; dMtmr6-RNAi*^{BL38340}. The following fly stocks used were from the Bloomington Drosophila Stock Center (BDSC): *UAS-CG3530*^{HMS01807}, and *UAS-Luciferase*^{35788}. The sequences for BDSC knockdown strains are available via the *Drosophila* RNAi Screening Center and Transgenic RNAi Project (DRSC/TRiP) at https://fgr.hms.harvard.edu. We used RNAi lines from Vienna Drosophila RNAi Center (VDRC): UAS-*Atg1*^{GD16133}, UAS-*CG3530*^{GD26216}. The sequences for VDRC knockdown strains are available for each at http://stockcenter.vdrc.at/control/main.

We thank the following researchers for mutant flies: Gabor Juhász for *Vps34*$^{\Delta m22}$ (Juhász et al., 2008) and Guang-Chao Chen for *Atg9*^{d51} (Wen et al., 2017).

Induction of cell clones and quantification

We induced RNAi clones in midgut or fat body cells by crossing virgin females of *y w hsFlp*; *pmCherry-Atg8a*; *Act >CD2 >GAL4* (> is FRT site), *UAS-nlsGFP/TM6B* (reference) or *y w hsFlp*; + ; *Act >CD2 >GAL4, UAS-nlsGFP/TM6B* to indicated transgenic RNAi lines. We induced *dMtmr6* mutant cell clones in midgut or fat body by crossing *yw hsFlp*; *FRT42D, ubi-GFP* virgin females to *FRT42D, dMtmr6Δ* males, and we induced *Vps34* and *Atg9* mutant clones by crossing *yw hsFlp*; *FRT42D, ubi-RFP*; *Lsp2*-Gal4 to either *yw hsFlp; FRT42D, Vps34*$^{\Delta m22}$*/cyo; dMtmr6-RNAi*^{BL38340} or *yw hsFLP; FRT42D, Atg9*^{d51}*/cyo; dMtmr6-RNAi*^{BL38340}. Following one-day egg lays, we heat-shocked embryos at 37°C for 10 minutes for RNAi clones or 1 hour for homozygous mutant clones. White prepupae were placed on wet filter paper for 2 h before dissection.

Starvation of larvae

We transferred feeding third instar larvae to 20% sucrose (starved) for 4 h or kept larvae in food (fed).

Immunolabeling and microscopy of *Drosophila* tissues

We dissected midguts or fat body in PBS (GIBCO), fixed tissues in 4% formaldehyde in PBS 0.1% Triton X-100 (PBS-TX) overnight at 4°C, blocked with 1% bovine serum albumin and 0.5% cold fish skin gelatin, and incubated overnight at 4°C with primary antibodies in PBS-TX. For immunolabeling, we used rabbit anti-GABARAP (1:100, from Cell Signaling Technologies, 13733), chicken anti-GFP (1:500, Abcam, catalogue number ab13970), rabbit anti-ref(2)p (1:100, Abcam, ab178440). We used Hoechst dye to stain DNA and the following secondary antibodies (1:250): anti-rabbit Alexa Fluor 546 (ThermoFisher, A-11035), anti-mouse 546 (Invitrogen, A-11003), or anti-rat Alexa Fluor 488 or 546. We mounted samples in VectaShield (Vector Lab). We imaged samples with a Zeiss LSM 700 confocal microscope. For LysoTracker Red (LTR) staining, we dissected tissues in PBS, transferred samples to LTR diluted in PBS (1:1000) on ice for 5 minutes, mounted samples in 80% glycerol (in PBS), and imaged immediately with a Zeiss AxioImager Z1 microscope. For Magic Red staining, we dissected tissues in PBS, followed by a 30 m incubation in Magic Red (diluted 1:10 in PBS, Magic Red Cathepsin B Assay, ImmunoChemistry, 937), a quick wash in PBS, and imaged immediately. For mCherry-Atg8a and GFP-2xFYVE imaging, we fixed samples briefly with 4% formaldehyde in PBS-TX, mounted in VectaShiled, and imaged samples with a Zeiss AxioImager Z1 microscope. We calculated p values using a paired t test for adjacent cells, an unpaired t test for two separate genotypes under one condition, and an ordinary two-way ANOVA for comparison

of multiple genotypes or conditions. Data is plotted as either min to max or the mean ± SEM.

Texas Red-avidin uptake assay

To visualize endocytosis, we dissected fat body from feeding third instar larvae and incubated it *ex vivo* with Texas Red-avidin (Invitrogen, A820) diluted in Schneider's media to a concentration of 80 μg/ml for 20 minutes, and then chased with 0.5% BSA in cold PBS for 10 minutes prior to overnight fixation with 4% formaldehyde. We washed the tissue three times (10 minutes per wash) with 0.1% Tween-20 in PBS and mounted in Vectashield (Vector Laboratories). We imaged samples with a Zeiss LSM 700 confocal microscope with 40x/1.30 Oil DIC M27 objective at room temperature (22 ºC) using Zeiss Zen Software, and processed images using ImageJ (NIH).

Cell Culture and Immunostaining

We cultured COS7 (ATCC, CRL-1651) and HeLa cells (ATCC, CCL-2) in DMEM supplemented with 10% FBS and penicillin-streptomycin at 37^0C and 5% CO_2). We applied experimental conditions and collected cells at a specific time point for either immunostaining or western blotting. For immunostaining, we fixed cells in 4% PFA for 20 min, permeabilized in 10μg/ml digitonin (Sigma, D141) for 15 min

at room temperature, and blocked with 5% goat serum for 60 min at room temperature. We incubated cells overnight at 4^0C in the following primary antibodies (diluted in 5% goat serum): rabbit anti-LC3B (1:1000, Abcam, ab48394), mouse monoclonal anti-LAMP1 (1:1000, BD Biosciences, 555798), mouse anti-Lamp2 (0.5 µg/mL, DSHB, H4B4), rabbit anti-p62 (1:2000, MBL, PM045), rabbit anti-TFEB (1:1000, Cell Signaling Technologies, 4240), and mouse anti-WIPI2 (1:500, Abcam, ab105459). After 3 washes with PBS, we incubated cells for 1 h at room temperature with Hoechst to stain nuclei and the following fluorescently-labeled secondary antibodies (1:250): anti-rabbit Alexa Fluor 546 (ThermoFisher, A-11035), anti-mouse 546 (Invitrogen, A-11003), or anti-rat Alexa Fluor 488 or 546. We mounted specimens with Vectashield, examined with a Zeiss LSM 700 confocal microscope with 63x/1.40 Oil DIC M27 objective at room temperature (22 ºC) using Zeiss Zen Software, and processed images using ImageJ (NIH). For serum starvation, we incubated cells in EBSS (Gibco). For Bafiloymycin treatment, we incubated cells for 12 hours in Bafilomycin A1 (20 µM, Sigma-Aldrich, B1793).

Transfection, RNA interference, and MTMR8 overexpression

For knockdown experiments, we transfected cells with either control or siRNA oligos using Invitrogen Lipofectamine RNAiMAX (ThermoFisher Scientific, 13778150), and cultured for 72 h prior to analyses. We purchased double-stranded siRNAs from GenePharma, and sequences are in Table S2. For MTMR8-

overexpression experiments, we transfected cells with Lipofectamine 2000 Transfection Reagent (ThermoFisher Scientific, 11668019) either as vehicle only or to deliver Myc-DDK-MTMR8 (Origene, RC201912), and cultured for 24 h prior to analyses.

HeLa cell gene editing

To generate MTMR8-C338S and MTMR8ΔPH HeLa cells, we delivered a CRISPR/Cas9 ribonucleoprotein complex containing tracrRNA:crRNA complex, Cas9 enzyme, and single-stranded donor oligonucleotides (ssODN), using electroporation with the Neon™ transfection system (MPK5000, Thermo Fisher Scientific). We acquired tracrRNA, crRNA, Cas9 and ssODN from Integrated DNA Technologies (IDT) and identified positive single cell clones by PCR amplification and Sanger sequencing. The gRNA and ssODN sequences are as follows.

MTMR8-C338S gRNA: GGTCCCATCCATCAGAACAA

MTMR8-C338S-ssODN:

TCTTGTCTTCACAGGCAGTGAAGGTAGAAAAGGCCAGTGTCTTAGTACATAG

TTCTGATGGATGGGACCGCACAGCACAAGTCTGCTCAGTGGCTAGCAT

MTMR8ΔPH gRNA – 5’: GGTAGAAAACGTGAAATTGG

MTMR8ΔPH gRNA – 3’: GCAGTGAAATATAAACCTCA

MTMR8ΔPH-ssODN:

GGTAACTTATTCAGTATTTTTTCCTCCAATAACAGGTAGAAAACGTGAAAAG
GTTTATATTTCACTGCTCAAGCTTTCTCAGCCAGGTAGTTATGATAGT

Immunoblotting assays

We washed mammalian cells 3 times with PBS, added lysis buffer (50 mM Tris-HCl, pH 7.5, 150 mM NaCl, 1 mM EDTA, 1% Triton X-100) supplemented with protease inhibitor cocktail (ThermoFisher, 78425), and incubated for 30 min on ice. We centrifuged homogenates at 13,000 rpm for 10 min at 4^0C. We subjected supernatants to SDS-PAGE electrophoresis, transferred proteins to 0.45 mm Immobilon-P PVDF membranes (Millipore, IPVH00010), and detected signals using the following primary antibodies: mouse monoclonal anti-LC3 (clone 4E12, 1:1000, MBL, M152-3), rabbit polyclonal anti-p62 (1:1000, MBL, PM045), mouse monoclonal anti-actin (1:2000, clone 7D2C10, Proteintech, 60008-1-Ig).

For fly tissues, we dissected fat body from larvae in PBS. We homogenized fat body in Laemmli buffer (0.1% glycerol, 2% SDS, 0.125 M Tris[pH 6.8], 0.05% β-mercaptoethanol, and 0.05% bromophenol blue) and boiled for 10 min at 100^0C. Equal amounts of proteins were separated on 12% SDS polyacrylamide gels, and we transferred proteins to 0.45 mm Immobilon-P PVDF membranes (Millipore, IPVH00010) according to standard procedures. We used the following primary antibodies: rabbit anti-GABARAP (1:1000, Cell Signaling Technology, 13733),

rabbit anti-Ref(2)p (1:1000, Abcam, ab178440), mouse anti-β-Tubulin (1:50, Developmental Studies Hybridoma Bank, E7), or mouse anti-β-actin (1:2000, Proteintech, 60008-1-Ig). We used the following secondary antibodies: HRP goat anti-mouse IgG (H+L) (1:5000, Thermo Fisher Scientific, 31430) and HRP goat anti-rabbit IgG (H+L) (1:5000, Invitrogen, 62-6120). We performed three independent biological replicates.

Embryonic phagocytic corpse clearance assays

Embryos of the appropriate developmental stage were collected from overnight apple juice plates, dechorionated in bleach for 90 seconds and mounted on double-sided sticky tape on glass slides in 10S Voltalef oil (VWR). *Srp*-Gal4, UAS-*LifeAct-GFP*/(*Cyo*) embryos were used as a control. We analyzed individual hemocytes, scoring the number of vacuoles at arbitrary time-points over a 20-minute time-lapse. Imaging was performed on a Zeiss LSM880 with Airyscan laser scanning confocal microscope. Z-stacks and time-lapse images were processed and analyzed in ImageJ (NIH), Adobe Photoshop, and Adobe Illustrator software. Graphical representations were generated in GraphPad Prism 8.

Electron Microscopy

For fly tissues, we dissected intestines in PBS (GIBCO) 2 hours after puparium formation, fixed in a solution of 2.5% glutaraldehyde and 2% paraformaldehyde in 0.1M sodium cacodylate buffer, pH 7.4 (Electron Microscopy Sciences) for 1 hour at room temperature followed by overnight fixation at 4°C in fresh fix. Following fixation, we washed the guts in 0.1M sodium cacodylate buffer, pH 7.4, post-fixed in 1% osmium tetroxide in distilled water for 1 hour at room temperature and washed in distilled water. Preparations were stained *en bloc* in 1% aqueous uranyl acetate for 1 hour at 4°C in the dark, washed in distilled water, dehydrated through a graded ethanol series, treated with propylene oxide and infiltrated in SPI-pon/Araldite for embedding. We cut ultrathin sections on a Leica UC7 microtome. Sections were stained with uranyl acetate and lead citrate and examined on a Phillips CM10 TEM. Images were taken down the length of the gut to ensure an unbiased approach. We reviewed all images and chose representative images for analyses. We measured area of organelles and cytoplasm in ImageJ (NIH), and graphical representations were generated in GraphPad Prism 8.

For COS7 cells, we prefixed cells in 50% media: 50% fix, 2.5% glutaraldehyde and 2% paraformaldehyde in 0.1M sodium cacodylate buffer, pH 7.4 (Electron Microscopy Sciences) for 5 minutes followed by fixation in full fix for 1 hour at room temperature. Cells were then washed with 0.1M cacodylate buffer, pH 7.4, post-fixed in 1% osmium tetroxide in distilled water for 1 hour at room temperature and washed in distilled water. Preparations were stained *en bloc* in

1% aqueous uranyl acetate over night at 4°C in the dark and then washed in distilled water. The cells were then scraped and pelleted. Cell pellets were embedded in agarose, dehydrated through a graded ethanol series, treated with propylene oxide and infiltrated in SPI-pon/Araldite for embedding. We cut ultrathin sections on a Leica UC7 microtome. Sections were stained with uranyl acetate and lead citrate and examined using a Phillips CM10 TEM.

RT-PCR

We collected RNA from fat body dissected from third instar larvae (*n*=10) using Trizol Reagent (Invitrogen) and treated with DNase. We generated cDNA from 1 µg of RNA, using Superscript III Reverse Transcriptase and oligo (dT) (Invitrogen, 18080051) according to manufacturer's instruction. cDNA of indicated genes was amplified by PCR using Power SYBR Green Master Mix (ThermoFisher, 4368577) according to manufacturer's instruction and the following specific primers:

actin5c forward primer 5'-GGATGGTCTTGATTCTGCTGG-3', reverse primer 5'-AGGTGGTTCCGCTCTTTTC-3', PCR product size: 146 bp; *dMtmr6* forward primer 5'-GACAGGATCTCCGCTACTCAT-3', reverse primer 5'-GCAGCGAAGTGTAGACATCGT-3', PCR product size: 98 bp; *Atg1* forward primer 5'- GTCGGGGAATATGAATACAGCTC -3', reverse primer 5'-GCATGTGTTTCTTGCGATGAC -3', PCR product size: 91 bp; *Atg18* forward primer 5'- GTGTTCGTCAACTTCAACCAGA -3', reverse primer 5'-

TGTCCAGGGTCGAGTCCAC -3', PCR product size: 100 bp; *Cp1* forward primer 5'-TCAACTACACTCTGCACAAGC-3', reverse primer 5'-GCCAGTCCACAGATTTGGG-3', PCR product size: 105 bp; *Mitf* forward primer 5'- AGTATCGGAGTAGATGTGCCAC -3', reverse primer 5'-CGCTGAGATATTGCCTCACTTG -3', PCR product size: 115 bp; *Ref(2)p* forward primer 5'- AATCGAGCTGTATCTTTTCCAGG -3', reverse primer 5'-AACGTGCATATTGCTCTCGCA -3', PCR product size: 148 bp. We resolved the PCR products on a 1.5% agarose gel.

QUANTIFICATION AND STATISTICAL ANALYSES

All experiments were performed independently at least three times, except for TEM. For mCherry-Atg8a, ref(2)p, LysoTracker Red, Texas Red-Avidin, or GABARAP antibody labeled puncta quantification, we chose at least 10 random images and counted the number of puncta in GFP-positive cells versus neighboring non-GFP cells. We examined an average of 20 cells for each group. For colocalization analyses, we used the EzColocalization plugin for ImageJ to determine the Pearson correlation coefficient per image or per region of interest (Stauffer et al., 2018). Statistical significance was analyzed by paired or unpaired t test for single comparisons and one-way ANOVA analysis for multiple comparisons as described in figure legends. A $P\ value < 0.05$ was considered

statistically significant. Statistics were performed using GraphPad Prism 8 software.

ACKNOWLEDGEMENTS

We thank the Bloomington Stock Center, the VDRC, and Well Genetics for flies, the Wolfe lab for use of their Neon™ Transfection system, and the Baehrecke lab and Yan Zhao for constructive comments. This work was supported by NIH grants R35GM131689 to EHB and 5T32CA130807-10, and Wellcome Trust Fellowship to WW (107940/Z/15/Z).

CHAPTER III

Discussion

Autophagy is regulated by numerous factors, including nutritional and developmental cues, molecules, and membrane dynamics. Phosphoinositide conversion mediates all aspects of autophagy from lysosome-mediated nutrient signaling to effector recruitment and membrane changes. My thesis work takes advantage of the nutrient- and hormone-regulated autophagy programs in larval *Drosophila* fat body and midgut, respectively. I discovered CG3530/dMtmr6 during a genetic screen for phosphatases that regulate midgut autophagy and focused my thesis work on investigating the role of CG3530/dMtmr6 in autophagy. To emphasize the conserved functions of human MTMR8, I used primate cell lines in which we can induce autophagy through nutrient restriction, like in *Drosophila* fat body. My work identified dMtmr6 and MTMR8 as conserved regulators of autophagic flux and endolysosomal homeostasis. Depletion of *dMtmr6* in starvation-induced fat body and developmental midgut autophagy impaired lysosome dysfunction and promoted the accumulation of large autolysosomes. Similarly, both *MTMR8*-knockdown cells and MTMR8 mutant cells harboring a truncation in the phosphoinositide-binding PH-GRAM domain accumulated autolysosomes. Meanwhile, a mutation in the MTMR8 catalytic phosphatase site affected autolysosome numbers and size, but to a lesser degree. Both *dMtmr6*- and *MTMR8*-depletion resulted in lysosomal acidification and activation of Mitf/TFEB, which promotes lysosome biogenesis and autophagy. However levels of the autophagy substrate ref(2)p/p62 remained high, which indicated that autophagic structures were generated, but not degraded. Depletion of *dMtmr6* also

impaired fluid phase endocytosis and phagocytosis, which are additional cellular degradation pathways that converge at the lysosome. Together, these data support a role for dMtmr6 and MTMR8 in lysosome function, thus advancing our understanding of how MTMRs regulate autophagy.

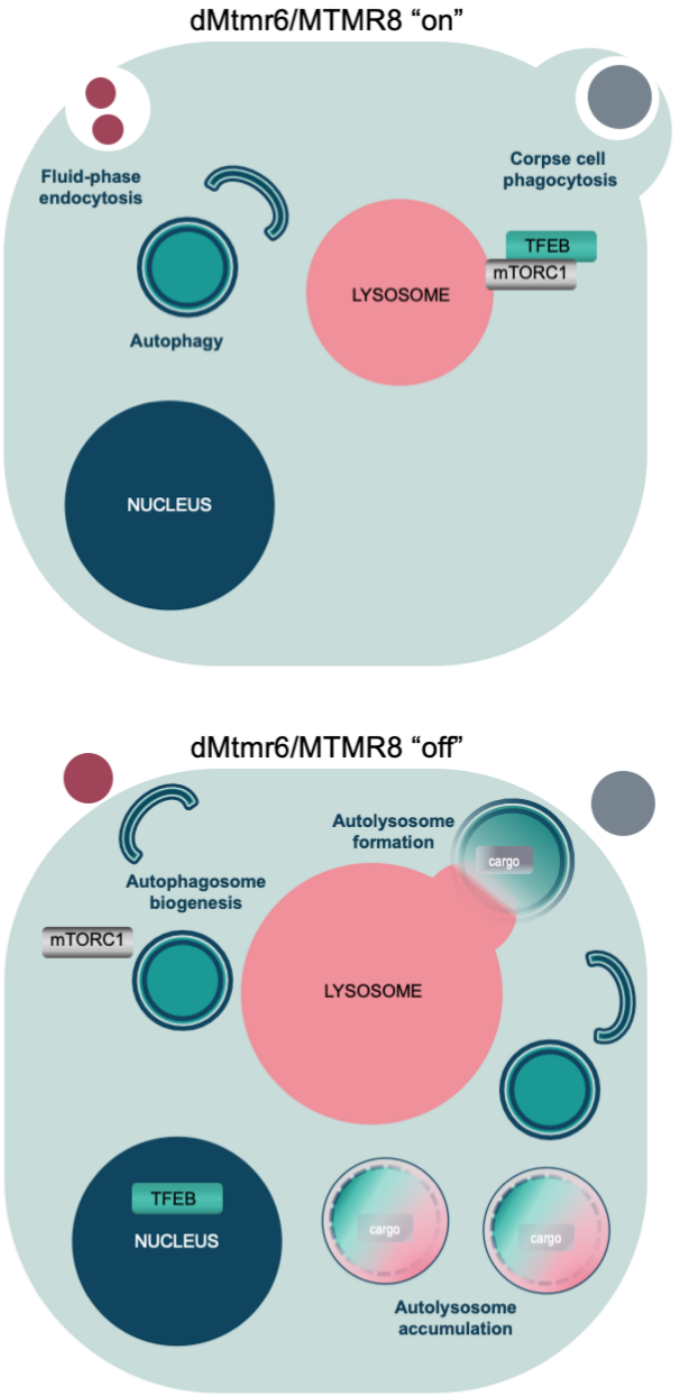

Figure 3.1. Graphical representation of cell status in a dMtmr6/MTMR8 “on” versus “off” state. dMtmr6/MTMR8 influence pathways that converge at the lysosome and maintain lysosomal homeostasis.

A role for dMtmr6 in autophagy

I identified dMtmr6 as a novel regulator of autophagy in *Drosophila* and provided evidence that *dMtmr6* depletion promotes autophagy and lysosome biogenesis, but degradation of autolysosomes was impaired.

dMtmr6 negatively regulates Drosophila autophagic flux

Previous studies of autophagy in *Drosophila* lack investigation of myotubularin-related phosphatases. A role for mtm in endolysosomal size maintenance exists (Velichkova et al., 2010), but *mtm* depletion failed to impair autophagic flux in our studies. However, reduced dMtmr6 function in multiple *Drosophila* tissues promoted accumulation of autophagic structures that included the ubiquitin-like autophagic membrane molecule Atg8a and the autophagic cargo adapter ref(2)p. These results indicate that in *dMtmr6*-depleted cells, excess undegraded autophagic material exists, which could be a result of enhanced autophagy induction, reduced lysosomal degradation, or a combination of both of these processes.

Our data indicate that cells with attenuated *dMtmr6* function both induce autophagy and reduce degradation of autolysosomal cargoes. We saw amplified autophagosome and lysosome biogenesis, as evidenced by heightened Mitf-target gene expression, cathepsin B protease activity, cathepsin L protein biogenesis, and endolysosomal acidification levels. We also saw diminished phospho- p70

S6K and Akt levels in nutrient rich conditions, a sign of attenuated growth signaling. However, when we dampened autophagy induction with Atg1-knockdown in *dMtmr6*-depleted fat body, ref(2)p and lipidated Atg8a protein levels intensified, which argues that dMtmr6 plays an Atg1-independent role in recruiting Atg8a and ref(2)p to membranes. Furthermore, Atg1 may promote some level of degradation in *dMtmr6*-depeleted fat body because, when compared to double *dMtmr6* and *Atg1*-RNAi knockdown cells they possess enhanced *Atg1* gene transcription but less ref(2)p and lipidated Atg8a. We further showed that the loss of either Vps34 or Atg9 only partially suppressed Atg8a puncta formation in *dMtmr6*-knockdown cells. These data suggest that dMtmr6 functions, at least in part, independent of Atg1, Vps34, and Atg9.

Despite seemingly blunted autophagic degradation, autolysosomes form in *dMtmr6*-depleted cells. We observed GFP signal-loss from our tandem fluorescent autophagy reporter, signifying recruitment to an acidic environment. Ultrastructural analyses of *dMtmr6* knockdown on intestine cells undergoing developmental autophagy contained enhanced amounts of the autolysosome compartment. Unlike the electron-dense autolysosomes in wild-type midgut cells, *dMtmr6*-knockdown cells contained large, predominantly electron-lucent autolysosomes with discrete pockets of electron dense material. Together, these results demonstrate that autolysosome formation remains intact in *dMtmr6*-depleted cells.

dMtmr6-associated defects converge at the lysosome

We show that *dMtmr6*-knockdown impairs additional membrane-mediated cellular degradation pathways. Both fluid-phase endocytosis and phagocytic uptake of apoptotic corpse cells by macrophages were reduced in cells with reduced *dMtmr6* function. These data are consistent with the idea that *dMtmr6* is required for lysosome function. During both endocytosis and phagocytosis, cells internalize extracellular matter in membrane-bound vesicles that are subsequently trafficked to the lysosome for degradation, albeit by different molecular cohorts. Indeed, evidence exists that several lysosomal storage disorders (LSDs), in which lysosomal function is impaired, possess reduced levels of fluid-phase endocytosis (Rappaport et al., 2016). In LSD cell lines, the severity of lysosomal cholesterol storage inversely correlates with endocytic uptake, and in wild-type cells, pharmacologically induced lysosomal cholesterol storage impairs endocytosis. Furthermore, a similar relationship exists between phagocytic degradation and lysosomal function (Wong et al., 2017). Both *Drosophila* and mammalian macrophages undergoing phagocytosis require lysosome function for degradation and additional phagocytic events. These studies reinforce our hypothesis that *dMtmr6*-knockdown impairs lysosome function.

While our data strongly support the idea that lysosome function requires dMtmr6, our studies fail to directly address which aspect of lysosome function is compromised. Indeed, lysosomal properties such as acidification, cathepsin B protease activity, and fusion with autophagosomes appear functional. However,

autolysosomes in *Drosophila* midguts are extremely large and electron lucent. This phenotype is strikingly similar to *Drosophila Fab1* and *Fig4* deficiencies (Rusten et al., 2007; Bharadwaj et al., 2016). The *Drosophila* ortholog of human PIKfyve, Fab1, is a PI(3)P 5-kinase with a conserved role in endolysosomal homeostasis, and Fig4 is a PI(3,5)P2 5-phosphatase that functions in complex with Fab1 (Mccartney et al., 2014). Loss of function mutations in either Fab1 or Fig 4 impairs lysosome function and promotes accumulation of swollen, autolysosomes. These data support a role for PI(3)P to PI(3,5)P2 interconversion in lysosome function and imply that *dMtmr6* might also participate in PI(3)P conversion at the lysosome. Future experiments should test if a genetic epistatic relationship exists between dMtmr6 and the Fab1/Fig4 complex.

dMtmr6 could mediate other trafficking processes

If impaired lysosome function is the driving factor in the *dMtmr6*-RNAi phenotype, then it will be important to define how dMtmr6 maintains lysosomal homeostasis. One possibility is that dMtmr6 facilitates lysosomal enzyme trafficking to lysosomes. Recently, *Drosophila* Rab6, a Rab GTPase that localizes to the Golgi, was identified as a regulator of autophagy and insulin-TOR signaling (Ayala et al., 2018). Like *dMtmr6*-depletion, Rab6 loss resulted in accumulation of large autolysosomes, an expanded lysosomal compartment in larval fat body cells, reduced TOR and Akt activities, and impaired lysosome function. Despite these similarities, some differences exist. Rab6 loss significantly affected fat body cell

size in an insulin signaling-dependent manner. By contrast, cells with reduced *dMtmr6* function do not have altered size, suggesting that dMtmr6 and Rab6 do not function in a similar manner. During insulin signaling, both ligand (insulin) and receptor (insulin receptor tyrosine kinase or InR) are internalized by endocytosis at the plasma membrane, and the receptor is later recycled back to the plasma membrane (Morcavallo et al., 2014). In Rab6-depleted cells, recycling failed, and InR accumulated in Lamp-GFP labeled vesicles. Further, these effects are specific to the role of Rab6 within the endomembrane system, and not the Golgi, although the authors provide evidence that Rab6 localizes to the Golgi, to lysosomes, and to autolysosomes presumably to facilitate lysosomal enzyme trafficking (Ayala et al., 2018). To investigate a role for dMtmr6 in lysosomal enzyme trafficking, future investigations could use fluorescently-tagged Rab6 as a reporter.

Previously, *dMtmr6* and its *C. elegans* ortholog, *mtm-6* were shown to play a role in protein secretion (Silhankova et al., 2010). Through analyses of endocytosis-defective *C. elegans* mutants, MTM-6 and MTM-9 were identified as required for efficient recycling of Wnt-binding proteins, which have important roles in development and disease. MTM-6 was specifically shown to function with SNX-3, a sorting nexin and PI-binding protein that plays a role in retromer function and is required for Wnt secretion (Silhankova et al., 2010; Harterink et al., 2011). However, knockdown of individual components in the MTM-6 mutant partially restored Wnt-signaling, which suggests that PI(3)P requires balanced levels. Wnt-signaling was also impaired in the *Drosophila* wing imaginal disc, a larval tissue

that gives rise to adult organs during metamorphosis. Interestingly, the *Drosophila* phenotype was atypical from other retromer-component mutants, which typically only possess impaired Wnt levels in Wnt-producing cells. Indeed, Wnt levels decreased in the entire *dMtmr6*-knockdown imaginal wing discs. These data are intriguing because they further support a role for *dMtmr6* in trafficking. Future studies should determine if dMtmr6 plays a direct role in retromer function or if the effect on Wnt-signaling in *Drosophila* is retromer-independent.

Another cellular trafficking process with similarities to autophagy is macropinocytosis. Through this endocytic process, cells engulf large volumes of extracellular fluids and solutes via actin-rich plasma membrane extensions. Once internalized, these membrane-enclosed fluids fuse with endolysosomal compartments where lysosomal hydrolases degrade macromolecules. Like all forms of membrane trafficking events described in this dissertation, macropinocytosis is regulated by phosphoinositides, especially at the plasma membrane during engulfment. To my knowledge, no *in vivo Drosophila* models of macropinocytosis exist. However, *Drosophila* Schneider 2 cells, are a commonly used fly cell line that can undergo both clathrin-mediated endocytosis and macropinocytosis during bacterial infection (Wei et al., 2019). Using this system, it would be possible to test if dMtmr6 also functions in macropinocytosis.

Implications of conserved dMtmr6 protein domains

The conservation of dMtmr6 protein domains suggests that these domains facilitate conserved functions. While we demonstrate that dMtmr6 loss hinders viability, we failed to analyze the contributions of either the phosphatase- or the FYVE-domain to autophagy. Indeed, *dMtmr6* might participate in PI(3)P hydrolysis, PI(3)P-binding via its FYVE domain, or both. We evaluated localization of an endosomal GFP-FYVE reporter in *dMtmr6*-depleted cells but did not see colocalization with the enlarged autolysosomes. Further, we tested localization of a putative PI(3,5)P2 reporter, and this failed to localize with autolysosomes (not shown). However, we did not test these reporters dually with lysosome markers. Therefore, future studies should test if *dMtmr6*-knockdown promotes GFP-FYVE recruitment to lysosomes. To address phosphatase function, we are currently generating a point mutation from cysteine to serine in the conserved catalytic cysteine residue (dMtmr6-C406S). Future studies should aim to characterize this mutant. Specifically, viability, autophagic flux, lysosome function, and changes in PI(3)P-binding protein reporter expression should be analyzed. Additionally, an effort should be made to produce a *dMtmr6* allele that lacks the FYVE domain to test if this affects autophagy and lysosome function.

One caveat to our study is that we lack evidence for *dMtmr6* cellular localization. As mentioned above, *dMtmr6* should bind PI(3)P via its conserved FYVE domain. Future work should aim towards developing fluorescently-tagged *dMtmr6* strains both with and without the FYVE domain to determine where

dMtmr6 localizes both in the presence and in the absence of active autophagy programs in the fat body and midgut. It will be important to resolve if *dMtmr6* localizes to autophagosomes, lysosomes, or elsewhere and if the FYVE domain is required for localization.

In human cells, MTMR8 interacts with its pseudophosphatase binding partner, MTMR9 for enhanced stability and activity (Zou et al., 2012b). The *Drosophila MTMR9* ortholog is *CG5026*. The protein product of this uncharacterized gene could play a conserved role in enhancing the function of dMtmr6. Future studies could address this question by generating a fluorescently tagged *CG5026* strain and using it in tandem with a tagged version of CG3530 to see if the two proteins colocalize or coimmunoprecipitate.

The epistatic relationship of dMtmr6 with other autophagy-related genes

How dMtmr6 functions in relation to other autophagy genes remains to be defined. We attempted to dissect where in the autophagy pathway dMtmr6 functions but were unable to draw a solid conclusion about the genetic relationship of dMtmr6 and other pathway components. As discussed above, when compared to *dMtmr6* knockdown alone, *Atg1- and dMtmr6* double-knockdown elevated ref(2)p and lipidated Atg8a levels in fat body from fed animals. It might be possible that when *dMtmr6* is depleted, endogenous Atg1 levels are sufficient to promote activation of other autophagy pathway components. When *Atg1* is simultaneously

downregulated, ref(2)p and Atg8a simply accumulate. However, *Atg1*-knockdown is not completely efficient, so some levels of Atg1 remain. Future experiments should test the effect of *dMtmr6*-knockdown in a clonal Atg1 null mutant setting.

If dMtmr6 is dephosphorylating PI(3)P or PI(3,5)P2, then it must function to counteract one or more kinases. We tested the effects of *dMtmr6* knockdown in *Vps34* mutant fat body cells. Vps34 is the sole *Drosophila* class III PI3K and is required for both endocytosis and autophagy. During starvation-induced autophagy in fat body, *Vps34* null mutant cells fail to form Atg8a puncta, and endolysosomal compartments fail to acidify (Juhasz et al., 2008). When we depleted *dMtmr6* in Vps34 null mutant fat body cells from fed animals, Atg8a puncta remained, albeit puncta numbers were less. We saw similar results in *dMtmr6*-depleted Atg9 null mutant cells. Thus, inhibiting some aspects of early autophagosome formation dampened but did not fully suppress the accumulation of Atg8a puncta in *dMtmr6*-knockdown cells. These data suggest that additional factors could be regulating the formation of autophagic structures in *dMtmr6*-absent cells. Alternatively, different mechanisms of Atg8a recruitment to lysosomal structures may exist that are influenced by *dMtmr6* in a *Vps34* and *Atg9* manner.

Mutations in ESCRT components were shown to result in Atg8a accumulation in fat body from fed animals (Rusten et al., 2007). In this setting, numerous autophagosomes were visible in the cytoplasm, but autolysosome formation failed. Based on our observation that autolysosomes form in *dMtmr6*-knockdown cells, we think it likely that *dMtmr6* functions downstream of ESCRT

proteins. However, ESCRT-mediated trafficking processes could contribute to the excess autophagic material present in *dMtmr6*-depleted cells, especially if some aspect of recycling is impaired. Therefore, future work should test if ESCRT-pathway components are required for autolysosome accumulation in *dMtmr6*-knockdown cells.

Many questions remain about the mechanistic role of *dMtmr6* in autophagy and lysosome homeostasis. Here, I have provided evidence that *dMtmr6* is critical for cellular degradation pathways. Future work should aim to better understand how *dMtmr6* functions in this pathway.

MTMR8 negatively regulates autophagic flux in primate cells

MTMR8 was shown to negatively regulate autophagy (Zou et al., 2012b; a). However, these analyses focused primarily on how MTMR8 functioned with MTMR9 to regulate autophagy. The authors largely ignored the effects of MTMR8 on its own because the effects of MTMR8 function were enhanced by its binding partner. This study also demonstrated that MTMR9 functions with MTMR6 to inhibit apoptosis, and the group previously showed that MTMR9 also physically interacts with MTMR7 (Zou et al., 2012a; Mochizuki and Majerus, 2003). Thus, MTMR9 plays a regulatory role for all three MTMR6 subfamily members, which has a significant impact on the analyses of MTMR8 in autophagy because *MTMR9* -loss or -overexpression experiments could influence its other binding partners and their

cellular functions. Our analyses focused solely on MTMR8, thereby providing a more refined picture of MTMR8's role in autophagy.

MTMR8 promotes autophagic degradation

Following our discovery that *dMtmr6*-knockdown in *Drosophila* led to large autophagic structures with degradation defects, we were excited to learn that *dMtmr6* had predicted human orthologs. Indeed, our data supported a conserved functional role for MTMR8 in autophagic flux because *MTMR8*-knockdown resulted in large, p62-containing autophagic puncta. Importantly, TEM analyses showed that *MTMR8* knockdown significantly influenced endolysosomal homeostasis when compared to control cells with enhanced lysosome, autophagosome, and autolysosome compartments throughout the cytoplasm. Immunofluorescence analyses further confirmed that what we saw in electron micrographs were autolysosomes because we saw large LC3B- and LAMP1-containing structures. Further, we showed that mutations in *MTMR8* significantly impaired lysosome homeostasis because, like in *MTMR8*-knockdown cells, acidified LAMP1 structures were larger than in wild-type cells. Further, mis-expression of MTMR8 in HeLa cells resulted in LC3B puncta formation, and decreased p62 and LC3B protein levels, further supporting that MTMR8 promotes degradation of autophagic structures. Unlike previous reports, which suggested that MTMR8's role in autophagy was significantly dependent upon cooperation with its binding partner, MTMR9, our data suggest that modulating MTMR8 levels

alone is sufficient to alter autophagic flux (Zou et al., 2012a; b).

MTMR8 and TFEB signaling

An important functional relationship exists between the lysosome, mTORC1, and TFEB (Settembre et al., 2012; Roczniak-Ferguson et al., 2012; Martina et al., 2012), making it intriguing that MTMR8 may function within this signaling axis. mTORC1 and TFEB colocalize at the lysosomal membrane. There, mTORC1 phosphorylates TFEB, resulting in 14-3-3 protein-binding to and inhibiting TFEB. Both starvation and lysosome dysfunction reduce mTORC1-dependent TFEB phosphorylation, which decreases interactions between 14-3-3 proteins and permits nuclear translocation. In the nucleus, TFEB promotes transcription of the CLEAR gene network (Coordinated Lysosomal Expression and Regulation network), which promotes lysosome biogenesis, autophagosome formation, autophagosome-lysosome fusion, and degradation (Settembre et al., 2011).

TFEB is also regulated by lysosomal Ca^{2+} signaling (Medina et al., 2015). Lysosomal Ca^{2+} release by the transient receptor potential (TRP) channel mucolipin 1 (MCOLN1/TRPML1) activates calcineurin, a phosphatase that binds and dephosphorylates TFEB, resulting in TFEB nuclear translocation. Further, TFEB requires MCOLN1-mediated calcineurin activation. Mutations in MCOLN1 cause the lysosomal storage disorder mucolipidosis type IV (MLIV, OMIM: 252650) which is characterized by increased autophagosome biosynthesis,

autophagosome accumulation, and delayed autophagosome-lysosome fusion (Vergarajauregui et al., 2008). Interestingly, MCOLN1 also regulates autophagy by a TFEB-independent mechanism. In addition to calcineurin, MCOLN1-mediated Ca^{2+} efflux activates calcium/calmodulin-dependent protein kinase kinase ß (CaMKKß) and AMP-activated protein kinase (AMPK), induces the Beclin1/VPS34 complex, and promotes PI(3)P production on isolation membranes (Scotto Rosato et al., 2019). Interestingly, MCOLN1 activation requires PI(3,5)P2-binding (Dong et al., 2010), and MCOLN1 promotes endolysosomal acidification in a PI(3,5)P2-dependent manner (Isobe et al., 2019).

Our data showed that TFEB nuclear localization was enhanced in *MTMR8*-depleted cells when compared to control cells. These data support our hypothesis that lysosomal degradation was impaired because lysosome dysfunction is known to promote TFEB activation. Despite this, we lack evidence that explains how MTMR8 maintains lysosomal homeostasis. Since PI(3)P is a known *MTMR8* substrate, it is possible and even likely, that MTMR8 maintains PI(3)P levels at degradative lysosomes. PI(3)P is a PIKfyve substrate required for PI(3,5)P2 synthesis. As introduced above, MCOLN1 activation by PI(3,5)P2 activates CaMKKß-induced autophagy. Therefore, it is interesting to speculate that in cells lacking MTMR8, PI(3)P accumulates, providing ample PIKfyve substrate for PI(3,5)P2 production, and thereby activating MCOLN1. Imbalanced phosphoinositide levels on the autolysosome can impair degradation (Palamiuc et al., 2020). Thus it is possible that MTMR8 is required to balance PI(3)P levels

upstream of PIKfyve. Future experiments should test if MTMR8 regulates MCOLN1-mediated TFEB-independent autophagy induction. For example, one could test the effects of CaMKKß-inhibition in *MTMR8* mutant cells. If *MTMR8* loss of function leads to increased MCOLN1 activation, then inhibiting CaMKKß should suppress LC3B accumulation.

MTMR8 conserved domains

MTMRs are characterized by their conserved protein domains, all of which contain a putative PI-binding PH-GRAM domain, a phosphatase domain, and a Coiled coil domain. While extensive analyses evaluated the roles of these conserved domains in other MTMRs, the MTMR6 subfamily remained unexplored. Our data provide the first analyses of the PH-GRAM and phosphatase domains in MTMR8. We showed that *MTMR8-C338S* HeLa cells produced large LAMP1-staining structures that are consistent with enlarged lysosomes. These data are consistent with a role for MTMR8 catalytic activity in maintaining lysosome homeostasis. We also showed that *MTMR8ΔPH* cells possessed large LC3B-containing LAMP1 structures, indicative of autolysosomes and consistent with the idea that the PH-GRAM domain is required for MTMR8 function, likely as a mechanism for lysosomal-membrane recruitment at PIs.

While our data support a role for MTMR8-mediated lysosomal homeostasis, we lack direct evidence that MTMR8 localizes to lysosomes and mediates

lysosomal PI(3)P hydrolysis. Future studies should generate fluorescently tagged MTMR8 fusion proteins both with and without the PH-GRAM domain to test if MTMR8 localizes to the lysosome and if that interaction is PH-GRAM-mediated. Furthermore, if MTMR8 hydrolyzes degradative lysosomal PI(3)P, then future analyses should evaluate the localization of PI(3)P binding proteins that are specific for late endolysosomes or autolysosomes. Unpublished work from our colleagues suggests that specific WIPI proteins may function at later stages in autophagy. Therefore, these WIPI proteins may function as tools to evaluate the relationship between MTMR8 and PI(3)P at autolysosomes. Indeed, an increase in lysosomal PI(3)P levels should be reflected by an increase in WIPI protein localization.

Our work introduces many intriguing possibilities about the role of MTMR8 in lysosome homeostasis and autophagy. Here, I have provided evidence that, like *Drosophila Mtmr6, MTMR8* is critical for autophagic degradation.

Significance of Findings

The enzymes that mediate reversible phosphorylation are drug target candidates in numerous human diseases, including cancer. Indeed, the ability to amplify or dampen a cellular process requires a functional knowledge of its molecular repertoire. A relatively understudied group of enzymes, myotubularin-related phosphatases mediate cellular membrane trafficking events throughout the endolysosomal system. Despite acknowledging a role for human MTMR8 in autophagy, research failed to further clarify MTMR8's contribution to this process. Additionally, Mtmr function has not be previously associated with autophagy in *Drosophila* I found that dMtmr6, and its human counterpart MTMR8, negatively regulate autophagy by promoting endolysosomal homeostasis. Reduced *dMtmr6* and *MTMR8* function promote accumulation of enlarged autolysosomes, which leads to endolysosomal imbalance and impairment of other endolysosomal processes. Overall, my study introduces dMtmr6 as an important molecule that promotes *in vivo* autophagic degradation and cell survival in *Drosophila* tissues, and further defines the role of MTMR8, a functional dMtmr6 ortholog, in mammalian autophagy.

Appendix A

Phosphoinositide phosphatase autophagy screen

Table A1 Predicted *Drosophila* phosphoinositide phosphatases. Predictions based on Flybase annotations, human orthologs, reagents tested, and results. Pepto-Bismol Pink box, reagent dysregulates developmental midgut autophagy; grey box, no defect in developmental midgut autophagy; white box, not tested.

Gene Symbol	Gene Name	Predicted	Human Ortholog	VDRC-RNAi (VDRC ID/stock library)	TRiP-RNAi (BDSC stock number)	Other
5Ptasel	5Ptasel		INPP5A			
CG3530	myotubularin-related phosphatase	mtmr6			38340	
			MTMR7	26216/GD	25864	
			MTMR8			P{XP}CG3530-d07361
			MTMR6			CG3530-KG01267 (BL14361)
						CG3530-CRISPR-RFP
CG3632	myotubularin-related phosphatase	mtmr3	MTMR4	26254/GD	38341	F001802
			MTMR3			
CG5026	myotubularin-related phosphatase	mtmr9	MTMR9	34916/GD	38309	
				34915/GD	57020	
EDTP	myotubularin-related phosphatase	mtmr14/ jumpy	Jumpy		41633	
					36917	
CG6707			PIP4P1			

CG6805			INPP5K			
Sbf	myotubularin-related phosphatase			22317/GD	57301	
					44004	
CG7956			INPP5F	22638/GD		
				22637/GD		
CG9389			IMPA1	44663/GD		
CG9391			IMPA1	23725/GD	60087	
CG9784			INPP5K	30098/GD		
CG14411	myotubularin-related phosphatase	mtmr10		17579/GD	40935	
				17576/GD		
CG15743			IMPAD1	42685/GD		
CG17026			IMPA2	32813/GD		
CG17027			IMPA1	50075/GD	51701	
CG17028			IMPA1	32819/GD	53320	
CG17029			IMPA1	32823/GD		
CG42271			INPP4A	100176/KK		
FIG4	FIG4 phosphoinositide 5-phosphatase		FIG4			
INPP5E	Inositol polyphosphate 5-phosphatase E		INPP5E		41701	
					34037	
Ipp	Inositol polyphosphate 1-phosphatase		INPP1	25625/GD	28028	
Mipp1	Multiple inositol polyphosphate phosphatase 1		MINPP1	8492/GD		
Mipp2	Multiple inositol		MINPP1	14163/GD		

	polyphosphate phosphatase 2					
mtm	myotubularin		MTMR2		38339	
			MTM1		31552	
			MTMR1			
Ocrl	Oculocerebrorenal syndrome of Lowe		INPP5B	34649/GD		
			OCRL			
Pten	Phosphatase and tensin homolog		PTEN	35731/GD	25841	
				101475/KK	33643	
PTPMT1	Protein tyrosine phosphatase mitochondrial 1		PTPMT1			
Sac1	Sac1 phosphatase		SACM1L	44376/GD	56013	
Synj	Synaptojanin		SYNJ1		44420	
CG7789		IMP-like			51028	

Appendix B

Mtmr3 negatively regulates autophagosome formation

Summary

During an *in vivo* RNAi screen for novel phosphatases that regulate autophagy, we identified Mtmr6 as essential to autophagic flux **(Chapter II)**. A member of the myotubularin-related (MTMR) family of 3-phosphatases, Mtmr6 is one of seven fly family members **(Table 1.2)**. We tested the additional six *Drosophila* MTMRs to explore their potential role in autophagy. Of the six, only CG3632/Mtmr3 elicited an effect on autophagy. Here I provide evidence that Mtmr3 negatively regulates both starvation-induced fat body and developmental midgut autophagy.

A summary of all stocks used in these analyses and the strength of their effects is listed in **Table B1**.

Table B1. Transgenic *Drosophila* strains tested in Mtmr3 analyses. In overexpression experiments, strong means that overexpression suppressed the normal biological response. In RNAi experiments, strong means that knockdown enhanced the normal biological response. Not tested (x).

CG3632/Mtmr3		Stock ID	Midgut			Fat
			Starved puncta	2 h APF puncta	2 h APF Cell size	Atg8a puncta
Over-expression	OE-Mtmr3	FlyORF: F001802	*no*	**strong**	**strong**	**strong**
RNAi	v26254	VDRC: v26254	x	*no*	*no*	*no effect*
	TRiP. HMS01808	BDSC: 38341	x	**strong**	*no*	**strong**
	stock no longer available	BDSC: 31552	x	**weak**	*no*	**weak**

Results

Some myotubularin-related phosphatases play a role in mammalian autophagy **(Chapter I, Part II)**. However, a role for the *Drosophila* MTMRs in autophagy remains unexplored. We clonally expressed RNAi towards all seven of the *Drosophila* MTMRs during autophagy-induced conditions in the larval fat body and midgut. Of the seven, we only saw a phenotype with *Mtmr3-RNAi* and *Mtmr6-RNAi* **(Chapter II, Table 2.1)**. Here I provide evidence that Mtmr3 negatively regulates Atg8a puncta formation. We used the FLP/FRT system to clonally co-express GFP and RNAi in tissues that express mCherry-Atg8a under the control of the Atg8a promoter.

As introduced in **Chapter I**, larval *Drosophila* fat body cells undergo autophagy in response to nutrient deprivation, and prolonged autophagy induction reduces cell size. Therefore, we evaluated the effects of *Mtmr3-RNAi* on mCherry-Atg8a expression in fat body from starved L3 larvae. When compared to adjacent wild-type control cells, fat body cells that co-express GFP and *Mtmr3-RNAi* remain the same size but contain significantly more Atg8a puncta that also occupies more area of the cell **(Fig B.1 A-D)**. These data establish Mtmr3 as a negative regulator of Atg8a puncta formation in response to nutrient restriction.

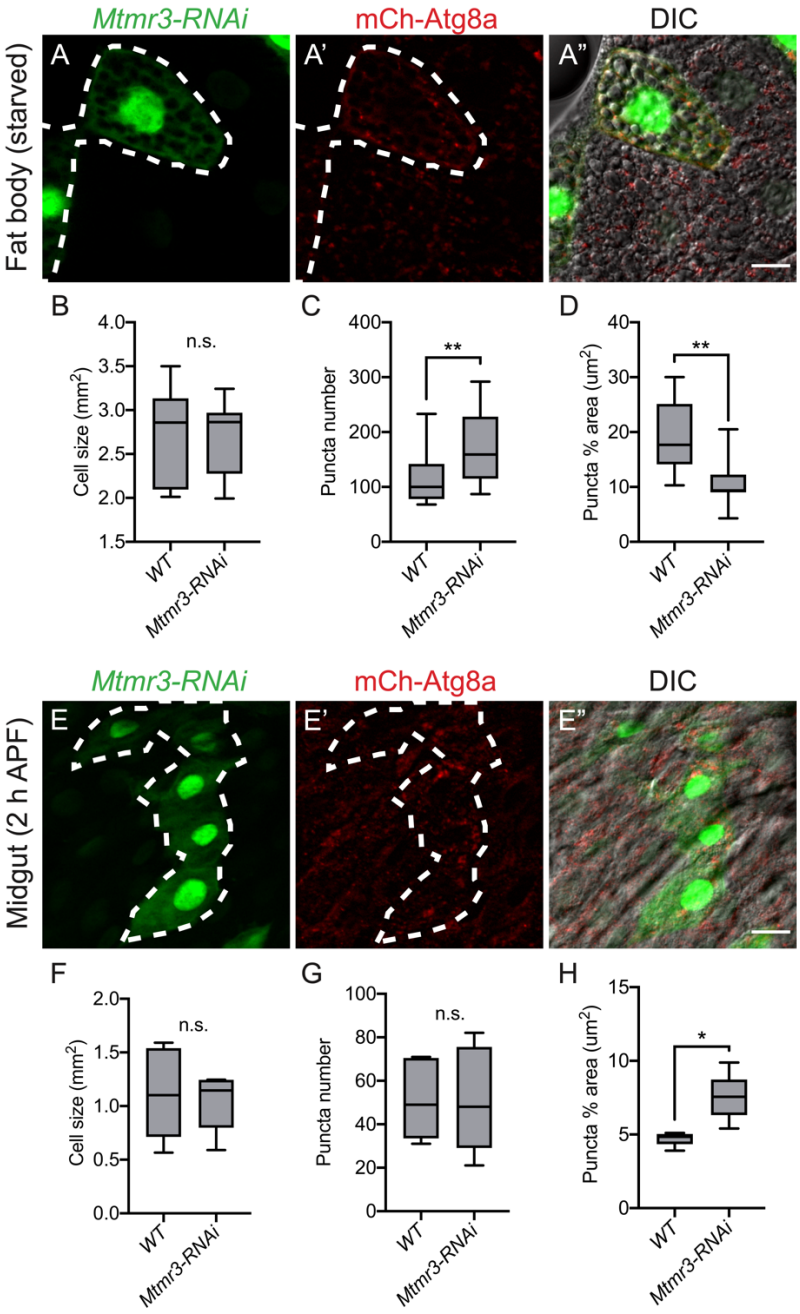

Figure B1. *Mtmr3*-depletion enhances Atg8a puncta formation following autophagy induction. (A) Representative image of fat body from starved L3 larvae expressing mCherry-Atg8a with clonal *Mtmr3* knockdown (green, white dashed line). Quantification of (B) cell size, (C) cellular Atg8a puncta number, and (D) the percentage of cellular area occupied by Atg8a puncta in wild-type (black) and *Mtmr3-RNAi* cells as represented in

(A). (E) Representative image of midgut from animals expressing mCherry-Atg8a with clonal *Mtmr3-RNAi* (green, white dashed line) taken at 2 hours after puparium formation (APF). Quantification of (F) cell size, (G) cellular Atg8a puncta number, and (H) the percentage of cellular area occupied by Atg8a puncta in wild-type (black) and *Mtmr3-RNAi* cells as represented in (E). Data information: in (B-D and F-G), data are presented as min and max ($n \geq 6$). Asterisks denote statistical significance (*$P < 0.05$ and **$P < 0.01$) using paired t test. Scale bars, 20 μm.

Larval midgut cells undergo developmental cell death by autophagy, and we can see high levels of autophagy 2 hours after puparium formation (2 h APF) **(Chapter I)**. Similar to fat body from starved larvae, we saw enhancement to Atg8a puncta **(Fig. B1 E)**. Cell size remained unaffected and puncta number was similar in both wild-type and *Mtmr3*-depleted cells, but Atg8a puncta occupied more area of the cell **(Fig. B1 F-H)**. These data are consistent with reports that loss of the *C. elegans* Mtmr3 ortholog, *mtm-3* causes autophagosome accumulation and impairs autolysosome formation and overexpression of a human MTMR3 phosphatase-inactive mutant allele induces autophagy (Wu et al., 2014; Hao et al., 2016).

We further hypothesized that if *Mtmr3* depletion can enhance Atg8a puncta formation, then *Mtmr3* overexpression (*OE-Mtmr3*) should suppress autophagy induction. Here, we tested the effects of *OE-Mtmr3* on starvation-induced autophagy in fat body and developmental midgut autophagy. As expected, Atg8a puncta formation was suppressed when we co-expressed GFP and *OE-Mtmr3* clonally in fat body from nutrient-deprived larvae **(Fig. B2 A)**. Cell size was not significantly affected, but the data trend toward a larger cell size in *OE-Mtmr3* cells compared to wild-type **(Fig B2 B)**. Significantly, *Mtmr3* overexpression suppressed Atg8a puncta number and puncta-occupied area in starved fat body **(Fig B2 C and D)**. Moreover, *Mtmr3* overexpression suppressed both cell size reduction and Atg8a puncta formation in 2 h APF midguts **(Fig B2 E-H)**. These data further support a regulatory role for Mtmr3 in autophagy induction.

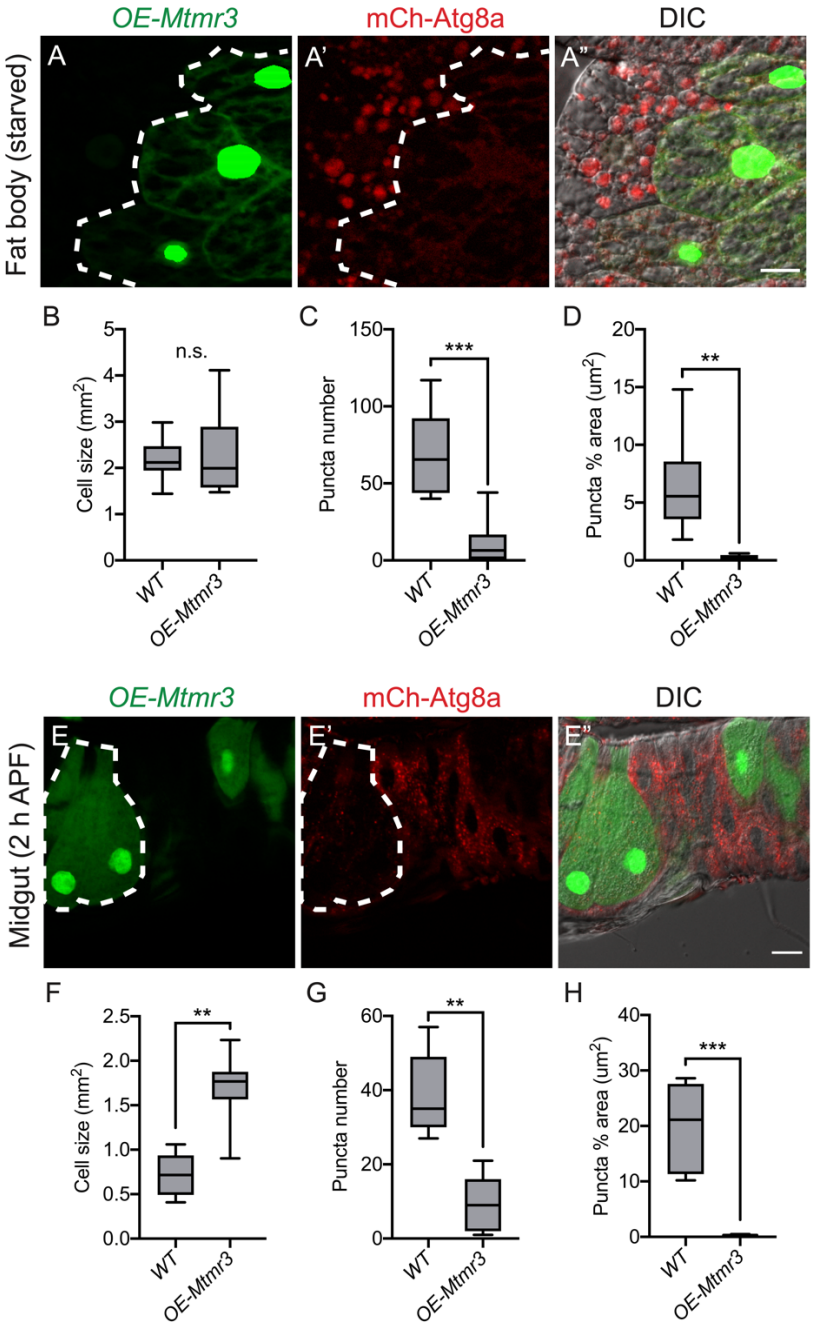

Figure B2. *Mtmr3*-overexpression suppresses Atg8a puncta formation and midgut cell size reduction following autophagy induction. (A) Representative image of fat body from starved L3 larvae expressing mCherry-Atg8a with clonal *Mtmr3* overexpression (OE-*Mtmr3*, green, white dashed line). Quantification of (B) cell size, (C) cellular Atg8a puncta

number, and (D) the percentage of cellular area occupied by Atg8a puncta in wild-type (black) and *OE-Mtmr3* cells as represented in (A). (E) Representative image of midgut from animals expressing mCherry-Atg8a with clonal *OE-Mtmr3* (green, white dashed line) taken at 2 hours after puparium formation (APF). Quantification of (F) cell size, (G) cellular Atg8a puncta number, and (H) the percentage of cellular area occupied by Atg8a puncta in wild-type (black) and *OE-Mtmr3* cells as represented in (E). Data information: in (B-D and F-G), data are presented as min and max ($n \geq 6$). Asterisks denote statistical significance (**$P < 0.01$ and ***$P < 0.001$) using paired t test. Scale bars, 20 μm.

Future directions

Mechanisms that regulate starvation-induced autophagy differ from those that regulate midgut autophagy during development. Furthermore, the mechanisms that underlie cell-size reduction during developmental midgut autophagy remain poorly understood. Here, I identified Mtmr3 as an additional regulator of midgut cell size reduction. Future experiments should explore the epistatic role of Mtmr3 in the cell-size reduction program.

Appendix C

dMtmr6 and MTMR8 association networks

We can identify potential interactions between genes of interest using predictive tools. The STRING database (string-db.org) uses known and predicted protein-protein interactions to generate representations of likely interactions, which can be helpful to generate hypotheses for empirical analyses. Here, I include predicted interactions between dMtmr6 **(Fig. C1 A)** and MTMR8 **(Fig. C1 B)** that have been clustered into five groups (five colors) based on the strength of evidence for their interactions. Future studies of either dMtmr6 or MTMR8 should evaluate these potential interactions for epistatic relationships, direct physical interactions, or both.

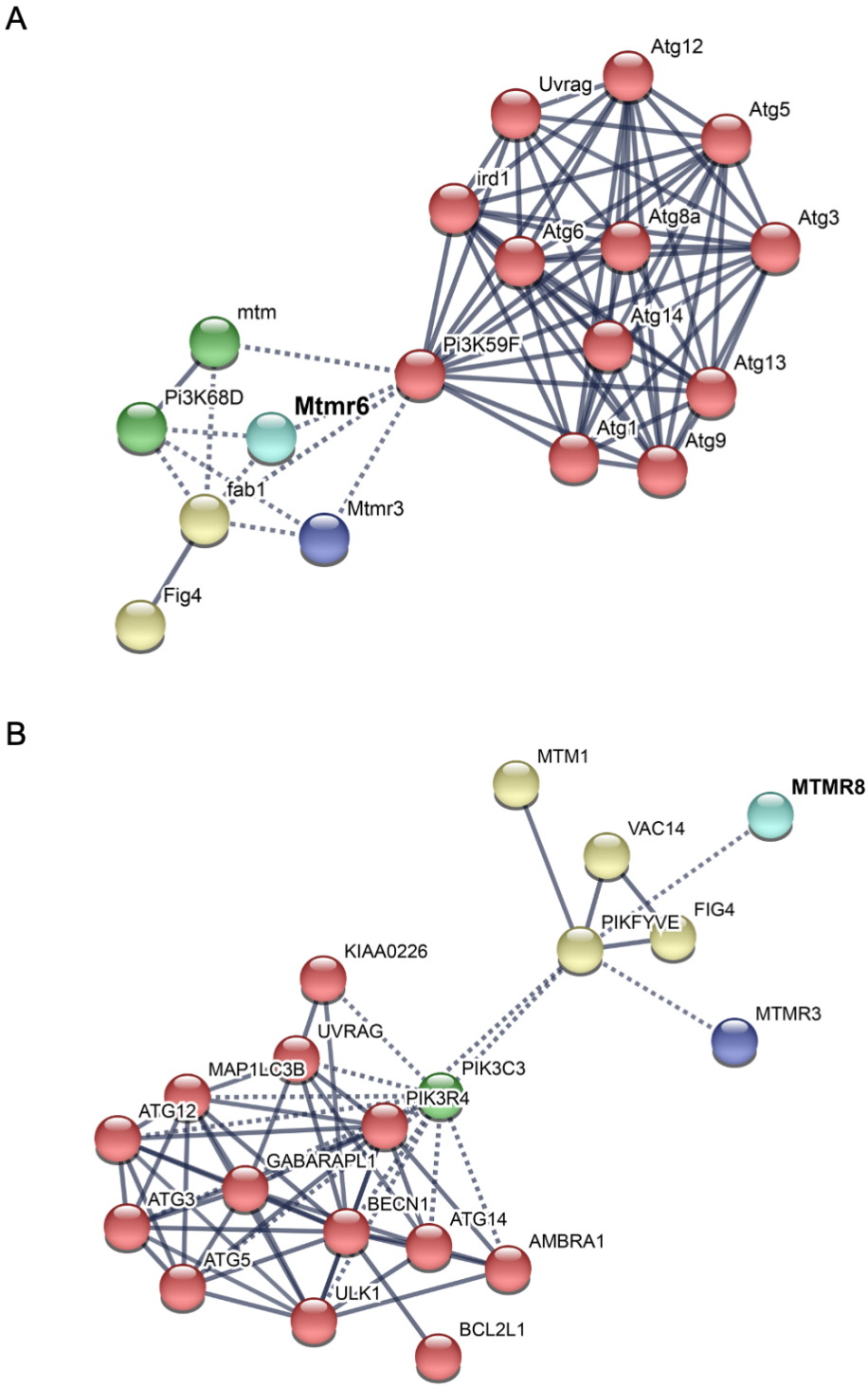

Figure C1. dMtmr6 and MTMR8 association networks. Representation of likely interactions for dMtmr6 (A) and MTMR8 (B) using a confidence score of 0.9 or

higher and sorted by K-means clustering into five groups (delineated by different colors). Network edge line thickness indicates data strength and is based on data support from the following interaction sources: textmining, experiments, databases, co-expression, neighborhood, gene fusion, and co-occurrence. Lines are represented as inter-cluster edges (dashed) and intra-cluster (solid) (Szklarczyk et al., 2019).

BIBLIOGRAPHY

Agarraberes, F.A., S.R. Terlecky, and J.F. Dice. 1997. An intralysosomal hsp70 is required for a selective pathway of lysosomal protein degradation. *J. Cell Biol.* 137:825–34. doi:10.1083/jcb.137.4.825.

Allen, E.A., and E.H. Baehrecke. 2020. Autophagy in animal development. *Cell Death Differ.* doi:10.1038/s41418-020-0497-0.

Amoasii, L., H. Hnia, and J. Laporte. 2012. Myotubularin phosphoinositide phosphatases in human diseases. *In* Curr. Top. Microbiol. Immuno. 209–233.

Anding, A.L., C. Wang, T.K. Chang, D.A. Sliter, C.M. Powers, K. Hofmann, R.J. Youle, and E.H. Baehrecke. 2018. Vps13D Encodes a Ubiquitin-Binding Protein that Is Required for the Regulation of Mitochondrial Size and Clearance. *Curr. Biol.* 28:287–295. doi:10.1016/j.cub.2017.11.064.

Arstila, A.U., and B.F. Trump. 1968. Studies on cellular autophagocytosis. The formation of autophagic vacuoles in the liver after glucagon administration. *Am. J. Pathol.* 53:687–733.

Ashford, T.P., and K.R. Porter. 1962. Cytoplasmic components in hepatic cell lysosomes. *J. Cell Biol.* 12:198–202. doi:10.1083/jcb.12.1.198.

Ayala, C.I., J. Kim, and T.P. Neufeld. 2018. Rab6 promotes insulin receptor and cathepsin trafficking to regulate autophagy induction and activity in Drosophila. *J. Cell Sci.* 131:jcs216127. doi:10.1242/jcs.216127.

Azzedine, H., A. Bolino, T. Taeb, N. Birouk, M. Di Duca, A. Bouhouche, S. Benamou, A. Mrabet, T. Hammadouche, T. Chkili, R. Gouider, R. Ravazzolo, A. Brice, J. Laporte, and E. Leguern. 2003. Mutations in MTMR13, a New Pseudophosphatase Homologue of MTMR2 and Sbf1, in Two Families with an Autosomal Recessive Demyelinating Form of Charcot-Marie-Tooth Disease Associated with Early-Onset Glaucoma. *Am. J. Hum. Genet*. 72:1141–1153.

Baehrecke, E.H. 2003. Autophagic programmed cell death in Drosophila. *Cell Death Differ.* 10:940–945. doi:10.1038/sj.cdd.4401280.

Balla, T. 2013. Phosphoinositides: tiny lipids with giant impact on cell regulation. *Physiol. Rev.* 93:1019–1137. doi:10.1152/physrev.00028.2012.

Beaulaton, J., and R.A. Lockshin. 1977. Ultrastructural study of the normal degeneration of the intersegmental muscles of Antheraea polyphemus and Manduca sexta (Insecta, lepidoptera) with particular reference to cellular autophagy. *J. Morphol.* 154:39–57. doi:10.1002/jmor.1051540104.

Berry, D.L., and E.H. Baehrecke. 2007a. Growth Arrest and Autophagy Are Required for Salivary Gland Cell Degradation in Drosophila. *Cell*. 131:1137–1148. doi:10.1016/j.cell.2007.10.048.

Berry, D.L., and E.H. Baehrecke. 2007b. Growth Arrest and Autophagy Are Required for Salivary Gland Cell Degradation in Drosophila. *Cell*. doi:10.1016/j.cell.2007.10.048.

Bharadwaj, R., K.M. Cunningham, K. Zhang, and T.E. Lloyd. 2016. FIG4 regulates lysosome membrane homeostasis independent of phosphatase function. *Hum. Mol. Genet.* 25:681–692. doi:10.1093/HMG/DDV505.

Bolino, A., A. Bolis, S.C. Previtali, G. Dina, S. Bussini, G. Dati, S. Amadio, U. Del Carro, D.D. Mruk, M.L. Feltri, C.Y. Cheng, A. Quattrini, and L. Wrabetz. 2004. Disruption of Mtmr2 CMT4B1-like neuropathy with myelin outfolding and impaired spermatogenesis. *J. Cell Biol.* 167:711–721. doi:10.1083/jcb.200407010.

Campa, C.C., J.P. Margaria, A. Derle, M. Del Giudice, M.C. De Santis, L. Gozzelino, F. Copperi, C. Bosia, and E. Hirsch. 2018. Rab11 activity and PtdIns(3)P turnover removes recycling cargo from endosomes. *Nat. Chem. Biol.* 14:801–810. doi:10.1038/s41589-018-0086-4.

Chang, T.-K., B. V Shravage, S.D. Hayes, C.M. Powers, R.T. Simin, J. Wade Harper, and E.H. Baehrecke. 2013. Uba1 functions in Atg7- and Atg3-independent autophagy. *Nat. Cell Biol.* 15:1067–78. doi:10.1038/ncb2804.

Cheng, S., Y. Wu, Q. Lu, J. Yan, H. Zhang, and X. Wang. 2013. Autophagy genes coordinate with the class II PI/PtdIns 3-kinase PIKI-1 to regulate apoptotic cell clearance in C. elegans. *Autophagy*. 9:2022–2032. doi:10.4161/auto.26323.

Chiang, H.L., S.R. Terlecky, C.P. Plant, and J.F. Dice. 1989. A role for a 70-kilodaton heat shock protein in lysosomal degradation of intracellular proteins. *Science (80-.).* 246:382–385. doi:10.1126/science.2799391.

Conradt, B., Y.C. Wu, and D. Xue. 2016. Programmed cell death during Caenorhabditis elegans development. *Genetics*. 203:1533–1562. doi:10.1534/genetics.115.186247.

Cormier, O., N. Mohseni, I. Voytyuk, and B.H. Reed. 2012. Autophagy can promote but is not required for epithelial cell extrusion in the amnioserosa of the Drosophila embryo. *Autophagy*. 8:252–264. doi:10.4161/auto.8.2.18618.

Coucouvanis, E., and G.R. Martin. 1995. Signals for death and survival: A two-step mechanism for cavitation in the vertebrate embryo. *Cell*. 83. doi:10.1016/0092-8674(95)90169-8.

Cuervo, A.M., and J.F. Dice. 1996. A receptor for the selective uptake and degradation of proteins by lysosomes. *Science (80-.).* 273:501–503. doi:10.1126/science.273.5274.501.

Cullen, P.J. 2011. Phosphoinositides and the regulation of tubular-based endosomal sorting. *In* Biochemical Society Transactions. 839–850.

Dang, H., Z. Li, E.Y. Skolnik, and H. Fares. 2004. Disease-related Myotubularins Function in Endocytic Traffic in Caenorhabditis elegans. *Mol. Biol. Cell*. 15:189–196. doi:10.1091/mbc.E03-08-0605.

Denton, D., B. Shravage, R. Simin, K. Mills, D.L. Berry, E.H. Baehrecke, and S. Kumar. 2009. Autophagy, Not Apoptosis, Is Essential for Midgut Cell Death in Drosophila. 19. 1741–1746 pp.

Dong, X.P., D. Shen, X. Wang, T. Dawson, X. Li, Q. Zhang, X. Cheng, Y. Zhang, L.S. Weisman, M. Delling, and H. Xu. 2010. PI(3,5)P2 controls membrane trafficking by direct activation of mucolipin Ca2+ release channels in the endolysosome. *Nat. Commun.* 1:38. doi:10.1038/ncomms1037.

Dooley, H.C., M. Razi, H.E.J. Polson, S.E. Girardin, M.I. Wilson, and S.A. Tooze. 2014. WIPI2 Links LC3 Conjugation with PI3P, Autophagosome Formation, and Pathogen Clearance by Recruiting Atg12–5-16L1. *Mol. Cell*. 55:238–252. doi:10.1016/j.molcel.2014.05.021.

Dowling, J.J., S.A. Moore, H. Kalimo, and B.A. Minassian. 2015. X-linked myopathy with excessive autophagy: a failure of self-eating. *Acta Neuropathol.* 129:383–90. doi:10.1007/s00401-015-1393-4.

Du, W., Q.P. Su, Y. Chen, Y. Zhu, D. Jiang, Y. Rong, S. Zhang, Y. Zhang, H. Ren, C. Zhang, X. Wang, N. Gao, Y. Wang, L. Sun, Y. Sun, and L. Yu. 2016. Kinesin 1 Drives Autolysosome Tubulation. *Dev. Cell*. 37:326–336. doi:10.1016/j.devcel.2016.04.014.

de Duve, C., B.C. Pressman, R. Gianetto, R. Wattiaux, and F. Appelmans. 1955. Tissue fractionation studies: Intracellular distribution patterns of enzymes in rat-liver tissue. *Biochem. J.* 60:604–617. doi:10.1042/bj0600604.

de Duve, C., and R. Wattiaux. 1966. Functions of Lysosomes. *Annu. Rev. Physiol.* 28:435–492. doi:10.1146/annurev.ph.28.030166.002251.

Efeyan, A., R. Zoncu, S. Chang, I. Gumper, H. Snitkin, R.L. Wolfson, O. Kirak, D.D. Sabatini, and D.M. Sabatini. 2012. Regulation of mTORC1 by the Rag GTPases is necessary for neonatal autophagy and survival. *Nature*. 493:679.

Funderburk, S.F., Q.J. Wang, and Z. Yue. 2010. The Beclin 1-VPS34 complex - at the crossroads of autophagy and beyond. *Trends Cell Biol.* 20:355–362.

doi:10.1016/j.tcb.2010.03.002.

Galluzzi, L., E.H. Baehrecke, A. Ballabio, P. Boya, J.M. Bravo-San Pedro, F. Cecconi, A.M. Choi, C.T. Chu, P. Codogno, M.I. Colombo, A.M. Cuervo, J. Debnath, V. Deretic, I. Dikic, E. Eskelinen, G.M. Fimia, S. Fulda, D.A. Gewirtz, D.R. Green, M. Hansen, J.W. Harper, M. Jäättelä, T. Johansen, G. Juhasz, A.C. Kimmelman, C. Kraft, N.T. Ktistakis, S. Kumar, B. Levine, C. Lopez-Otin, F. Madeo, S. Martens, J. Martinez, A. Melendez, N. Mizushima, C. Münz, L.O. Murphy, J.M. Penninger, M. Piacentini, F. Reggiori, D.C. Rubinsztein, K.M. Ryan, L. Santambrogio, L. Scorrano, A.K. Simon, H. Simon, A. Simonsen, N. Tavernarakis, S.A. Tooze, T. Yoshimori, J. Yuan, Z. Yue, Q. Zhong, and G. Kroemer. 2017. Molecular definitions of autophagy and related processes. *EMBO J.* 36:1811–1836. doi:10.15252/embj.201796697.

Ganley, I.G., D.H. Lam, J. Wang, X. Ding, S. Chen, and X. Jiang. 2009. ULK1·ATG13·FIP200 complex mediates mTOR signaling and is essential for autophagy. *J. Biol. Chem.* 284:12297–12305. doi:10.1074/jbc.M900573200.

Gillooly, D.J. 2000. Localization of phosphatidylinositol 3-phosphate in yeast and mammalian cells. *EMBO J.* 19:4577–4588. doi:10.1093/emboj/19.17.4577.

Golic, K.G., and S. Lindquist. 1989. The FLP recombinase of yeast catalyzes site-specific recombination in the drosophila genome. *Cell*. 59:499–509. doi:10.1016/0092-8674(89)90033-0.

Grimsley, C., and K.S. Ravichandran. 2003. Cues for apoptotic cell engulfment: Eat-me, don't eat-me and come-get-me signals. *Trends Cell Biol.* 13:648–656. doi:10.1016/j.tcb.2003.10.004.

Guo, L., C. Martens, D. Bruno, S.F. Porcella, H. Yamane, S.M. Caucheteux, J. Zhu, and W.E. Paul. 2013. Lipid phosphatases identified by screening a mouse phosphatase shRNA library regulate T-cell differentiation and protein kinase B AKT signaling. *Proc Natl Acad Sci U S A*. 110:1849–56. doi:10.1073/pnas.1305070110.

Hao, F., T. Itoh, E. Morita, K. Shirahama-Noda, T. Yoshimori, and T. Noda. 2016. The PtdIns3-phosphatase MTMR3 interacts with mTORC1 and suppresses its activity. *FEBS Lett.* 590:161–173. doi:10.1002/1873-3468.12048.

Harterink, M., F. Port, M.J. Lorenowicz, I.J. McGough, M. Silhankova, M.C. Betist, J.R.T. Van Weering, R.G.H.P. Van Heesbeen, T.C. Middelkoop, K. Basler, P.J. Cullen, and H.C. Korswagen. 2011. A SNX3-dependent retromer pathway mediates retrograde transport of the Wnt sorting receptor Wntless and is required for Wnt secretion. *Nat. Cell Biol.* doi:10.1038/ncb2281.

Hasegawa, J., R. Iwamoto, T. Otomo, A. Nezu, and M. Hamasaki. 2016.

Autophagosome – lysosome fusion in neurons requires INPP 5 E , a protein associated with Joubert syndrome. 35:1853–1867.

Hasegawa, J., B.S. Strunk, and L.S. Weisman. 2017. PI5P and PI(3,5)P2: Minor, but Essential Phosphoinositides. 42:49–60.

Heckmann, B.L., and D.R. Green. 2019. LC3-associated phagocytosis at a glance. *J. Cell Sci.* doi:10.1242/jcs.222984.

Holman, S.K., T. Morgan, G. Baujat, V. Cormier-Daire, T.J. Cho, M. Lees, J. Samanich, D. Tapon, H.D. Hove, A. Hing, R. Hennekam, and S.P. Robertson. 2013. Osteopathia striata congenita with cranial sclerosis and intellectual disability due to contiguous gene deletions involving the WTX locus. *Clin. Genet.* 83:251–256. doi:10.1111/j.1399-0004.2012.01905.x.

Hotta, K., T. Kitamoto, A. Kitamoto, S. Mizusawa, T. Matsuo, Y. Nakata, S. Kamohara, N. Miyatake, K. Kotani, R. Komatsu, N. Itoh, I. Mineo, J. Wada, M. Yoneda, A. Nakajima, T. Funahashi, S. Miyazaki, K. Tokunaga, H. Masuzaki, T. Ueno, K. Hamaguchi, K. Tanaka, K. Yamada, T. Hanafusa, S. Oikawa, H. Yoshimatsu, T. Sakata, Y. Matsuzawa, K. Nakao, and A. Sekine. 2011. Association of variations in the FTO, SCG3 and MTMR9 genes with metabolic syndrome in a Japanese population. *J. Hum. Genet.* 56:647–651. doi:10.1038/jhg.2011.74.

Huang, S., K. Jia, Y. Wang, Z. Zhou, and B. Levine. 2013. Autophagy genes function in apoptotic cell corpse clearance during C. Elegans embryonic development. *Autophagy*. 9:1–12. doi:10.4161/auto.22352.

Isobe, Y., K. Nigorikawa, G. Tsurumi, S. Takemasu, S. Takasuga, S. Kofuji, and K. Hazeki. 2019. PIKfyve accelerates phagosome acidification through activation of TRPML1 while arrests aberrant vacuolation independent of the Ca 2+ channel. *J. Biochem.* 165:75–84. doi:10.1093/jb/mvy084.

Itakura, E., C. Kishi-Itakura, and N. Mizushima. 2012. The Hairpin-type Tail-Anchored SNARE Syntaxin 17 Targets to Autophagosomes for Fusion with Endosomes/Lysosomes. *Cell*. 151:1256–1269. doi:10.1016/j.cell.2012.11.001.

Itakura, E., and N. Mizushima. 2010. Characterization of autophagosome formation site by a hierarchical analysis of mammalian Atg proteins. *Autophagy*. 6:764–776. doi:10.4161/auto.6.6.12709.

Jenzer, C., E. Simionato, C. Largeau, V. Scarcelli, C. Lefebvre, and R. Legouis. 2019. Autophagy mediates phosphatidylserine exposure and phagosome degradation during apoptosis through specific functions of GABARAP/LGG-1 and LC3/LGG-2. *Autophagy*. 15:228–241. doi:10.1080/15548627.2018.1512452.

Jeschke, A., and A. Haas. 2016. Deciphering the roles of phosphoinositide lipids in phagolysosome biogenesis. *Commun. Integr. Biol.* 9:e1174798. doi:10.1080/19420889.2016.1174798.

Juhasz, G., J.H. Hill, Y. Yan, M. Sass, E.H. Baehrecke, J.M. Backer, and T.P. Neufeld. 2008. The class III PI(3)K Vps34 promotes autophagy and endocytosis but not TOR signaling in Drosophila. *J. Cell Biol.* 181:655–666. doi:10.1083/jcb.200712051.

Juhász, G., J.H. Hill, Y. Yan, M. Sass, E.H. Baehrecke, J.M. Backer, and T.P. Neufeld. 2008. The class III PI(3)K Vps34 promotes autophagy and endocytosis but not TOR signaling in *Drosophila*. *J. Cell Biol.* 181:655–666. doi:10.1083/jcb.200712051.

Kamada, Y., T. Funakoshi, T. Shintani, K. Nagano, M. Ohsumi, and Y. Ohsumi. 2000. Tor-Mediated Induction of Autophagy via an Apg1 Protein Kinase Complex. *J. Cell Biol.* 150:1507–1513. doi:10.1083/jcb.150.6.1507.

Ketel, K., M. Krauss, A.-S. Nicot, D. Puchkov, M. Wieffer, R. Müller, D. Subramanian, C. Schultz, J. Laporte, and V. Haucke. 2016. A phosphoinositide conversion mechanism for exit from endosomes. *Nature*. 529:408–412. doi:10.1038/nature16516.

Kim, G.H.E., R.M. Dayam, A. Prashar, M. Terebiznik, and R.J. Botelho. 2014. PIKfyve inhibition interferes with phagosome and endosome maturation in macrophages. *Traffic*. 15:1143–1163. doi:10.1111/tra.12199.

Komatsu, M., S. Waguri, T. Ueno, J. Iwata, S. Murata, I. Tanida, J. Ezaki, N. Mizushima, Y. Ohsumi, Y. Uchiyama, E. Kominami, K. Tanaka, and T. Chiba. 2005. Impairment of starvation-induced and constitutive autophagy in Atg7-deficient mice. *J. Cell Biol.* 169:425–434. doi:10.1083/jcb.200412022.

Kuma, A., M. Hatano, M. Matsui, A. Yamamoto, H. Nakaya, T. Yoshimori, Y. Ohsumi, T. Tokuhisa, and N. Mizushima. 2004a. The role of autophagy during the early neonatal starvation period. *Nature*. 432:1032–1036. doi:10.1038/nature03029.

Kuma, A., M. Hatano, M. Matsui, A. Yamamoto, H. Nakaya, T. Yoshimori, Y. Ohsumi, T. Tokuhisa, and N. Mizushima. 2004b. The role of autophagy during the early neonatal starvation period. *Nature*. 432:1032–1036. doi:10.1038/nature03029.

Laporte, J., F. Bedez, A. Bolino, and J.-L. Mandel. 2003. Myotubularins, a large disease-associated family of cooperating catalytically active and inactive phosphoinositides phosphatases. *Hum. Mol. Genet.* 12 Spec No:R285-92. doi:10.1093/hmg/ddg273.

Laporte, J., L.J. Hu, C. Kretz, J.L. Mandel, P. Kioschis, J.F. Coy, S.M. Klauck, A.

Poustka, and N. Dahl. 1996. A gene mutated in X-linked myotubular myopathy defines a new putative tyrosine phosphatase family conserved in yeast. *Nat. Genet.* 13:175–182. doi:10.1038/ng0696-175.

De Lartigue, J., H. Polson, M. Feldman, K. Shokat, S.A. Tooze, S. Ur, and M.J. Clague. 2009. PIKfyve Regulation of Endosome-Linked Pathways. *Traffic*. 10:883–893. doi:10.1111/j.1600-0854.2009.00915.x.

Lawrence, R.E., and R. Zoncu. 2019. The lysosome as a cellular centre for signalling, metabolism and quality control. *Nat. Cell Biol.* 21:133–142. doi:10.1038/s41556-018-0244-7.

Lee, C.-Y., B.A.K. Cooksey, and E.H. Baehrecke. 2002. Steroid Regulation of Midgut Cell Death during Drosophila Development. *Dev. Biol.* 250:101–111. doi:10.1006/dbio.2002.0784.

Lee, C.Y., and E.H. Baehrecke. 2001. Steroid regulation of autophagic programmed cell death during development. *Development*. 128:1443–1455.

Lee, C.Y., E.A. Clough, P. Yellon, T.M. Teslovich, D.A. Stephan, and E.H. Baehrecke. 2003. Genome-wide analyses of steroid- and radiation-triggered programmed cell death in Drosophila. *Curr. Biol.* 13:350–357. doi:10.1016/S0960-9822(03)00085-X.

Lee, T. V., H.E. Kamber Kaya, R. Simin, E.H. Baehrecke, and A. Bergmann. 2016. The initiator caspase Dronc is subject of enhanced autophagy upon proteasome impairment in Drosophila. *Cell Death Differ.* 23:1555–1564. doi:10.1038/cdd.2016.40.

De Leo, M.G., L. Staiano, M. Vicinanza, A. Luciani, A. Carissimo, M. Mutarelli, A. Di Campli, E. Polishchuk, G. Di Tullio, V. Morra, E. Levtchenko, F. Oltrabella, T. Starborg, M. Santoro, D. di Bernardo, O. Devuyst, M. Lowe, D.L. Medina, A. Ballabio, and M.A. De Matteis. 2016. Autophagosome–lysosome fusion triggers a lysosomal response mediated by TLR9 and controlled by OCRL. *Nat. Cell Biol.* 18:839–850. doi:10.1038/ncb3386.

Levin, R., S. Grinstein, and D. Schlam. 2015. Phosphoinositides in phagocytosis and macropinocytosis. *Biochim. Biophys. Acta - Mol. Cell Biol. Lipids*. 1851:805–823. doi:10.1016/j.bbalip.2014.09.005.

Levine, B., and D.J. Klionsky. 2004. Development by self-digestion: Molecular mechanisms and biological functions of autophagy. *Dev. Cell*. 6:463–477. doi:10.1016/S1534-5807(04)00099-1.

Levine, B., and G. Kroemer. 2019. Biological Functions of Autophagy Genes: A Disease Perspective. *Cell*. 176:11–42. doi:10.1016/j.cell.2018.09.048.

Li, W., W. Zou, Y. Yang, Y. Chai, B. Chen, S. Cheng, D. Tian, X. Wang, R.D.

Vale, and G. Ou. 2012. Autophagy genes function sequentially to promote apoptotic cell corpse degradation in the engulfing cell. *J. Cell Biol.* 197:27–35. doi:10.1083/jcb.201111053.

Lin, L., F.S.L.M. Rodrigues, C. Kary, A. Contet, M. Logan, R.H.G. Baxter, W. Wood, and E.H. Baehrecke. 2017a. Complement-Related Regulates Autophagy in Neighboring Cells. *Cell*. 170:158-171.e8. doi:10.1016/j.cell.2017.06.018.

Lin, Y., J. Zhao, H. Wang, J. Cao, and Y. Nie. 2017b. MiR-181a modulates proliferation, migration and autophagy in AGS gastric cancer cells and downregulates MTMR3. *Mol. Med. Rep.* 15:2452–2456. doi:10.3892/mmr.2017.6289.

Liu, G.Y., and D.M. Sabatini. 2020. mTOR at the nexus of nutrition, growth, ageing and disease. *Nat. Rev. Mol. Cell Biol.* 21:183–203. doi:10.1038/s41580-019-0199-y.

Locke, M., and J. V. Collins. 1965. The structure and formation of protein granules in the fat body of an insect. *J. Cell Biol.* 26:857–884. doi:10.1083/jcb.26.3.857.

Lorenzo, O., S. Urbe, and M.J. Clague. 2006. Systematic analysis of myotubularins: heteromeric interactions, subcellular localisation and endosomerelated functions. *J. Cell Sci.* 119:2953–2959. doi:10.1242/jcs.03040.

Lystad, A.H., and A. Simonsen. 2016. Phosphoinositide-binding proteins in autophagy. *FEBS Lett.* 590:2454–2468. doi:10.1002/1873-3468.12286.

Maekawa, M., S. Terasaka, Y. Mochizuki, K. Kawai, Y. Ikeda, N. Araki, E.Y. Skolnik, T. Taguchi, and H. Arai. 2014. Sequential breakdown of 3-phosphorylated phosphoinositides is essential for the completion of macropinocytosis. *Proc. Natl. Acad. Sci.* 111:E978–E987. doi:10.1073/pnas.1311029111.

Martin, D.N., and E.H. Baehrecke. 2004. Caspases function in autophagic programmed cell death in Drosophila. *Development*. 131:275–284. doi:10.1242/dev.00933.

Martina, J.A., Y. Chen, M. Gucek, and R. Puertollano. 2012. MTORC1 functions as a transcriptional regulator of autophagy by preventing nuclear transport of TFEB. *Autophagy*. 8:903–914. doi:10.4161/auto.19653.

Matsunaga, K., T. Noda, and T. Yoshimori. 2009. Binding Rubicon to cross the Rubicon. *Autophagy*. 5:876–877. doi:10.4161/auto.9098.

Mccartney, A.J., Y. Zhang, and L.S. Weisman. 2014. Phosphatidylinositol 3,5-

bisphosphate: Low abundance, high significance. *BioEssays*. 36:52–64. doi:10.1002/bies.201300012.

McPhee, C.K., M.A. Logan, M.R. Freeman, and E.H. Baehrecke. 2010. Activation of autophagy during cell death requires the engulfment receptor Draper. *Nature*. 465:1093–1097. doi:10.1038/nature09127.

Medina, D.L., S. Di Paola, I. Peluso, A. Armani, D. De Stefani, R. Venditti, S. Montefusco, A. Scotto-Rosato, C. Prezioso, A. Forrester, C. Settembre, W. Wang, Q. Gao, H. Xu, M. Sandri, R. Rizzuto, M.A. De Matteis, and A. Ballabio. 2015. Lysosomal calcium signalling regulates autophagy through calcineurin and TFEB. *Nat. Cell Biol.* 17:288–299. doi:10.1038/ncb3114.

Mei, J., Z. Li, and J.F. Gui. 2009. Cooperation of Mtmr8 with PI3K regulates actin filament modeling and muscle development in zebrafish. *PLoS One*. 4. doi:10.1371/journal.pone.0004979.

Mei, J., S. Liu, Z. Li, and J.F. Gui. 2010. Mtmr8 is essential for vasculature development in zebrafish embryos. *BMC Dev. Biol.* 10. doi:10.1186/1471-213X-10-96.

Meléndez, A., Z. Tallóczy, M. Seaman, E.L. Eskelinen, D.H. Hall, and B. Levine. 2003. Autophagy genes are essential for dauer development and life-span extension in C. elegans. *Science (80-.).* 301:1387–1391. doi:10.1126/science.1087782.

Mellén, M.A., E.J. de la Rosa, and P. Boya. 2008. The autophagic machinery is necessary for removal of cell corpses from the developing retinal neuroepithelium. *Cell Death Differ.* 15:1279–1290. doi:10.1038/cdd.2008.40.

Mellén, M.A., E.J. De La Rosa, and P. Boya. 2009. Autophagy is not universally required for phosphatidyl-serine exposure and apoptotic cell engulfment during neural development. *Autophagy*. 5:964–972. doi:10.4161/auto.5.7.9292.

Mercer, T.J., A. Gubas, and S.A. Tooze. 2018. A molecular perspective of mammalian autophagosome biogenesis. *J. Biol. Chem.* 293:5386–5395. doi:10.1074/jbc.R117.810366.

Mochizuki, Y., and P.W. Majerus. 2003. Characterization of myotubularin-related protein 7 and its binding partner, myotubularin-related protein 9. *Proc. Natl. Acad. Sci. U. S. A.* 100:9768–73. doi:10.1073/pnas.1333958100.

Mohan, M., L.C. Chandra, W. Torben, P.P. Aye, X. Alvarez, and A.A. Lackner. 2014. miR-190b Is Markedly Upregulated in the Intestine in Response to Simian Immunodeficiency Virus Replication and Partly Regulates Myotubularin-Related Protein-6 Expression. *J. Immunol.* 193:1301–1313. doi:10.4049/jimmunol.1303479.

Mohseni, N., S.C. McMillan, R. Chaudhary, J. Mok, and B.H. Reed. 2009. Autophagy promotes caspase-dependent cell death during Drosophila development. *Autophagy*. 5:329–338. doi:10.4161/auto.5.3.7444.

Mony, V.K., S. Benjamin, and E.J. O'Rourke. 2016. A lysosome-centered view of nutrient homeostasis. *Autophagy*. 12:619–631. doi:10.1080/15548627.2016.1147671.

Morcavallo, A., M. Stefanello, R. V. Iozzo, A. Belfiore, and A. Morrione. 2014. Ligand-mediated endocytosis and trafficking of the insulin-like growth factor receptor I and insulin receptor modulate receptor function. *Front. Endocrinol. (Lausanne).* 5:220. doi:10.3389/fendo.2014.00220.

Mulakkal, N.C., P. Nagy, S. Takats, R. Tusco, G. Juhász, and I.P. Nezis. 2014. Autophagy in drosophila: From historical studies to current knowledge. *Biomed Res. Int.* 2014. doi:10.1155/2014/273473.

Nakamura, S., and T. Yoshimori. 2017. New insights into autophagosome–lysosome fusion. *J. Cell Sci.* 130:1209–1216. doi:10.1242/jcs.196352.

Nakatogawa, H. 2013. Two ubiquitin-like conjugation systems that mediate membrane formation during autophagy. *Essays Biochem.* 55:39–50. doi:10.1042/BSE0550039.

Napolitano, G., and A. Ballabio. 2016. TFEB at a glance. *J. Cell Sci.* 129:2475–2481. doi:10.1242/jcs.146365.

Nelson, C., V. Ambros, and E.H. Baehrecke. 2014. miR-14 Regulates Autophagy during Developmental Cell Death by Targeting ip3-kinase 2. *Mol. Cell*. 56:376–388. doi:10.1016/j.molcel.2014.09.011.

Neukomm, L.J., A.-S. Nicot, J.M. Kinchen, J. Almendinger, S.M. Pinto, S. Zeng, K. Doukoumetzidis, H. Tronchère, B. Payrastre, J.F. Laporte, and M.O. Hengartner. 2011. The phosphoinositide phosphatase MTM-1 regulates apoptotic cell corpse clearance through CED-5–CED-12 in C. elegans. *Development*. 138.

Nicot, A.S., and J. Laporte. 2008. Endosomal phosphoinositides and human diseases. *Traffic*. 9:1240–1249. doi:10.1111/j.1600-0854.2008.00754.x.

Ohsumi, Y. 2001. Molecular dissection of autophagy: Two ubiquitin-like systems. *Nat. Rev. Mol. Cell Biol.* 2:211–216. doi:10.1038/35056522.

Oppelt, A., E.M. Haugsten, T. Zech, H.E. Danielsen, A. Sveen, V.H. Lobert, R.I. Skotheim, and J. Wesche. 2014. PIKfyve, MTMR3 and their product PtdIns5P regulate cancer cell migration and invasion through activation of Rac1. *Biochem. J.* 461:383–390. doi:10.1042/BJ20140132.

Oppelt, A., V.H. Lobert, K. Haglund, A.M. MacKey, L.E. Rameh, K. Liestøl, K.

Oliver Schink, N. Marie Pedersen, E.M. Wenzel, E.M. Haugsten, A. Brech, T. Erik Rusten, H. Stenmark, and J. Wesche. 2013. Production of phosphatidylinositol 5-phosphate via PIKfyve and MTMR3 regulates cell migration. *EMBO Rep.* 14:57–64. doi:10.1038/embor.2012.183.

Palamiuc, L., A. Ravi, and B.M. Emerling. 2020. Phosphoinositides in autophagy: current roles and future insights. *FEBS J.* 287:222–238. doi:10.1111/febs.15127.

Palmieri, M., R. Pal, H.R. Nelvagal, P. Lotfi, G.R. Stinnett, M.L. Seymour, A. Chaudhury, L. Bajaj, V. V. Bondar, L. Bremner, U. Saleem, D.Y. Tse, D. Sanagasetti, S.M. Wu, J.R. Neilson, F.A. Pereira, R.G. Pautler, G.G. Rodney, J.D. Cooper, and M. Sardiello. 2017. MTORC1-independent TFEB activation via Akt inhibition promotes cellular clearance in neurodegenerative storage diseases. *Nat. Commun.* 8:14338. doi:10.1038/ncomms14338.

Di Paolo, G., and P. De Camilli. 2006. Phosphoinositides in cell regulation and membrane dynamics. *Nature*. 443:651–657. doi:10.1038/nature05185.

Pham, H.Q., K. Yoshioka, H. Mohri, H. Nakata, S. Aki, K. Ishimaru, N. Takuwa, and Y. Takuwa. 2018. MTMR4, a phosphoinositide-specific 3'-phosphatase, regulates TFEB activity and the endocytic and autophagic pathways. *Genes to Cells*. 1–18. doi:10.1111/gtc.12609.

Qu, X., Z. Zou, Q. Sun, K. Luby-Phelps, P. Cheng, R.N. Hogan, C. Gilpin, and B. Levine. 2007. Autophagy Gene-Dependent Clearance of Apoptotic Cells during Embryonic Development. *Cell*. 128:931–946. doi:10.1016/j.cell.2006.12.044.

Raess, M.A., B.S. Cowling, D.L. Bertazzi, C. Kretz, B. Rinaldi, J.M. Xuereb, P. Kessler, N.B. Romero, B. Payrastre, S. Friant, and J. Laporte. 2017a. Expression of the neuropathy-associated MTMR2 gene rescues MTM1-associated myopathy. *Hum. Mol. Genet.* 26:3736–3748. doi:10.1093/hmg/ddx258.

Raess, M.A., S. Friant, B.S. Cowling, and J. Laporte. 2017b. WANTED – Dead or alive: Myotubularins, a large disease-associated protein family. *Adv. Biol. Regul.* 63:49–58. doi:10.1016/j.jbior.2016.09.001.

Rappaport, J., R.L. Manthe, M. Solomon, C. Garnacho, and S. Muro. 2016. A Comparative Study on the Alterations of Endocytic Pathways in Multiple Lysosomal Storage Disorders. *Mol. Pharm.* 13:357–368. doi:10.1021/acs.molpharmaceut.5b00542.

Reed, B.H., R. Wilk, F. Schöck, and H.D. Lipshitz. 2004. Integrin-dependent apposition of Drosophila extraembryonic membranes promotes morphogenesis and prevents anoikis. *Curr. Biol.* 14:372–380. doi:10.1016/j.cub.2004.02.029.

Reggiori, F., and C. Ungermann. 2017. Autophagosome Maturation and Fusion. *J. Mol. Biol.* 429:486–496. doi:10.1016/j.jmb.2017.01.002.

Robinson, F.L., and J.E. Dixon. 2006. Myotubularin phosphatases: policing 3-phosphoinositides. *Trends Cell Biol.* 16:403–412. doi:10.1016/j.tcb.2006.06.001.

Roczniak-Ferguson, A., C.S. Petit, F. Froehlich, S. Qian, J. Ky, B. Angarola, T.C. Walther, and S.M. Ferguson. 2012. The transcription factor TFEB links mTORC1 signaling to transcriptional control of lysosome homeostasis. *Sci. Signal.* 5. doi:10.1126/scisignal.2002790.

Rong, Y., M. Liu, L. Ma, W. Du, H. Zhang, Y. Tian, Z. Cao, Y. Li, H. Ren, C. Zhang, L. Li, S. Chen, J. Xi, and L. Yu. 2012. Clathrin and phosphatidylinositol-4,5-bisphosphate regulate autophagic lysosome reformation. *Nat. Cell Biol.* 14:924–934. doi:10.1038/ncb2557.

Rong, Y., C.K. McPhee, C. McPhee, S. Deng, L. Huang, L. Chen, M. Liu, K. Tracy, E.H. Baehrecke, E.H. Baehreck, L. Yu, and M.J. Lenardo. 2011. Spinster is required for autophagic lysosome reformation and mTOR reactivation following starvation. *Proc. Natl. Acad. Sci. U. S. A.* 108:7826–31. doi:10.1073/pnas.1013800108.

Rubinsztein, D.C., P. Codogno, and B. Levine. 2012. Autophagy modulation as a potential therapeutic target for diverse diseases. *Nat. Rev. Drug Discov.* 11:709–730. doi:10.1038/nrd3802.

Ruck, A., J. Attonito, K.T. Garces, L. Núnez, N.J. Palmisano, Z. Rubel, Z. Bai, K.C.Q. Nguyen, L. Sun, B.D. Grant, D.H. Hall, and A. Meléndez. 2011. The Atg6/Vps30/Beclin 1 ortholog BEC-1 mediates endocytic retrograde transport in addition to autophagy in C. elegans. *Autophagy*. 7:386–400. doi:10.4161/auto.7.4.14391.

Rusten, T.E., K. Lindmo, G. Juhász, M. Sass, P.O. Seglen, A. Brech, and H. Stenmark. 2004. Programmed autophagy in the Drosophila fat body is induced by ecdysone through regulation of the PI3K Pathway. *Dev. Cell*. 7:179–192. doi:10.1016/j.devcel.2004.07.005.

Rusten, T.E., T. Vaccari, K. Lindmo, L.M.W. Rodahl, I.P. Nezis, C. Sem-Jacobsen, F. Wendler, J.-P. Vincent, A. Brech, D. Bilder, and H. Stenmark. 2007. ESCRTs and Fab1 Regulate Distinct Steps of Autophagy. 17. 1817–1825 pp.

Saitoh, T., N. Fujita, T. Hayashi, K. Takahara, T. Satoh, H. Lee, K. Matsunaga, S. Kageyama, H. Omori, T. Noda, N. Yamamoto, T. Kawai, K. Ishii, O. Takeuchi, T. Yoshimori, and S. Akira. 2009. Atg9a controls dsDNA-driven dynamic translocation of STING and the innate immune response. *Proc. Natl. Acad. Sci. U. S. A.* 106:20842–20846. doi:10.1073/pnas.0911267106.

Saitoh, T., N. Fujita, M.H. Jang, S. Uematsu, B.G. Yang, T. Satoh, H. Omori, T. Noda, N. Yamamoto, M. Komatsu, K. Tanaka, T. Kawai, T. Tsujimura, O. Takeuchi, T. Yoshimori, and S. Akira. 2008. Loss of the autophagy protein Atg16L1 enhances endotoxin-induced IL-1β production. *Nature*. 456:264–268. doi:10.1038/nature07383.

Salvador, N., C. Aguado, M. Horst, and E. Knecht. 2000. Import of a cytosolic protein into lysosomes by chaperone-mediated autophagy depends on its folding state. *J. Biol. Chem.* 275:27447–27456. doi:10.1074/jbc.M001394200.

Sanchez-Juan, P., M.T. Bishop, Y.S. Aulchenko, J.P. Brandel, F. Rivadeneira, M. Struchalin, J.C. Lambert, P. Amouyel, O. Combarros, J. Sainz, A. Carracedo, A.G. Uitterlinden, A. Hofman, I. Zerr, H.A. Kretzschmar, J.L. Laplanche, R.S.G. Knight, R.G. Will, and C.M. van Duijn. 2012. Genome-wide study links MTMR7 gene to variant Creutzfeldt-Jakob risk. *Neurobiol. Aging*. 33:1487.e21-1487.e28. doi:10.1016/j.neurobiolaging.2011.10.011.

Santambrogio, L., and A.M. Cuervo. 2011. Chasing the elusive mammalian microautophagy. *Autophagy*. doi:10.4161/auto.7.6.15287.

Sardiello, M., M. Palmieri, A. Di Ronza, D.L. Medina, M. Valenza, V.A. Gennarino, C. Di Malta, F. Donaudy, V. Embrione, R.S. Polishchuk, S. Banfi, G. Parenti, E. Cattaneo, and A. Ballabio. 2009. A gene network regulating lysosomal biogenesis and function. *Science (80-.).* 325:473–477. doi:10.1126/science.1174447.

Saxton, R.A., and D.M. Sabatini. 2017. mTOR Signaling in Growth, Metabolism, and Disease. *Cell*. 168:960–976. doi:10.1016/j.cell.2017.02.004.

Scharrer, B. 1966. Ultrastructural study of the regressing prothoracic glands of blattarian insects. *Zeitschrift für Zellforsch. und Mikroskopische Anat.* 69:1–21. doi:10.1007/BF00406264.

Schin, K., and H. Laufer. 1973. Studies of programmed salivary gland regression during larval-pupal transformation in Chironomus thummi. *Exp. Cell Res.* 82:335–340. doi:10.1016/0014-4827(73)90350-9.

Schin, K.S., and U. Clever. 1965. Lysosomal and Free Acid Phosphatase in Salivary Glands of Chironomus tentans. *Science (80-.).* 150:1053–1055. doi:10.1126/science.150.3699.1053.

Schink, K.O., K.-W. Tan, and H. Stenmark. 2016. Phosphoinositides in Control of Membrane Dynamics. *Annu. Rev. Cell Dev. Biol.* 32:143–171. doi:10.1146/annurev-cellbio-111315-125349.

Schnorrer, F., C. Schönbauer, C.C.H. Langer, G. Dietzl, M. Novatchkova, K. Schernhuber, M. Fellner, A. Azaryan, M. Radolf, A. Stark, K. Keleman, and

B.J. Dickson. 2010. Systematic genetic analysis of muscle morphogenesis and function in Drosophila. *Nature*. 464:287–291. doi:10.1038/nature08799.

Scott, R.C., O. Schuldiner, and T.P. Neufeld. 2004. Role and regulation of starvation-induced autophagy in the Drosophila fat body. *Dev. Cell*. 7:167–78. doi:10.1016/j.devcel.2004.07.009.

Scotto Rosato, A., S. Montefusco, C. Soldati, S. Di Paola, A. Capuozzo, J. Monfregola, E. Polishchuk, A. Amabile, C. Grimm, A. Lombardo, M.A. De Matteis, A. Ballabio, and D.L. Medina. 2019. TRPML1 links lysosomal calcium to autophagosome biogenesis through the activation of the CaMKKβ/VPS34 pathway. *Nat. Commun.* 10:5630. doi:10.1038/s41467-019-13572-w.

Senderek, J., C. Bergmann, S. Weber, U.P. Ketelsen, H. Schorle, S. Rudnik-Schöneborn, R. Büttner, E. Buchheim, and K. Zerres. 2003. Mutation of the SBF2 gene, encoding a novel member of the myotubularin family, in Charcot-Marie-Tooth neuropathy tye 4B2/11p15. *Hum. Mol. Genet.* 12:349–356. doi:10.1093/hmg/ddg030.

Settembre, C., A. Fraldi, D.L. Medina, and A. Ballabio. 2013. Signals from the lysosome: a control centre for cellular clearance and energy metabolism. *Nat. Rev. Mol. Cell Biol.* 14:283–296. doi:10.1038/nrm3565.

Settembre, C., C. Di Malta, V.A. Polito, M.G. Arencibia, F. Vetrini, S. Erdin, S.U. Erdin, T. Huynh, D. Medina, P. Colella, M. Sardiello, D.C. Rubinsztein, and A. Ballabio. 2011. TFEB links autophagy to lysosomal biogenesis. *Science (80-.).* 332:1429–1433. doi:10.1126/science.1204592.

Settembre, C., R. Zoncu, D.L. Medina, F. Vetrini, S. Erdin, S. Erdin, T. Huynh, M. Ferron, G. Karsenty, M.C. Vellard, V. Facchinetti, D.M. Sabatini, and A. Ballabio. 2012. A lysosome-to-nucleus signalling mechanism senses and regulates the lysosome via mTOR and TFEB. *EMBO J.* 31:1095–1108. doi:10.1038/emboj.2012.32.

Sheffield, D.A., M.R. Jepsen, S.J. Feeney, M.C. Bertucci, A. Sriratana, M.J. Naughtin, J.M. Dyson, R.L. Coppel, and C.A. Mitchell. 2019. The myotubularin MTMR4 regulates phagosomal phosphatidylinositol 3-phosphate turnover and phagocytosis. *J. Biol. Chem.* doi:10.1074/jbc.RA119.009133.

Silhankova, M., F. Port, M. Harterink, K. Basler, H.C. Korswagen, H. Azzedine, A. Bolino, T. Taieb, N. Birouk, M. Di Duca, A. Bouhouche, S. Benamou, A. Mrabet, T. Hammadouche, T. Chkili, R. Gouider, R. Ravazzolo, A. Brice, J. Laporte, E. LeGuern, C. Banziger, D. Soldini, C. Schutt, P. Zipperlen, G. Hausmann, K. Basler, K. Bartscherer, N. Pelte, D. Ingelfinger, M. Boutros, T. Belenkaya, Y. Wu, X. Tang, B. Zhou, L. Cheng, Y. Sharma, D. Yan, E.

Selva, X. Lin, F. Blondeau, J. Laporte, S. Bodin, G. Superti-Furga, B. Payrastre, J. Mandel, A. Bolino, M. Muglia, F. Conforti, E. LeGuern, M. Salih, D. Georgiou, K. Christodoulou, I. Hausmanowa-Petrusewicz, P. Mandich, A. Schenone, A. Gambardella, F. Bono, A. Quattrone, M. Devoto, A. Monaco, C. Cao, J. Backer, J. Laporte, E. Bedrick, A. Wandinger-Ness, C. Cao, J. Laporte, J. Backer, A. Wandinger-Ness, M. Stein, Q. Ch'ng, L. Williams, Y. Lie, M. Sym, J. Whangbo, C. Kenyon, H. Clevers, D. Coudreuse, G. Roel, M. Betist, O. Destree, H. Korswagen, D. Cowing, C. Kenyon, P. Cullen, H. Dang, Z. Li, E. Skolnik, H. Fares, G. Di Paolo, P. De Camilli, S. Eaton, D. Eisenmann, S. Kim, H. Fares, I. Greenwald, A. Fire, S. Harrison, et al. 2010. Wnt signalling requires MTM-6 and MTM-9 myotubularin lipid-phosphatase function in Wnt-producing cells. *EMBO J.* 29:4094–105. doi:10.1038/emboj.2010.278.

Sou, Y.S., S. Waguri, J.I. Iwata, T. Ueno, T. Fujimura, T. Hara, N. Sawada, A. Yamada, N. Mizushima, Y. Uchiyama, E. Kominami, K. Tanaka, and M. Komatsu. 2008. The Atg8 conjugation system is indispensable for proper development of autophagic isolation membranes in mice. *Mol. Biol. Cell*. 19:4762–4775. doi:10.1091/mbc.E08-03-0309.

Sridhar, S., B. Patel, D. Aphkhazava, F. Macian, L. Santambrogio, D. Shields, and A.M. Cuervo. 2013. The lipid kinase PI4KIIIβ preserves lysosomal identity. *EMBO J.* 32:324–339. doi:10.1038/emboj.2012.341.

Srivastava, S., L. Di, O. Zhdanova, Z. Li, S. Vardhana, Q. Wan, Y. Yan, R. Varma, J. Backer, H. Wulff, M.L. Dustin, and E.Y. Skolnik. 2009. The class II phosphatidylinositol 3 kinase C2β is required for the activation of the K+ channel KCa3.1 and CD4 T-cells. *Mol. Biol. Cell*. 20:3783–3791. doi:10.1091/mbc.E09-05-0390.

Srivastava, S., K. Ko, P. Choudhury, Z. Li, A.K. Johnson, V. Nadkarni, D. Unutmaz, W.A. Coetzee, and E.Y. Skolnik. 2006. Phosphatidylinositol-3 phosphatase myotubularin-related protein 6 negatively regulates CD4 T cells. *Mol. Cell. Biol.* 26:5595–602. doi:10.1128/MCB.00352-06.

Srivastava, S., Z. Li, L. Lin, G. Liu, K. Ko, W.A. Coetzee, and E.Y. Skolnik. 2005. The Phosphatidylinositol 3-Phosphate Phosphatase Myotubularin- Related Protein 6 (MTMR6) Is a Negative Regulator of the Ca 22 -Activated K 2 Channel K Ca 3 . 1. *Society*. 25:3630–3638. doi:10.1128/MCB.25.9.3630.

Stauffer, W., H. Sheng, and H.N. Lim. 2018. EzColocalization: An ImageJ plugin for visualizing and measuring colocalization in cells and organisms. *Sci. Rep.* 8. doi:10.1038/s41598-018-33592-8.

Steinmuller, R., A. Lantigua-Cruz, R. Garcia-Garcia, M. Kostrzewa, D. Steinberger, and U. Muller. 1997. Evidence of a third locus in X-linked recessive spastic paraplegia [1]. *Hum. Genet.* 100:287–289.

doi:10.1007/s004390050507.

Stoka, V., V. Turk, and B. Turk. 2016. Lysosomal cathepsins and their regulation in aging and neurodegeneration. *Ageing Res. Rev.* 32:22–37. doi:10.1016/j.arr.2016.04.010.

Szklarczyk, D., A.L. Gable, D. Lyon, A. Junge, S. Wyder, J. Huerta-Cepas, M. Simonovic, N.T. Doncheva, J.H. Morris, P. Bork, L.J. Jensen, and C. Von Mering. 2019. STRING v11: Protein-protein association networks with increased coverage, supporting functional discovery in genome-wide experimental datasets. *Nucleic Acids Res.* 47:D607–D613. doi:10.1093/nar/gky1131.

Taguchi-Atarashi, N., M. Hamasaki, K. Matsunaga, H. Omori, N.T. Ktistakis, T. Yoshimori, and T. Noda. 2010. Modulation of local Ptdins3P levels by the PI phosphatase MTMR3 regulates constitutive autophagy. *Traffic*. 11:468–478. doi:10.1111/j.1600-0854.2010.01034.x.

Takacs-Vellai, K., T. Vellai, A. Puoti, M. Passannante, C. Wicky, A. Streit, A.L. Kovacs, and F. Müller. 2005. Inactivation of the autophagy Gene bec-1 triggers apoptotic cell death in C. elegans. *Curr. Biol.* 15:1513–1517. doi:10.1016/j.cub.2005.07.035.

Takáts, S., P. Nagy, Á. Varga, K. Pircs, M. Kárpáti, K. Varga, A.L. Kovács, K. Hegedus, and G. Juhász. 2013. Autophagosomal Syntaxin17-dependent lysosomal degradation maintains neuronal function in Drosophila. *J. Cell Biol.* 201:531–539. doi:10.1083/jcb.201211160.

Takeshige, K., M. Baba, S. Tsuboi, T. Noda, and Y. Ohsumi. 1992. Autophagy in yeast demonstrated with proteinase-deficient mutants and conditions for its induction. *J. Cell Biol.* 119:301–311. doi:10.1083/jcb.119.2.301.

Tamagaki, A., M. Shima, R. Tomita, M. Okumura, M. Shibata, S. Morichika, H. Kurahashi, J.C. Giddings, A. Yoshioka, and Y. Yokobayashi. 2000. Segregation of a pure form of spastic paraplegia and NOR insertion into Xq11.2. *Am. J. Med. Genet.* 94:5–8. doi:10.1002/1096-8628(20000904)94:1<5::AID-AJMG2>3.0.CO;2-O.

Tang, L., Y. Tong, H. Cao, S. Xie, Q. Yang, F. Zhang, Q. Zhu, L. Huang, Q. Lü, Y. Yang, D. Li, M. Chen, C. Yu, W. Jin, Y. Yuan, and N. Tong. 2014. The MTMR9 rs2293855 polymorphism is associated with glucose tolerance, insulin secretion, insulin sensitivity and increased risk of prediabetes. *Gene*. 546:150–155. doi:10.1016/j.gene.2014.06.028.

Theodosiou, N.A., and T. Xu. 1998. Use of FLP/FRT System to Study Drosophila Development. *Methods Enzymol.* 14:355–365.

Thumm, M., R. Egner, B. Koch, M. Schlumpberger, M. Straub, M. Veenhuis, and

D.H. Wolf. 1994. Isolation of autophagocytosis mutants of Saccharomyces cerevisiae. *FEBS Lett.* 349:275–280. doi:10.1016/0014-5793(94)00672-5.

Thurmond, J., J.L. Goodman, V.B. Strelets, H. Attrill, L.S. Gramates, S.J. Marygold, B.B. Matthews, G. Millburn, G. Antonazzo, V. Trovisco, T.C. Kaufman, B.R. Calvi, N. Perrimon, S.R. Gelbart, J. Agapite, K. Broll, L. Crosby, G. Dos Santos, D. Emmert, K. Falls, V. Jenkins, C. Sutherland, C. Tabone, P. Zhou, M. Zytkovicz, N. Brown, P. Garapati, A. Holmes, A. Larkin, C. Pilgrim, P. Urbano, B. Czoch, R. Cripps, and P. Baker. 2019. FlyBase 2.0: The next generation. *Nucleic Acids Res.* 47:D759-765. doi:10.1093/nar/gky1003.

Tsukada, M., and Y. Ohsumi. 1993. Isolation and characterization of autophagy-defective mutants of Saccharomyces cerevisiae. *FEBS Lett.* 333:169–174. doi:10.1016/0014-5793(93)80398-E.

Velentzas, P.D., L. Zhang, G. Das, T.K. Chang, C. Nelson, W.R. Kobertz, and E.H. Baehrecke. 2018. The Proton-Coupled Monocarboxylate Transporter Hermes Is Necessary for Autophagy during Cell Death. *Dev. Cell*. 47:281–293. doi:10.1016/j.devcel.2018.09.015.

Velichkova, M., J. Juan, P. Kadandale, S. Jean, I. Ribeiro, V. Raman, C. Stefan, and A.A. Kiger. 2010. Drosophila Mtm and class II PI3K coregulate a PI(3)P pool with cortical and endolysosomal functions. *J. Cell Biol.* 190:407–425. doi:10.1083/jcb.200911020.

Vergarajauregui, S., P.S. Connelly, M.P. Daniels, and R. Puertollano. 2008. Autophagic dysfunction in mucolipidosis type IV patients. *Hum. Mol. Genet.* 17:2723–2737. doi:10.1093/hmg/ddn174.

Wallroth, A., and V. Haucke. 2018. Phosphoinositide conversion in endocytosis and the endolysosomal system. *J. Biol. Chem.* 293:1526–1535. doi:10.1074/jbc.R117.000629.

Wang, H., H.Q. Sun, X. Zhu, L. Zhang, J. Albanesi, B. Levine, and H. Yin. 2015. GABARAPs regulate PI4P-dependent autophagosome: Lysosome fusion. *Proc. Natl. Acad. Sci. U. S. A.* 112:7015–7020. doi:10.1073/pnas.1507263112.

Wang, Y., X. Lei, C. Gao, Y. Xue, X. Li, H. Wang, and Y. Feng. 2019a. MiR-506-3p suppresses the proliferation of ovarian cancer cells by negatively regulating the expression of MTMR6. *J. Biosci.* 44:126. doi:10.1007/s12038-019-9952-9.

Wang, Z., M. Zhang, R. Shan, Y.J. Wang, J. Chen, J. Huang, L.Q. Sun, and W.B. Zhou. 2019b. MTMR3 is upregulated in patients with breast cancer and regulates proliferation, cell cycle progression and autophagy in breast cancer cells. *Oncol. Rep.* 42:1915–1923. doi:10.3892/or.2019.7292.

Waugh, M.G. 2016. Chromosomal Instability and Phosphoinositide Pathway Gene Signatures in Glioblastoma Multiforme. *Mol. Neurobiol.* 53:621–630. doi:10.1007/s12035-014-9034-9.

Weavers, H., I.R. Evans, P. Martin, and W. Wood. 2016. Corpse Engulfment Generates a Molecular Memory that Primes the Macrophage Inflammatory Response. *Cell*. 1–14. doi:10.1016/j.cell.2016.04.049.

Wei, P., M. Ning, M. Yuan, X. Li, H. Shi, W. Gu, W. Wang, and Q. Meng. 2019. Spiroplasma eriocheiris enters drosophila schneider 2 cells and relies on clathrin-mediated endocytosis and macropinocytosis. *Infect. Immun.* 87:e00233-19. doi:10.1128/IAI.00233-19.

Weidner, P., M. Söhn, T. Gutting, T. Friedrich, T. Gaiser, J. Magdeburg, P. Kienle, H. Ruh, C. Hopf, H.-M. Behrens5, C. Röcken, T. Hanoch, R. Seger, M.P.A. Ebert, and E. Burgermeister. 2016. Myotubularin-related protein 7 inhibits insulin signaling in colorectal cancer. *Oncotarget*. 7:50490–50506. doi:10.18632/oncotarget.10466.

Wen, J.K., Y.T. Wang, C.C. Chan, C.W. Hsieh, H.M. Liao, C.C. Hung, and G.C. Chen. 2017. Atg9 antagonizes TOR signaling to regulate intestinal cell growth and epithelial homeostasis in Drosophila. *Elife*. 6:e29338. doi:10.7554/eLife.29338.

Wilson, P.W.F., R.B. D'Agostino, H. Parise, L. Sullivan, and J.B. Meigs. 2005. Metabolic syndrome as a precursor of cardiovascular disease and type 2 diabetes mellitus. *Circulation*. 112:3066–3072. doi:10.1161/CIRCULATIONAHA.105.539528.

Wollert, T., D. Yang, X. Ren, H.H. Lee, Y.J. Im, and J.H. Hurley. 2009. The ESCRT machinery at a glance. *J. Cell Sci.* 122:2163–2166. doi:10.1242/jcs.029884.

Wong, C.O., S. Gregory, H. Hu, Y. Chao, V.E. Sepúlveda, Y. He, D. Li-Kroeger, W.E. Goldman, H.J. Bellen, and K. Venkatachalam. 2017. Lysosomal Degradation Is Required for Sustained Phagocytosis of Bacteria by Macrophages. *Cell Host Microbe*. 21:719–730. doi:10.1016/j.chom.2017.05.002.

Wu, Y., S. Cheng, H. Zhao, W. Zou, S. Yoshina, S. Mitani, H. Zhang, and X. Wang. 2014. PI3P phosphatase activity is required for autophagosome maturation and autolysosome formation. *EMBO Rep.* 15:973–981. doi:10.15252/embr.201438618.

Wucherpfennig, T., M. Wilsch-Bräuninger, and M. González-Gaitán. 2003. Role of *Drosophila* Rab5 during endosomal trafficking at the synapse and evoked neurotransmitter release. *J. Cell Biol.* 161:609–624. doi:10.1083/jcb.200211087.

Xue, Y., H. Fares, B. Grant, Z. Li, A.M. Rose, S.G. Clark, and E.Y. Skolnik. 2003. Genetic Analysis of the Myotubularin Family of Phosphatases in Caenorhabditis elegans. *J. Biol. Chem.* 278:34380–34386. doi:10.1074/jbc.M303259200.

Yanagiya, T., A. Tanabe, A. Iida, S. Saito, A. Sekine, A. Takahashi, T. Tsunoda, S. Kamohara, Y. Nakata, K. Kotani, R. Komatsu, N. Itoh, I. Mineo, J. Wada, H. Masuzaki, M. Yoneda, A. Nakajima, S. Miyazaki, K. Tokunaga, M. Kawamoto, T. Funahashi, K. Hamaguchi, K. Tanaka, K. Yamada, T. Hanafusa, S. Oikawa, H. Yoshimatsu, K. Nakao, T. Sakata, Y. Matsuzawa, N. Kamatani, Y. Nakamura, and K. Hotta. 2007. Association of single-nucleotide polymorphisms in MTMR9 gene with obesity. *Hum. Mol. Genet.* 16:3017–3026. doi:10.1093/hmg/ddm260.

Yang, Z., and D.J. Klionsky. 2010. Mammalian autophagy: Core molecular machinery and signaling regulation. *Curr. Opin. Cell Biol.* 22:124–131. doi:10.1016/j.ceb.2009.11.014.

Yoshii, S.R., and N. Mizushima. 2017. Monitoring and measuring autophagy. *Int. J. Mol. Sci.* pii: E186. doi:10.3390/ijms18091865.

Yu, L., Y. Chen, and S.A. Tooze. 2018a. Autophagy pathway: Cellular and molecular mechanisms. *Autophagy*. 14:207–215. doi:10.1080/15548627.2017.1378838.

Yu, L., Y. Chen, and S.A. Tooze. 2018b. Autophagy pathway: Cellular and molecular mechanisms. *Autophagy*. 14:207–215. doi:10.1080/15548627.2017.1378838.

Yu, L., C.K. Mcphee, L. Zheng, G.A. Mardones, Y. Rong, J. Peng, N. Mi, Y. Zhao, Z. Liu, F. Wan, D.W. Hailey, V. Oorschot, J. Klumperman, E.H. Baehrecke, and M.J. Lenardo. 2010. Termination of autophagy and reformation of lysosomes regulated by mTOR. *Nature*. 465:942–946. doi:10.1038/nature09076.

Zhang, H., and E.H. Baehrecke. 2015. Eaten alive: novel insights into autophagy from multicellular model systems. *Trends Cell Biol.* 25:376–387. doi:10.1016/j.tcb.2015.03.001.

Zoncu, R., R.M. Perera, D.M. Balkin, M. Pirruccello, D. Toomre, and P. De Camilli. 2009. A Phosphoinositide Switch Controls the Maturation and Signaling Properties of APPL Endosomes. *Cell*. 136:1110–1121. doi:10.1016/j.cell.2009.01.032.

Zou, J., S.C. Chang, J. Marjanovic, and P.W. Majerus. 2009a. MTMR9 increases MTMR6 enzyme activity, stability, and role in apoptosis. *J. Biol. Chem.* 284:2064–2071. doi:10.1074/jbc.M804292200.

Zou, J., P.W. Majerus, D.B. Wilson, A. Schrade, S.-C. Chang, and M.P. Wilson. 2012a. The Role of Myotubularin-related Phosphatases in the Control of Autophagy and Programmed Cell Death. *Adv. Biol. Regul.* 52:282–289. doi:10.1016/j.advenzreg.2011.10.001.The.

Zou, J., C. Zhang, J. Marjanovic, M. V Kisseleva, P.W. Majerus, and M.P. Wilson. 2012b. Myotubularin-related protein (MTMR) 9 determines the enzymatic activity, substrate specificity, and role in autophagy of MTMR8. *Proc. Natl. Acad. Sci. U. S. A.* 109:9539–44. doi:10.1073/pnas.1207021109.

Zou, W., Q. Lu, D. Zhao, W. Li, J. Mapes, Y. Xie, and X. Wang. 2009b. Caenorhabditis elegans myotubularin MTM-1 negatively regulates the engulfment of apoptotic cells. *PLoS Genet.* 5:e1000679. doi:10.1371/journal.pgen.1000679.